ParisTech
INSTITUT DES SCIENCES ET TECHNOLOGIES
PARIS INSTITUTE OF TECHNOLOGY

TELECOM ParisTech

2014-ENST-0075

EDITE - ED 130

Doctorat ParisTech

T H È S E

pour obtenir le grade de docteur délivré par

TELECOM ParisTech

Spécialité « Électronique et Communication »

présentée et soutenue publiquement par

Ayşe ÜNSAL

le 27 Novembre 2014

Méthodes de transmission d'échantillons continus pour les réseaux de capteurs

Directeur de thèse : **Raymond KNOPP**

Jury

M. Michael C. Gastpar, Professeur, École Polytechnique Fédérale de Lausanne	Rapporteur
M. Deniz GÜNDÜZ, Assist. Professeur , Imperial College London	Rapporteur
M. Dirk SLOCK, Professeur, EURECOM	Examinateur
Mme. Aline ROUMY, Chargée de Recherche, INRIA	Examinateur
M. Pierre DUHAMEL, Professeur, CNRS	Examinateur

TELECOM ParisTech
école de l'Institut Télécom - membre de ParisTech

THÈSE

DISSERTATION

In Partial Fulfillment of the Requirements
for the Degree of Doctor of Philosophy
from TELECOM ParisTech

Specialization: Wireless Communications

Ayşe Ünsal

Transmission of Analog Source Samples for Remote and Distributed Sensing

Defended on November 27, 2014 before a committee composed of:

Reviewers	Prof. Michael C. Gastpar, EPFL, Switzerland
	Assist. Prof. Deniz Gündüz, Imperial College London, United Kingdom
Examiners	Prof. Dirk Slock, EURECOM, France
	Dr. Aline Roumy, INRIA, France
	Prof. Pierre Duhamel, CNRS, France
Thesis Supervisor	Prof. Raymond Knopp, EURECOM, France

Acknowledgements

It is my pleasure to thank people who made this thesis possible with their support in some way.

Götz Trenkler is doubtless the first name I would like to thank, who was my inspiration to get a Ph.D. degree by simply being a concrete example of the kind of academic I want to be. I consider this thesis as the initial step in that direction, which I was able to take thanks to Raymond. Based on my experiences over the last four years, I can say that despite his exceptional mind, Raymond's modesty and respect for his students distinguish him from a great portion of today's research society. It is not only his technical capabilities what let him earn the respect of the people working under him, but also simply the way he treats them. His challenging stubbornness enabled me to try harder which ended up improving what we produced further. I am grateful to him for being hard on me to let me 'grow into' a better researcher and I am proud of the work we produced together.

Surely, the difficulties which I faced over the last four years were not only technical. Even if we take the language out of the equation moving into a foreign country may become unbearable especially at the very beginning. Thanks to my local family composed by three beautiful ladies with extraordinarily strong characters, Melek, Leyla and Neslihan, my life in Antibes was filled with countless good memories.

Finally, I would like to thank my family for their endless support. It is an everlasting assurance to know that I would still have their unconditional love and faith in me even if I had the greatest failure.

Abstract

This thesis considers transmission of sporadic random samples in three scenarios which can be summarized as a single source with remote sensing, dual and multiple source cases with distributed and remote sensing. The protocol and the transmission strategy is reminiscent of reverse ARQ protocols and we show how it can be used for energy-limited sensors making use of future broadband cellular networks. To begin with, a low-latency, two-way parameter modulation-estimation protocol for wide-band channels which is inspired by the classical scheme in [1] is presented and analyzed in terms of its asymptotic behaviour with non-coherent detection on both pure line-of sight and more general fading channels.

We proceed with introducing lower bounds on the reconstruction error for transmission of two continuous correlated random vectors sent over a sum channel with and without feedback both for uniform and normal distributions. Additionally, the novel protocol from the first part is extended to the dual-source case and its asymptotic performance is analyzed and an upper bound on the distortion level is derived for two rounds considering the extreme case of high correlation among the sources for each distribution.

Lastly, lower bounds are derived for the reconstruction error of a single normally or uniformly-distributed finite-dimensional vector imperfectly measured by a network of sensors and transmitted with finite energy to a common receiver via an additive white Gaussian noise asynchronous multiple access channel. Transmission makes use of a perfect causal feedback link to the encoder connected to each sensor. The retransmission protocol from the first part is further extended to this more general network scenario, for which asymptotic upper-bounds on the reconstruction error are provided. Both the upper and lower-bounds show that collaboration can be achieved through energy accumulation under certain circumstances.

Résumé

Cette thèse porte sur la transmission d'échantillons aléatoires et intempestifs pour trois scénarios de réseaux sans-fils. Un canal point-a-point avec un capteur à distance, puis un canal a accès-multiple avec deux observations corrélées provenant de deux capteurs à distance et finalement un canal a accès-multiple avec de multiples observations bruitées du même échantillon. Le protocole de transmission étudie dans les trois cas ressemble à un protocole de retransmission (ARQ) inversé. Ce type de protocole trouve son origine dans le schéma classique propose dans [1]. Un protocole bidirectionnel à faible latence pour la modulation-estimation à travers des canaux large-bande est présenté et par la suite analyse en terme de sa performance asymptotique avec la détection non-cohérente sur divers canaux radio-mobiles.

Nous continuons par le développement de bornes inférieures sur l'erreur de reconstructions pour la transmission de deux vecteurs aléatoires corrélés à travers un canal à accès-multiples.Le nouveau protocole de la première partie de cette thèse est généralise pour ce cas. Sa performance asymptotique est analysée et une borne supérieure sur la distorsion à la reconstruction est présentée pour une transmission en deux rondes.

Finalement, des bornes inférieures sur l'erreur de reconstruction pour la transmission d'un vecteur de dimension finie mesurée de manière imparfaite par un réseaux de capteurs sont présentées. La transmission utilise une liaison de retour causal parfaite vers l'encodeur de chaque capteur.Le protocole est modifiée pour ce scenario plus général et des bornes supérieures sur l'erreur de reconstruction de la source commune sont présentées.

Contents

List of Figures

Acronyms

The main acronyms used in this thesis are given hereafter. The meaning of an acronym is usually indicated once at its first appearance in the text.

4G	Fourth Generation
5G	Fifth Generation Wireless Systems
ACK	Acknowledgment
ARQ	Automatic Repeat Request
CEO	Central Estimating Officer
DAMGN	Discrete-time additive Gaussian noise
NACK	Negative-Acknowledgment
AWGN	Additive White Gaussian Noise
GMAC	Gaussian Multiple Access Channel
HARQ	Hybrid Automatic Repeat Request
HDMI	High-Definition Multimedia Interface
JSCC	Joint Source-Channel Coding
LTE	Long Term Evolution
M2M	Machine-to-machine
MAC	Multiple Access Channel
MAP	Maximum a Posteriori Probability
ML	Maximum Likelihood
MSE	Mean Squared Error
MMSE	Minimum Mean Squared Error
PRACH	Physical Random Access Channel
PDF	Probability Density Function
PPM	Pulse-Position Modulation
OFDM	Orthogonal Frequency Division Multiplexing
SK	Schalkwijk-Kailath
SNR	Signal to Noise Ratio

Chapter 1

Introduction

1.1 Motivation

Claude Shannon in 1948 through his milestone paper [2] showed that separate source and channel coding does not cause any loss of optimality (in terms of reliable transmission) as long as the coding block-length tends to infinity. This result has been proven to hold in very few instances. Nevertheless, because of the optimality in the single-source case, this is the main reason for treating the source and channel coding separately in traditional solutions. From a networking standpoint, it is also convenient to separate the two operations since protocols are simpler to design since digital data can be multiplexed. However, these practical implementations incur high delays, that translates to is latency, and large complexity due to the extremely long block-lengths that have to be used. By combining the efforts of the channel and source code, a new technique, known as joint source-channel coding (JSCC), is obtained.It might be expected that this technique will provide significant improvements in the case of a source with significant redundancy combined with a channel with high noise levels. This is due to the fact that in this case traditional, or separated source and channel coding would first use source coding in order to remove redundancy and afterwards utilize channel coding to insert additional redundancy. Thus it is not surprising that this is not the most efficient approach even when the block-length is allowed to grow boundlessly.

A modern example of a system using joint-source channel approaches (although not analog) would be the current HDMI standard on top of OFDM transmission used for short-range wireless transmission of high-definition video with sub-1 ms latency. This makes use of variable signal levels in the

transformed source signal (audio/video) with unequal error protection at the physical layer for the different levels of importance of the source signals. Here the "analog" information is not encoded using a source code at all aside from scalar quantization. This significantly minimizes latency and mimics the linear coding described in the upcoming subsection. The most important remark to stress is that this approach is used to *minimize latency.*

Another reason motivating the use of novel joint-source and channel coding paradigms would be the time scales corresponding to the source and channel bandwidths. In sensor networks, for instance, the sources may be characterized by a few independent samples of an analog phenomenon that need to be transmitted very sporadically across a wide-band channel. This would be the case arising when we integrate low-cost/power analog sensors to LTE infrastructure. Here the ergodicity of the source is not a degree of freedom that can be exploited in the coding system. Interestingly enough, the ultimate performance (in terms of reconstruction fidelity at the receiver) achievable by a coding scheme for this reasonably simple problem remains unknown, although upper and lower bounds on performance are easily found.

The key issue is that digital transmission for small amounts of typically analog data will induce overhead which is wasteful, especially for massive networks of simple nodes. Joint source-channel coding (JSCC), which combines the efforts of the channel and source code, addresses such problems. In this study, we consider JSCC for transmission of multiple spatially distributed samples of a slowly time-varying random field. Our primary objective is to provide asymptotic performance measures and realizable, simple transmission strategies for large one-hop sensor networks. We model systems where each sensor measures signals with a finite and small number of source dimensions, in comparison to the number of channel dimensions. This is motivated by applications such as remote sensing using broadband wireless infrastructure (e.g. cellular networks) where sensors take sporadic samples of a random event, feed them back to the network via base stations and subsequently return to an idle state to conserve power. As a result, we do not consider coding of sequences of samples, but rather exploit spatial expansion and correlation between a network of sensors with independent observation noise. Since the applications target wireless networks, it is reasonable to assume a feedback-based transmission strategy, and both the asymptotic results as well as the transmission strategy studied here will exploit feedback. The latter allows for simple and energy-efficient strategies, even if feedback is not required for optimality.

1.2 Problem Definition and Background

Imagine the simplest scenario of one sensor node tracking a slowly time-varying random sequence and sending its observations to a receiver over a

wireless channel. The source is denoted by a random variable U of zero mean and variance $\sigma_u^2 = 1$, representing a single realization of the random sequence at a particular time t. The sensor should be seen as a tiny device with strict energy constraints. The communication channel between the sender and the receiver is an additive white Gaussian noise channel. An important question is how to efficiently encode the random variable U for transmission, and what performance can be achieved upon reconstruction as a function of the energy used to achieve this transmission. As an example, the sensor could be sporadically sending analog information (temperature, magnetic field, current, speed, etc.) to a collecting node. The traffic would be very low-rate (vanishing) and potentially requiring low-latency. The latter could arise for two reasons, either reactivity of an actuating element in the network or to minimize energy consumption in the sensing node itself by using discontinuous transmission and reception. Here the latency of the transmission is directly related to the "on"-time of communication circuitry of the sensing node. This example captures the essence of some so-called *machine-type communications*, a term which refers to machines (including sensors) interconnected via cellular networks and exchanging information autonomously.

For this scenario, the slowly time-varying characteristic of the source has two main impacts on the way the coding problem should be addressed: firstly, the time between two observations is long, and the sensor should not wait for a sequence of observations to encode it. Therefore, the sensor will encode only one observation before sending it through the channel. Secondly, for each source realization the channel can potentially be used over many signal dimensions, for instance by encoding over a wide-bandwidth in the frequency-domain. This would be the case for sensors connected directly to fourth-generation cellular networks. Hence, we can reasonably assume that there is no constraint on the dimensionality of the channel codebook. The latter condition amounts to saying that very low-rate codes should be used. In [3], the authors state three main requirements which need to be satisfied for the 5G technology to contain machine-type communication (or machine-to-machine communication, M2M) which can be listed as supporting systems with a high number of connected devices, maintaining low-rate and low-latency. This thesis introduces system models and transmission strategies which try to meet these three main requirements of 5G.

We focus our attention on the case where unitary samples of the source are transmitted sporadically due to slow time-variation as explained above in the motivation. We review the related studies in two main groups as the single and multiple source systems.

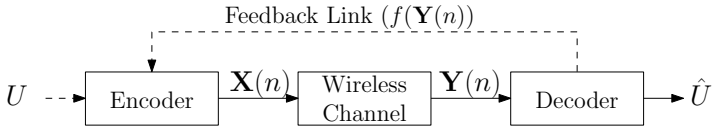

Figure 1.1: Single-Source System Model

1.2.1 Single Source Problem

The single-source model is depicted in Figure (1.1) where an encoder maps one realization of the source U into $\mathbf{X} \triangleq (X_1, \ldots, X_N)$ where N denotes the dimension of the channel input. We will make use of causal feedback so that the encoder may also depend on past channel outputs, that is $X_i = f(U, Y_1, \cdots, Y_{i-1})$. $\mathbf{X}$ is then sent across the channel corrupted by a white Gaussian noise sequence $\mathbf{Z}$, and is received as $\mathbf{Y}$. The receiver is a mapping function which tries to construct an estimate $\widehat{U}$ of U given $\mathbf{Y}$. The fidelity criterion that we wish to minimize is the MSE distortion defined as $D \triangleq \mathbb{E}[(U - \widehat{U})^2]$, under the mean energy constraint $\mathbb{E}[||\mathbf{X}||^2] \leq \mathcal{E}$. It is well-known that the linear encoder (i.e. $X = \sqrt{\mathcal{E}}U$) achieves the best performance under the mean energy constraint for the special case $N = 1$ [4–6]. In fact, a lower bound on the distortion over all possible encoders and decoders is easily derived in [4] using classical information theory, and given by

$$D \geq e^{-2\mathcal{E}/N_0} \tag{1.1}$$

where $N_0/2$ is the channel noise per dimension. Note that, the form of (1.1) is adapted to a discrete-time complex Gaussian channel with noise variance $N_0/2$ to make the comparisons easier with our information theoretic lower bounds in the further chapters. Goblick's information theoretic bound given above was derived through defining the channel capacity and the rate-distortion function in terms of the channel SNR, more precisely he obtained the minimum distortion in estimating the source message as a function of the channel SNR which leads to the output SNR in a continuous-time channel with limited bandwidth. At the end of the procedure the reconstruction error is composed solely by the quantization process applied to the source.

The $e^{-\mathcal{E}/3N_0}$ behaviour for Goblick's digital scheme was described in [7, 8]. Figure (1.2) is a pictorial representation of Goblick's scheme where the B bit uniform quantization is followed by 2^B-ary orthogonal modulation to transmit the source U using the energy $\mathcal{E}$ which achieves the same performance with [9]. Several schemes can achieve $e^{-\mathcal{E}/3N_0}$ both with and without coherent detection and for both normally and uniformly distributed U. The importance of Goblick's work [4] comes from the method he chose. To the best of our knowledge the first digital scheme for unlimited bandwidth based on scalar quantization and orthogonal modulation was described by Goblick in [4], which is also the quantization/modulation strategy used in this

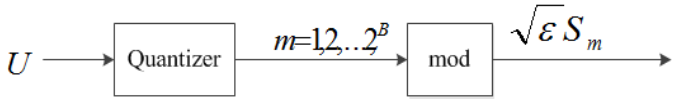

Figure 1.2: Goblick's Digital Scheme

thesis, and the performance loss with respect to (1.1) was heuristically argued to be on the order of 6-9 dB. Unlike Goblick and all three achievable schemes proposed in this thesis, Wozencraft-Jacobs use [9, pg:623-624] pulse position modulation (PPM) as shown in Figure (1.3). A comparison in [8] with best-known joint medium-resolution source-channel codes [10] for high channel to source bandwidth ratios shows that simple hybrid (yet separated) joint-source channel techniques can outperform non-linear mappings. Such optimization for a different power constraint can be found in the literature for example in [11] and [12], where the authors try to bound the optimal number of quantization bits that minimizes distortion.

For the case of a point-to-point channel without feedback, the most recent and significant studies are presented by Merhav in [13,14] for AWGN channels and discrete-memoryless channels, respectively. In [13,15] the best-known lower bound for the reconstruction fidelity without feedback, with coherent detection and unlimited channel bandwidth behaves as $e^{-\mathcal{E}/2N_0}$ for uniformly-distributed U where $\mathcal{E}$ is the energy used for transmission of U. In fact, the author achieves this lower-bound on the MSE through the threshold he defines on the maximum exponential rate of that the error probability decay in estimating $|U-\hat{U}|$ rather than concentrating on the MSE as the performance criterion itself. In order to prove this threshold on the error probability of $|U-\hat{U}|$, he adapts the well-known Ziv-Zakai bound [16] to his case with M hypotheses instead of 2 and the derivation proceeds as the Chazan-Zakai bound [17]. Basically, the author defines the following generalized hypothesis testing problem

$$\mathcal{H}_i : \mathbf{y} = \mathbf{x}(t, u + i\Delta) + \mathbf{z} \tag{1.2}$$

for $i \in \{1, \cdots, M\}$ and the signal model defined as $y(t) = x(t,u) + n(t)$ for $t \in [0,T)$ where $x(t,u)$ is the waveform with a power of S, parametrized by u under the assumption of $u + i\Delta \in [-1/2, 1/2)$. Merhav comes up with a bound on the error probability of the optimum ML detector in choosing from M hypotheses through expanding Ziv-Zakai's derivation. After he uses this result to obtain the second moment on the estimation error of U. In the upcoming chapter which focuses on the single source case, we benefited from the results of [13] to discuss the tightness of our bounds from our achievable scheme for the no-feedback-case. In a following study [14], the author generalizes his results to a certain extend and provides

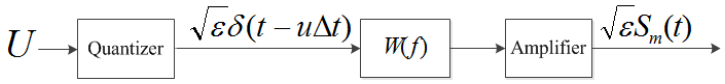

Figure 1.3: Pulse-position modulation

both upper and lower bounds for the best achievable exponential decay of $E|\hat{U}-U|^m, \quad m \geq 0$ in a discrete memoryless channel. Ziv-Zakai and Chazan-Zakai bounds are extended to the vector parameter estimation case in [18].

Feedback-based schemes

In two-way systems, for example cellular networks, we could clearly imagine the use of reliable feedback from the down-link, with vanishing probability of error (i.e. perfect feedback). The main drawback is the requirement of energy for receiver which would impact the overall energy budget of the sensing node. Although it is difficult to model, protocol latency becomes an issue for overall energy consumption. Some of the earliest work in analog transmission of low-bandwidth sources assumed feedback as shown in Figure (1.1) with the presence of the feedback signal $f(\mathbf{Y}(n))$. Through two-way communication, stochastic control approaches [19, 20] can achieve, at least asymptotically, the lower bound on distortion in (1.1). This comes at the expense of delay, since, as in many adaptive systems, the feedback system must converge to minimize distortion. It is reasonable to assume that both can be extended to non-coherent detection and even broadband frequency-selective channels for diversity. However, the underlying estimation strategies will quickly become quite involved.

As mentioned above following Goblick's original work, with an addition of a noiseless feedback link to the system, using coherent detection and unlimited channel bandwidth, the classical closed-loop schemes described in [19] asymptotically achieves (1.1). In comparison to [4], the proposed scheme is differentiated by not being quantized neither coded. The iterative transmission scheme for unitary samples of the source proceeds as follows for the first couple of iterations. $x_1 = a_1 U$ is transmitted where U is normally distributed with the following parameters $N(0, N_0)$. At the receiver end, $y_1 = x_1 + n_1$ is received and $v_1 = y_1/a_1$ is computed, where $n_i, i = 1, 2, \cdots$, denotes the additive Gaussian white channel noise with zero mean and variance σ^2. Using v_1, the first maximum a posteriori probability (MAP) estimate of U is obtained as $\hat{U}_1 = \frac{a_1^2 v_1}{\frac{1}{N_0} a_1^2}$ and it is fed back. On the second iteration the transmitter sends $x_2 = a_2[U - \hat{U}_1]$, which is received as $y_2 = x_2 + n_2$. The second MAP of U is computed through $v_2 = \frac{y_2}{a_2} + \hat{U}_1$ as

$\hat{U}_2 = \frac{a_1^2 v_1 + a_2^2 v_2}{(1\ N_0) + a_1^2 + a_2^2}$ and fed back. This procedure could be repeated upto N iterations and eventually the authors obtain [4, eq. 21] without quantizing the source nor coding on the channel where they add a perfect feedback link to the system. It should be noted that both [4] and [19] consider unlimited channel bandwidth for a normally distributed source and coherent detection but unlike Goblick's digital scheme non-coherent detection is not applicable to [19]. As a second drawback, the scheme requires perfect feedback to achieve (1.1). The paper differs from Schalkwijk's previous work [21] with respect to the source statistics where the author uses uniform distribution with band-limited signals and feedback.

In a fairly recent paper [22], Gallager and Nakiboğlu study the case treated in the first part of [21] (which is [23]) with no bandwidth constraints by Schalkwijk and Kailath where the authors aim to benefit from feedback using a linear encoding function in a discrete-time additive Gaussian noise channel (DAMGN) with perfect feedback. In [23], the authors build a coding scheme upon the Robbins-Monro stochastic approximation procedure and consequently come up with a result of that the error probability decreases faster than exponentially with signaling duration. In [22], the authors showed that the error probability can decrease with block length, say n, where the exponential order of the decay is a linear function of n besides introducing a new lower bound the error probability for the same problem.

The achievable schemes proposed and analyzed based on their asymptotic performances in this thesis are inspired by the transmission scheme for channels with perfect feedback using a blockwise decision by Yamamoto and Itoh [1] which in fact is the modified Schalkwijk-Barron scheme [24]. The original paper provides an error exponent for sequential feedback schemes [1] is applicable to both discrete memoryless channels and AWGN channels. The modification is made by replacing Viterbi's sequential decision feedback [25] by blockwise decision and a fixed length transmission. One round of transmission in both of the studies by Yamamoto-Itoh and Schalkwijk-Barron is composed by two phases which are called as the message mode, where the source message is transmitted and fed back, and the control mode where transmission of the control message and feedback occur. Although the latter shows the same performance with the original Schalkwijk-Barron scheme for the AWGN case, modified scheme outperforms [24] for the discrete memoryless channel.

1.2.2 Multiple Source Problem

An important generalization to the case of multiple sensing nodes with spatially-correlated information is as shown in Figure (1.4). In particular we are interested in the case where correlated random variables are transmitted over multiple-access channels, where the information of the sources are sent through an AWGN channel. The main issue is how to do the encoding with

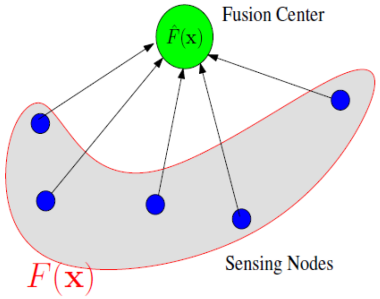

Figure 1.4: Multi-sensor Sampling and Transmission of a Random-Field

respect to the performance to be achieved upon reconstruction as a function of the required energy. The key element in the multi-sensor scenario being to exploit the correlation, which is assumed to be known, both at the transmitter and receiver. Moreover, we aim to determine the operating regimes for such a multiple-access system in terms of the role correlation plays in determining the energy efficiency.

The multiple source problem can be seen as the CEO (Central Estimating Officer) problem as named in the literature with some differences. The original problem is introduced and formulated in [26, 27] for a discrete-memoryless source X. As shown in Figure (1.5), the CEO in a sensor network is interested in the information of a source $\{X(t)\}_{t=1}^{\infty}$ which cannot be obtained directly thus the CEO uses L agents which observe a noisy version of the source independently. The agents send their observations, $Y_i(t) = X(t) + N_i(t)$, to the CEO which is subject to a finite sum rate constraint R. Here the Gaussian observation noise is denoted by $N_i(t)$ which is i.i.d. $\forall i = 1, \cdots, L$ and $t = 1, \cdots, n, \cdots$. The CEO tries to reconstruct $\{X(t)\}_{t=1}^{\infty}$ which results in $D(R)$, the distortion-rate function of the source $X(t)$. The authors in [27] determined the minimal error frequency asymptotically in both L and R. [28] studies a special case of the problem where they consider the source $\{X(t)\}_{t=1}^{\infty}$ as an i.i.d Gaussian random variable and show the asymptotic performance of the distortion as both L and R tend to infinity. There are many studies in the literature which address this problem in different settings. [29] discusses the problem in a multi-terminal source-channel communication system with correlated sources transmitted over a MAC without being subject to a channel noise and provides the rate-distortion region of the multi-terminal source coding. [30] can be given as yet another example which explores the CEO problem where the authors introduce the rate-region for the quadratic Gaussian case whereas in a quite recent paper [31] comes up with an upper bound on the rate-distortion region of the vector Gaussian CEO problem for the noisy observation case.

One of the main differences between the multiple source problem in the

way that is addressed in Chapter 4 of this thesis and several studies in the literature briefly mentioned above is that all the results obtained in Chapter 4 are considered in the context of zero-rate, i.e. vanishing rate. Another major difference can be stated as the focus on the transmission of unitary samples of the source message instead of doing sequential coding as already mentioned above in problem definition and will be highlighted in further chapters. Lastly, we combine the original CEO problem with a multiple-access channel and discuss the performance of a system with correlated analog sources over a GMAC with a feedback link from the receiver to each encoder as will be discussed in detail in Chapter 4.

With respect to the the multiple source scenarios, the authors in [32] and [33] derive a threshold signal-to-noise ratio (SNR) through the correlation between the sources so that below this threshold, minimum distortion is attained by uncoded transmission in a Gaussian multiple access channel with and without feedback, respectively. In these works, the authors consider transmission of a memoryless bi-variate normal source and the distortion can be characterized by two regimes as a function of the relationship between the channel SNR and the correlation between the sources. [32] the authors set a condition, which basically consists of upper bounds on the rate-distortion functions of each source and both sources jointly, in order to achieve distortion pair (D_1, D_2). Secondly, following [34–36] they prove the high-SNR distortion asymptotics (D_1^*, D_2^*) through source-channel separation which is given by for the symmetric case of $D_1^* = D_2^* = D^*(\sigma^2, \rho, P, N)$

$$\lim_{P/N\to\infty} \sqrt{P/N} D^*(\sigma^2, \rho, P, N) = \sigma^2 \sqrt{\frac{1-\rho^2}{4}}, \tag{1.3}$$

where $\rho \in [0, 1]$ with equal source variance σ^2 and equal power constraints on each source P with noise variance N. And finally, for the uncoded scheme the authors of [32] present the following result

$$D^*(\sigma^2, \rho, P, N) = \sigma^2 \frac{P(1-\rho^2)+N}{2P(1+\rho)+N}, \tag{1.4}$$

having an SNR not exceeding $\frac{\rho}{1-\rho^2}$. Note that, (1.4) is obtained through disregarding feedback since feedback is useful only above the given threshold of SNR for separate source-channel coding as shown in [37].

In a similar vein, [38, 39] approaches to the problem from the point of view of both the performance and required energy. The paper discusses the trade off between the energy the system consumes and the achieved distortion in transmitting source message(s) over channels subject to noise. That is done by defining an information theoretic function called energy-distortion function $E(D)$ which basically shows the required energy in order to attain a target distortion D without setting any constraints on the number of channel uses per source sample. It was shown that the separation based scheme

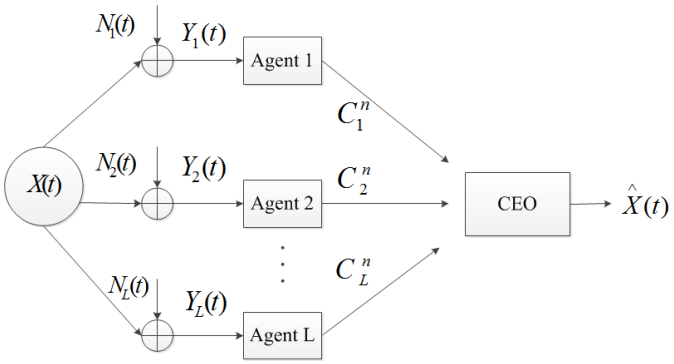

Figure 1.5: CEO Network configuration

is optimal for the point-to-point channel however it cannot be carried on to multiple-source problem with correlated sources. In particular, the authors consider the case with two correlated Gaussian sources which transmit their information over a GMAC with perfect feedback and derive a lower bound on $E(D)$ and an upper bound for Schalkwijk-Kailath (SK) scheme, which is shown to outperform the source-channel separation by numerical analysis. In [39, 40], to be able to reduce the consumed energy in a sensor network, the authors benefit from the feedback link to allow the sensors to cooperate with each other and again as in [38], no constraints are set on the number of the channel uses. The paper proves that the source and channel separation is optimal for a single sensor and shows that separation is no longer optimal for a system with multiple sensors thus the author come up with an upper and a lower-bound on their energy-distortion function $E(D)$. The two different schemes studied here are an uncoded SK and source-channel separation with unlimited bandwidth per source sample. For a system with multiple sensors without feedback, [41] has shown that the optimality of the uncoded transmission with respect to the trade off between the energy and distortion.

[42] is yet another example that studies transmitting two correlated Gaussian sources over a GMAC and aims at achieving the minimum possible distortion to recover the transmitted information. The authors use joint-source channel coding to estimate the linear functions of the two sources which are subject to average power constraints and provide a scheme based on lattice coding and lower-bounds on the reconstruction error in estimating the correlated source information through two different settings of this linear function. In the first case, which is inspired by [35, 43], the choice of the function allows to reduce the system two a parallel channel and goes around the dependence as turning it into a conditional independence among the two sources whereas the second setting allows collaboration between the transmitters. Besides the two lower bounds a lattice based coding scheme is

introduced and it was shown that for a high enough SNR, i.e. $SNR > 0.5$, for any linear function to be chosen the distortion can be made very close to the lower bound derived.

In one of the further chapters, in Chapter 4, we will show that the resulting MSE for the special case of a vector channel with a Gaussian input ([44, eq: 27]) meets our results of the lower bound derived on the reconstruction error of a single random vector measured by a network of sensors and multiple source vectors which are transmitted to a common receiver over a GMAC with a perfect causal feedback link to the encoder connected to each sensor. In [44], Guo et al. set the following relationship between the mutual information of the channel SNR and the minimum mean squared error (MMSE) in Gaussian channels for both scalar and vector input signals irrespective of its statistics.

$$\frac{\mathrm{d}}{\mathrm{dsnr}} I(\mathrm{snr}) = \frac{\mathrm{MMSE}(\mathrm{snr})}{2}. \tag{1.5}$$

Consider the simple case of a scalar channel with the pair of (X, Y) denoting the input and output signals through the following definition of $Y = \sqrt{\mathrm{snr}}X + N$ where snr is non-negative and the noise signal N is normally distributed with zero mean and unit variance. Thus the mutual information in (1.5) is basically $I(X;Y) = I(X; \sqrt{\mathrm{snr}}X + N)$ whereas the MMSE is defined by $\mathrm{MMSE}(\mathrm{snr}) = \mathrm{MMSE}(X|\sqrt{\mathrm{snr}}X + N)$.

Even though we focus all our attention to the systems with analog source information, it is worth mentioning of a system with discrete sources, in [45], a coding strategy based on separate source and channel coding is introduced for a network information flow with discrete correlated sources. In the described model, the authors set the conditions for which perfect reconstruction of the messages from the encoder nodes can be achieved.

1.3 Outline and Contributions

In the upcoming chapter, we introduce a two-way low-latency protocol for a single source transmitting analog information over a non-coherent AWGN channel. In spirit, this is very similar to the first phase of the 4G random-access procedure described above. The analytical exponential behavior of the protocol with respect to the reconstruction error for estimating the source-message is observed and discussed subject to the energy used by the protocol for different number of rounds. This is followed by the discussion regarding the effect of the feedback error on the distortion-energy trade-off made in subsection 2.1.2. Additionally, for the case of one-shot transmission without feedback, in subsection 2.1.3 we extend Merhav's recent lower-bounds derived in [13] for the problem addressed here, in order to provide the tightest numerical lower-bounds on performance. This is followed by numerical analysis for a more general wireless channel model in

Section 2.2. In subsection 2.2.1, we provide adaptations of Goblick's and Merhav's lower-bounds for the more general fading channel models. The numerical analysis results for a chosen configuration of the fading channel model are given in Section 2.3 together with the results of the non-coherent AWGN channel. The numerical results are also contrasted with the best-known theoretical lower-bounds on the reconstruction fidelity.

In Chapter 3, subsections 3.1.1 and 3.1.2, we describe the considered system model of the addressed problem for the dual-source case. In Section 3.2 of the same chapter, we proceed with introducing three different lower bounds on the reconstruction error of estimating the source vectors based on different ranges in which the correlation coefficient between the two sources is defined. In Section 3.3, we present new results which aim to show the benefit of feedback regarding optimality, yet with minimal latency through a two-way protocol and its asymptotic performance of reconstruction error is analyzed for two correlated continuous sources. In the final Section 3.4 of this chapter, we present numerical results to discuss the analytical outcomes obtained in Sections 3.2 and 3.3. The derivations of the lower bounds and the distortion terms from the achievable scheme are given in detail in Appendix 6.2.

Following the single and dual-source cases, Chapter 4 treats the most general problem of a network of sensors measuring a single normally or uniformly-distributed finite-dimensional vector which is after transmitted to a mutual receiver over an additive white Gaussian noise asynchronous multiple-access channel. In Section 4.1, we give a description of the general model to explain the problem addressed. It is followed by the derivation of the information-theoretic lower bounds on the reconstruction error in estimating both the single vector and its combination with the observation noise. In Section 4.4, we provide an M-sensor adaptation of Yamamoto's protocol [1] for a uniformly-distributed source with uniform observation error along with the analysis of its asymptotic performance. In Section 4.5, we present the numerical results for a slightly different protocol and the lower bounds derived in 4.2. Chapter 5 consists of the comparisons between the obtained results for each case in the previous chapters 2, 3 and 4 and the conclusions drawn upon them.

Chapter 2

Point-to-point channel

The main contribution of this chapter is to analyze the use of a retransmission protocol for the transmission of scalar quantized analog samples in terms of the energy-efficiency as a function of the reconstruction fidelity. It is shown that there is a very significant benefit at the expense of two-way exchanges in comparison to a one-shot transmission of the parameter. The efficient use of such a protocol calls for joint optimization of the parameter quantization and modulation. It is important to note that in our scenario we are driven to assume unknown channels (i.e. non-coherent reception) in the formulation of the problem. Since the information content is very small, additional overhead for channel estimation is not warranted and thus, it is unreasonable to assume the channel state (i.e. channel amplitude and phase) be known to either the transmitter or receiver. In what follows, simplifying steps in the derivation of lower-bounds will result in equivalent formulations for known channels, however the proposed schemes will not make use of channel state information at either end of the transmission chain. The analysis is carried out for line-of-sight and non line-of-sight channels and we consider both the case of perfect and imperfect feedback. We furthermore provide new lower-bounds on the performance of such feedback-based schemes as well as numerical evaluation of recent bounds [13] for one-shot transmission. These bounds allow us to assess how close the proposed schemes are to fundamental limits.

In the upcoming section, we introduce a two-way low-latency protocol for a single source transmitting analog information over a non-coherent AWGN channel. In spirit, this is very similar to the first phase of the 4G random-access procedure described above. The analytical exponential behavior of the protocol with respect to the reconstruction error for estimating

the source-message is observed and discussed subject to the energy used by the protocol for different number of rounds. This is followed by the discussion regarding the effect of the feedback error on the distortion-energy trade-off made in subsection 2.1.2. Additionally, for the case of one-shot transmission without feedback, in subsection 2.1.3 we extend Merhav's recent lower-bounds derived in [13] for the problem addressed here, in order to provide the tightest numerical lower-bounds on performance. This is followed by numerical analysis for a more general wireless channel model in Section 2.2. In subsection 2.2.1, we provide adaptations of Goblick's and Merhav's lower-bounds for the more general fading channel models. The numerical analysis results for a chosen configuration of the fading channel model are given in Section 2.3 together with the results of the non-coherent AWGN channel from Section 2.1. The numerical results are also contrasted with the best-known theoretical lower-bounds on the reconstruction fidelity.

2.1 Asymptotic Performance of a Novel Two-Way Protocol

Let us consider now a protocol applied to the transmission of isolated analog samples with non-coherent reception. This will serve as a motivating example for the use of feedback with low-latency achieving asymptotically near-optimal distortion performance. In the analysis, we first focus on a simple non-coherent AWGN channel with a one dimensional source letter.

The protocol consists of two phases, a data phase and a control phase. In our adaptation the two phases compose one round of the protocol. A source sample quantized to B bits is encoded into one of 2^B N-dimensional messages $\mathbf{S}_m$, with $m = 1, 2, \cdots, 2^B$ and each message is transmitted with equal energy $\sqrt{\mathcal{E}_{\mathrm{D},i}}$, where $\mathcal{E}_{\mathrm{D},i}$ denotes the energy of the data phase on the i^{th} round. Upon reception, the receiver computes the maximum-likelihood message, $\hat{m}(\mathbf{Y}_D)$, based on the N-dimensional observation

$$\mathbf{Y}_D = \sqrt{\mathcal{E}_{\mathrm{D},i}} \mathrm{e}^{j\Phi_i} \mathbf{S}_m + \mathbf{Z} \tag{2.1}$$

where the subscript D represents the data phase of the protocol. The random phase sequence ϕ_i is assumed to be i.i.d. with uniform distribution on $[0, 2\pi)$. The N-dimensional vector noise sequence z_i is complex, circularly symmetric, has zero-mean and autocorrelation $N_0\mathbf{I}_{N\times N}$.

This type of transmission can exactly model any low-rate transmission strategy based on orthogonal modulation. For instance, to further put this in the context of the random-access procedure 4G-LTE systems, the $\mathbf{S}_m$ can represent the so-called *PRACH preamble* [46], where $m = 0, 1, \cdots, 63$, and conveys the 6-bit message (MSG1) described in Section 1.1. The preamble in 4G-LTE is a Zadoff-Chu roots-of-unity sequence which usually occupies $N =$

839 signaling dimensions for $B = 6$ information bits. Orthogonality over time-dispersive channels is guaranteed through up to 64 cyclic time-shifts of $\mathbf{S}_m$ coupled with the use of a cyclic extension. For very dispersive channels (i.e. with delay-spreads longer than the cyclic-shift between preambles), fewer than 64 (and hence longer) cyclic time-shifts can be used at the expense of using multiple preamble sequences which are quasi-orthogonal.

After the first data phase, the receiver feeds $\hat{m}$ back to the encoder via the noiseless feedback link. Let the corresponding error event be denoted E_i. After the data phase, the encoder enters the control phase and informs the receiver whether or not its decision was correct via a signal $\sqrt{\mathcal{E}_{\mathrm{C},i}}\mathbf{S}_c$ of energy $\sqrt{\mathcal{E}_{\mathrm{C},i}}$ if the decision is incorrect and $\mathbf{0}$ if the decision was correct. $\mathcal{E}_{\mathrm{C},i}$ here denotes the energy of the control phase in the i^{th} round. During the control phase the receiver observes $\mathbf{Y}_C$. Let $y_C = \mathbf{Y_C}^H\mathbf{S}_C$ and assume a detector of the form $\mathrm{e} = \mathcal{I}\left(|y_C|^2 > \lambda\mathcal{E}_{\mathrm{C},i}\right)$ where $\mathcal{I}(\cdot)$ is the indicator function and λ is a threshold to be optimized and included within the interval $[0, 1)$. $E_{\mathrm{e}\to\mathrm{c},i}$ corresponds to an uncorrectable error since it acknowledges an error as correct decoding and $E_{\mathrm{c}\to\mathrm{e},i}$ represents a mis-detected acknowledged error declaring correct decoding as incorrect. If the receiver correctly decodes the control signal and it signals that the data phase was correct after the completion of the first round, with probability $\Pr(E_1^c)(1 - \Pr(E_{\mathrm{c}\to\mathrm{e},1}))$, the protocol halts, otherwise another identical round is initiated by the receiver. The retransmission probability, i.e. the probability of going on for a second round, is $\Pr(E_1)(1-\Pr(E_{\mathrm{e}\to\mathrm{c},1}))$. This on-off signaling guarantees that with probability $\Pr(E_1^c)(1 - \Pr(E_{\mathrm{c}\to\mathrm{e},1}))$ the transmitter will not expend more than $\mathcal{E}_{\mathrm{D},1}$ joules, which should be close to one. After each data phase, the receiver computes the ML or MAP message $\hat{m}_i(\mathbf{Y}_1, \cdots, \mathbf{Y}_i)$ based on all observations up to round i with error event E_i. The same control phase is repeated and the protocol is terminated after two rounds. The reconstruction error of the source message is obtained by calculating the mean squared error distortion through $D = D_q(1 - P_e) + D_eP_e$ which can be bounded further for a uniform source U on $(-\sqrt{3}, \sqrt{3})$ (i.e. a source with zero mean and unit variance) by

$$D\left(\mathcal{E}, N_0, N, \lambda\right) \leq 2^{-2B}(1 - P_e) + 2P_e \tag{2.2}$$

where P_e is the total probability of error, D_q represents the distortion caused by the quantization process and D_e corresponds to the MSE distortion for the case where an error was made. The error probability at the end of second round is defined and consequently bounded by

$$\begin{aligned} P_{\mathrm{e}} &= \Pr(E_1)\Pr(E_{\mathrm{e}\to\mathrm{c},1}) + \Pr(E_1)(1 - \Pr(E_{\mathrm{e}\to\mathrm{c},1}))\Pr(E_2|E_1) \\ &\quad + (1 - \Pr(E_1))\Pr(E_{\mathrm{c}\to\mathrm{e},1})\Pr(E_2|E_1^c) \\ &\overset{(a)}{\leq} \Pr(E_1)\Pr(E_{\mathrm{e}\to\mathrm{c},1}) + \Pr(E_2). \end{aligned} \tag{2.3}$$

In step (a) the conclusive expression is obtained through bounding $\Pr(E_{\mathrm{c}\to\mathrm{e},1})$ and $(1-\Pr(E_{\mathrm{e}\to\mathrm{c},1}))$ by 1. The probability of an uncorrectable error in round i, which is defined as $\Pr\left(|\sqrt{\mathcal{E}_{\mathrm{C},i}}+z_c|^2 \leq \lambda\mathcal{E}_{\mathrm{C},i}\right)$, is obtained as

$$\Pr(E_{\mathrm{e}\to\mathrm{c},i}) = 1 - \mathrm{Q}_1\left(\sqrt{\frac{2\mathcal{E}_{\mathrm{C},i}}{N_0}}, \sqrt{\frac{2\lambda\mathcal{E}_{\mathrm{C},i}}{N_0}}\right), \tag{2.4}$$

where $\mathrm{Q}_1(\alpha,\beta)$ is the first-order Marcum-Q function and $z_C = \mathbf{S}_C^H\mathbf{Z}$ is a circularly-symmetric Gaussian zero-mean random variable with variance N_0. Furthermore, we have the recent bound on the $\mathrm{Q}_1(\alpha,\beta)$ for $\alpha > \beta$ from [47, eq:4] which is very useful for bounding (2.4) as

$$\Pr(E_{\mathrm{e}\to\mathrm{c},i}) \leq 1/2\exp\left(-\frac{(\sqrt{\lambda}-1)^2\mathcal{E}_{\mathrm{C},i}}{N_0}\right). \tag{2.5}$$

The probability of a mis-detected acknowledged error is obtained as

$$\begin{aligned}\Pr(E_{\mathrm{c}\to\mathrm{e},i}) &= \Pr\left(|z_C|^2 > \lambda\mathcal{E}_{\mathrm{C},i}\right)\\ &= \mathrm{e}^{-\frac{\lambda\mathcal{E}_{\mathrm{C},i}}{N_0}}.\end{aligned} \tag{2.6}$$

Lastly, the probability of making an error on a particular round j, $\Pr(E_j) \leq 2^B P_2(j)$ can be derived using [48, eq:12.1-24]

$$P_2(j) \leq \frac{1}{2^{2j-1}} e^{-\gamma/2} \sum_{n=0}^{j-1} c_n \left(\frac{\gamma}{2}\right)^n \tag{2.7}$$

where $c_n = 1/n! \sum_{k=0}^{j-1-n} \binom{2j-1}{k}$ and γ represents the signal to noise ratio.

The average energy used by the protocol after two rounds is

$$\mathcal{E} = \mathcal{E}_{\mathrm{D},1} + \Pr(E_1)\left(\mathcal{E}_{\mathrm{C},1} + \mathcal{E}_{\mathrm{D},2}\right). \tag{2.8}$$

$\mathcal{E}_{\mathrm{D},2}$ here denotes the required energy for retransmission, which is the energy to be used in the data phase of the second round. Clearly if $\Pr(E_1)$ is small, then the protocol achieves marginally more than $\mathcal{E}_{\mathrm{D},1}$ joules per source symbol.

The detection rule is given using [48, Chapter 12, eq:12.1-16] considering the two possible decision variables assuming (k) is transmitted as $U_k = |\sqrt{\mathcal{E}_{D,1}}+N_k|^2$ $U_{k'} = |N_{k'}|^2$ where $U_k = |\langle \mathbf{Y}_1, \mathbf{S}_{m_k}\rangle|^2$. An error is committed if $U_{k'}$ is greater than U_k. The union bound on $P_e(k)$ is defined as

$$P_e(k) \leq \sum_{(k')\neq(k)} \Pr\left(u_k < u_{k'}|(k)\right) \tag{2.9}$$

The conditional probability of $U_k < U_{k'}$ given (k) is transmitted becomes for the first round

$$\Pr(U_k < U_{k'}|k) = \Pr(U_k < U_{k'}) = \Pr(|\sqrt{\mathcal{E}_{D,1}} + N_k|^2 < |N_{k'}|^2) \tag{2.10}$$

whereas for the second round, we have cumulatively the following probability

$$\begin{aligned}\Pr(U_k < U_{k'}|k) &= \Pr(U_k < U_{k'}) \\ &= \Pr(|\sqrt{\mathcal{E}_{D,1}} + N_{k,1}|^2 + |\sqrt{\mathcal{E}_{D,2}} + N_{k,2}|^2 < |N_{k',1}|^2 + |N_{k',2}|^2)\end{aligned} \tag{2.11}$$

Bounds on the error probabilities of both rounds are attained through (2.7) and given by

$$\Pr(E_1) \leq 2^{B-1} \mathrm{e}^{-\frac{\mathcal{E}_{\mathrm{D},1}}{2N_0}}, \tag{2.12}$$

$$\Pr(E_2) \leq 2^{B-3} \left(1 + 3\frac{\mathcal{E}_{\mathrm{D},1} + \mathcal{E}_{\mathrm{D},2}}{N_0}\right) \mathrm{e}^{-\frac{\mathcal{E}_{\mathrm{D},1}+\mathcal{E}_{\mathrm{D},2}}{2N_0}} \tag{2.13}$$

where (2.12) corresponds to (2.10) which is equivalent to $P_2(1)$ and (2.13) is obtained through (2.11) equivalently by $P_2(2)$.

For the case of $N = 1$, i.e. the protocol terminates without retransmission, we obtain the bound on the reconstruction error in estimating U as given in the following. The error probability defined by (2.3) consists of the probability of making an error in the first round $\Pr(E_1)$ solely, since there is no use of the control phase given that there will not be a second round to retransmit the message. Thus, through substitution of $P_e \leq 2^{B-1}\mathrm{e}^{-\frac{\mathcal{E}_{\mathrm{D},1}}{2N_0}}$ into the distortion (2.2), we get the following bound

$$D\left(\mathcal{E}, N_0, 1, \lambda\right) \leq \mathrm{e}^{-2B\ln 2} + \mathrm{e}^{B\ln 2 - \frac{\mathcal{E}_{\mathrm{D},1}}{2N_0}}. \tag{2.14}$$

By setting the two exponentials in (2.14) equal, it can be seen that 2^{-B} is in the same order of $\mathrm{e}^{-\frac{\mathcal{E}_{\mathrm{D},1}}{6N_0}}$. In other words, the upper bound (2.14) is obtained as $D\left(\mathcal{E}, N_0, 1, \lambda\right) \leq 2\mathrm{e}^{-\frac{\mathcal{E}_{\mathrm{D},1}}{3N_0}}$ for a single round. In the same way, for $N = 2$ the resulting distortion is bounded by

$$\begin{aligned}D\left(\mathcal{E}, N_0, 2, \lambda\right) \leq\ & \mathrm{e}^{-2B\ln 2} + \mathrm{e}^{(B-1)\ln 2 - \frac{\mathcal{E}_{\mathrm{D},1}}{2N_0} - \left(1+\lambda-2\sqrt{\lambda}\right)\frac{\mathcal{E}_{\mathrm{C},1}}{N_0}} \\ &+ \left(1 + 3\frac{\mathcal{E}_{\mathrm{D},1} + \mathcal{E}_{\mathrm{D},2}}{N_0}\right) \mathrm{e}^{(B-2)\ln 2 - \frac{\mathcal{E}_{\mathrm{D},1}+\mathcal{E}_{\mathrm{D},2}}{2N_0}}\end{aligned} \tag{2.15}$$

through substituting (2.3) with (2.12), (2.13) and (2.5) for $i = 1$ into the distortion (2.2). By equating the three exponentials of (2.15) we have that $\mathcal{E}_{\mathrm{C},1} = \frac{\mathcal{E}_{\mathrm{D},2}}{2(1+\lambda-2\sqrt{\lambda})}$. In order for $\Pr(E_1)$ to be exponentially bounded away from zero so that $\mathcal{E}$ can be made arbitrarily close to $\mathcal{E}_{\mathrm{D},1}$, we define $\mathcal{E}_{D,2} =$

$(2-\mu)\mathcal{E}_{D,1}$ where μ is an arbitrary constant satisfying $\mu \in (0,2)$. Finally, we obtain the bound on the distortion at the end of the second round as given by

$$D\left(\mathcal{E}, N_0, 2, \lambda\right) \leq \mathrm{e}^{-\frac{\mathcal{E}_{\mathrm{D},1}(1-\mu/3)}{N_0}} \left(3 + 3\frac{\mathcal{E}_{\mathrm{D},1} + \mathcal{E}_{\mathrm{D},2}}{N_0}\right). \tag{2.16}$$

Note that, at the end of the second round, 2^{-B} is in the same order of $\mathrm{e}^{-\frac{\mathcal{E}_{\mathrm{D},1}(1-\mu/3)}{2N_0}}$.

It is worth mentioning that (1.1) and the limiting expression in [19, eq.15] is achieved to within a factor of 1/2 in the energy using only two rounds and, moreover, with non-coherent reception. Even though it is possible to obtain $\exp\{-\frac{2\mathcal{E}_{\mathrm{D},1}}{N_0}\}$ (i.e. twice better than the performance in (2.16)) by changing the relationship between the energies used in the different rounds, this causes the average energy used by the protocol to exceed $\mathcal{E}_{\mathrm{D},1}$, the energy used in the data phase of the first round. In other words, going on to further rounds cannot provide asymptotically better results in terms of distortion unless the energy used by the protocol is increased. This result is analytically proved in the following subsection 2.1.1 and will be supported through numerical evaluation of the above bounds in Section 2.3. Closing the gap with (1.1) using non-coherent reception is, therefore, still open and a subject of our current effort. In Section 2.1.2, we investigate the case when the feedback link from the decoder to the encoder is not perfect and discuss the effect of a possible error in feedback on the exponential behavior of the reconstruction error. Note that, for modeling systems where both the transmitter and receiver are subject to the constraints on energy usage, one would have to consider the energy consumption of the feedback link, and we also shed some light on this issue in 2.1.2.

2.1.1 Third round and after

Assume that the protocol is not terminated after the second round, so it goes on one more round to do another retransmission. Hereafter, we will show that the asymptotic performance (2.16) achieved in two rounds cannot be improved unless the average energy the protocol consumes is increased. The probability of error for $N = 3$ can be simply bounded as in (2.3)

$$P_{\mathrm{e}}^{(3)} \leq \sum_{i=1}^{2} \Pr(E_i) \Pr(E_{\mathrm{e}\to\mathrm{c},i}) + \Pr(E_3) \tag{2.17}$$

with

$$\Pr(E_3) \leq 2^{B-5}\mathrm{e}^{-\frac{\mathcal{E}_{\mathrm{D},1}+\mathcal{E}_{\mathrm{D},2}+\mathcal{E}_{\mathrm{D},3}}{2N_0}} \left(16 + 6\frac{\mathcal{E}_{\mathrm{D},1} + \mathcal{E}_{\mathrm{D},2} + \mathcal{E}_{\mathrm{D},2}}{N_0} + 1/2\left(\frac{\mathcal{E}_{\mathrm{D},1} + \mathcal{E}_{\mathrm{D},2} + \mathcal{E}_{\mathrm{D},2}}{N_0}\right)^2\right) \tag{2.18}$$

which is equivalent to $P_2(3)$ representing the cumulative error probability at the end of the third round where $\mathcal{E}_{\mathrm{D},3}$ denotes the energy used in the corresponding round. The uncorrectable error in one round is independent of the uncorrectable error in another round, so that (2.5) can be used also for the second round with $\mathcal{E}_{\mathrm{C},2}$. The distortion at the end of third round is bounded as

$$D\left(\mathcal{E}, N_0, 3, \lambda\right) \leq K_1 \mathrm{e}^{-2B\ln 2} + K_2 \mathrm{e}^{(B+1)\ln 2 - \frac{\mathcal{E}_{\mathrm{D},1}+2\left(1-\sqrt{\lambda}\right)^2\mathcal{E}_{\mathrm{C},1}}{2N_0}} + K_3 \mathrm{e}^{(B-1)\ln 2 - \frac{\mathcal{E}_{\mathrm{D},1}+\mathcal{E}_{\mathrm{D},2}+2\left(1-\sqrt{\lambda}\right)^2\mathcal{E}_{\mathrm{C},2}}{2N_0}} + K_4 \mathrm{e}^{(B-3)\ln 2 - \frac{\mathcal{E}_{\mathrm{D},1}+\mathcal{E}_{\mathrm{D},2}+\mathcal{E}_{\mathrm{D},3}}{2N_0}} \tag{2.19}$$

where $K_4 = O((\mathcal{E}_{\mathrm{D},1} + \mathcal{E}_{\mathrm{D},2})^2)$. By equating the coefficients in the four exponentials of (2.19), we obtain the following relationships between the energies $\mathcal{E}_{\mathrm{D},2} = \mathcal{E}_{\mathrm{D},3} = \mathcal{E}_{\mathrm{C},2} 2(1-\sqrt{\lambda})^2$ and $\mathcal{E}_{\mathrm{C},1} = 2\mathcal{E}_{\mathrm{C},2}$. The final form of the upper bound on the distortion level at the end of the third round becomes

$$D\left(\mathcal{E}, N_0, 3\right) \leq K_{D_3} \mathrm{e}^{-\frac{\mathcal{E}_{\mathrm{D},1}(1-2\mu_2/3)}{N_0}} \tag{2.20}$$

where we defined $\mathcal{E}_{\mathrm{D},2} = \mathcal{E}_{\mathrm{D},3} = (1-\mu_2)\mathcal{E}_{\mathrm{D},1}$ to assure the average energy used by protocol for three rounds to be arbitrarily close to the energy only in the first round. μ_2 is an arbitrary constant satisfying $\mu_2 \in (0,1)$. This result proves that the asymptotic performance achieved in two rounds cannot be improved with more rounds.

2.1.2 The case of imperfect feedback

One might consider the case of an imperfect feedback link in the system described and analyzed above. Let $P_{\mathrm{fb},1}$ denote the following error probability $\Pr(\hat{\hat{m}} = m | \hat{m} \neq m)$ whereas $P_{\mathrm{fb},2} = \Pr(\hat{\hat{m}} \neq m | \hat{m} = m)$. Here m denotes the transmitted message, $\hat{m}$ and $\hat{\hat{m}}$ denote the messages decoded at the receiver and transmitter (after the feedback phase) respectively. The overall energy used by the protocol in this scenario becomes

$$\mathcal{E} = \mathcal{E}_{\mathrm{D},1} + \mathcal{E}_{\mathrm{C},1} \Pr(E_1)\left(1 - P_{\mathrm{fb},1}\right) + \mathcal{E}_{\mathrm{D},2}\left[\Pr(E_1)(1 - P_{\mathrm{fb},1}) + \left(1 - \Pr(E_1)\right) P_{\mathrm{fb},2}\right] \tag{2.21}$$

whereas the error probability at the end of the second round yields

$$\begin{aligned} P_{\mathrm{e}} = {} & \Pr(E_1)(1 - P_{\mathrm{fb},1}) \Pr(E_{\mathrm{e}\to\mathrm{c},1}) + \Pr(E_1) P_{\mathrm{fb},1} \\ & + \Pr(E_1)(1 - P_{\mathrm{fb},1})(1 - \Pr(E_{\mathrm{e}\to\mathrm{c},1})) \Pr(E_2 | E_1) \\ & + (1 - \Pr(E_1))(1 - P_{\mathrm{fb},2}) \Pr(E_{\mathrm{c}\to\mathrm{e},1}) \Pr(E_2 | E_1^c) \\ & + (1 - \Pr(E_1)) P_{\mathrm{fb},2}(1 - \Pr(E_{\mathrm{e}\to\mathrm{c},1}) \Pr(E_2 | E_1^c) \\ & \overset{(a)}{\leq} \Pr(E_1)\left(\Pr(E_{\mathrm{e}\to\mathrm{c},1}) + P_{\mathrm{fb},1}\right) + \Pr(E_2). \end{aligned} \tag{2.22}$$

In step (a), $(1-P_{\text{fb},1})$, $(1-\Pr(E_{\text{e}\to\text{c},1}))$ and $\Pr(E_{\text{c}\to\text{e},1})$ is upper bounded by 1. Clearly, if $P_{\text{fb},1} = P_{\text{fb},2} = 0$ this case boils down to the perfect feedback scenario studied above and the expressions on average energy (2.21) and error probability (2.22) given above yield (2.8) and (2.3), respectively. Now, we apply the modified error probability given above to the overall distortion term (2.2). In order to obtain the same exponential behavior of $e^{-\mathcal{E}_{\text{D},1}/N_0}$ like in (2.16), $P_{\text{fb},1}$ should be upper-bounded by the uncorrectable error $\frac{1}{2}\exp\left\{-\frac{(\sqrt{\lambda}-1)^2\mathcal{E}_{C,1}}{N_0}\right\}$ given earlier by (2.4). With respect to the energy consumption, we can say that in addition to the error probability in the first round, vanishing $P_{\text{fb},2}$ guarantees the energy consumed by two rounds of the protocol to be upper bounded by the energy which is used by the data phase of the first round.

In order to characterize the amount energy required for feedback we consider an explicit scheme for feedback. The receiver uses waveform $\mathbf{S}_{\hat{m}}$ on the feedback link with energy $\mathcal{E}_{\text{fb}}$ so that the received signal is

$$\mathbf{Y}_{\text{fb}} = \sqrt{\mathcal{E}_{\text{fb}}}e^{j\Phi}\mathbf{S}_{\hat{m}} + \mathbf{Z} \tag{2.23}$$

In order to determine if message m was received correctly, the transmitter projects on waveform $\mathbf{S}_m$ and computes the statistic $U = |\langle \mathbf{Y}_{\text{fb}}, \mathbf{S}_m|^2$ which is compared to a threshold $\lambda_{\text{fb}}\mathcal{E}_{\text{fb}}$. The important feedback probability is then

$$P_{\text{fb},1} = \Pr\left(|\langle \mathbf{Y}_{\text{fb}}, \mathbf{S}_m\rangle|^2 \geq \lambda_{\text{fb}}\mathcal{E}_{\text{fb}}\right) = e^{-\frac{\lambda_{\text{fb}}\mathcal{E}_{\text{fb}}}{N_0}}. \tag{2.24}$$

As a result, in order for $P_{\text{fb},1}$ to be on the same exponential order as $\Pr(E_{\text{e}\to\text{c},1})$ we require that $\mathcal{E}_{\text{fb}} = \frac{1-\mu/2}{\lambda_{\text{fb}}}\mathcal{E}_{d,1}$ and that the energy used by the protocol approaches $\frac{\lambda_{\text{fb}}+1-\mu/2}{\lambda_{\text{fb}}}\mathcal{E}_{d,1}$. The main conclusion is that when we account for the energy consumption required by the feedback link, it reduces the reconstruction fidelity in a non-negligible manner under a total energy constraint. In the primary application scenario considered here, namely energy-constrained sensors transmitting to cellular basestations, we believe that this does not pose a significant problem. Basestations are power constrained and not short-term energy constrained and if the aggregate downlink traffic dedicated to feedback for sensors is an order of magnitude less than other downlink services, this energy consumption is insigificant. If such schemes were to be used for transmission between energy-constrained devices, the benefits may be significantly reduced.

2.1.3 Lower-bounds on Distortion

The first set of bounds all rely on channel state knowledge at the receiving end which clearly is also a bound for the case where the channel phases are unknown. The simplest bound is Goblick's bound which in our case of a

uniform random variable on $[-\sqrt{3},\sqrt{3})$ is given by

$$D_G(\mathcal{E},N_0) \geq \frac{6}{\pi e} e^{-\frac{2\mathcal{E}}{N_0}}. \tag{2.25}$$

For the case of a single round without feedback we use the recent bounds from Merhav in [13] which are adaptations of the Ziv-Zakai lower-bound [16] on mean-squared error for parameter modulation-estimation. We consider only the case of zero-rate transmission in the context of [13] and adapt the results to the normalized uniform distribution considered here. We have the following bound on the distribution of distortion

$$\Pr\left(|U-\hat{U}| > \frac{\sqrt{3}}{M}\right) \geq \frac{\sqrt{3}}{M} Q\left(\sqrt{\frac{\mathcal{E}}{N_0}\frac{M}{M-2}}\right). \tag{2.26}$$

The right-hand side of (2.26) is the weakest version of Shannon's lower-bound on M-ary transmission over an AWGN channel [49, eq. 82]. Through the use of the Chebyshev inequality, this results in the following lower-bound on the distortion

$$D_{M1}(\mathcal{E},N_0) \geq \max_M \frac{3\sqrt{3}}{M^3} Q\left(\sqrt{\frac{\mathcal{E}}{N_0}\frac{M}{M-2}}\right). \tag{2.27}$$

A tighter version makes use of Shannon's best bound [49, eq. 81] yielding

$$D_{M2}(\mathcal{E},N_0) \geq \max_M \frac{6\sqrt{3}}{M^4} \sum_{n=2}^{M} Q\left(\sqrt{\frac{\mathcal{E}}{N_0}\frac{n}{n-1}}\right). \tag{2.28}$$

As suggested in [13, eq.23] an even tighter version based on [49, eq. 81] is derived using

$$\begin{aligned} D_{M3}(\mathcal{E},M,N_0) &= 2\int_0^{2\sqrt{3}} d\Delta\cdot\Delta(2\sqrt{3}-(\lfloor 2\sqrt{3}/\Delta\rfloor-1)\Delta)\cdot\Pr\left(|U-\hat{U}|>\Delta\right) \\ &\geq 2\left(\int_0^{\sqrt{3}/M} d\Delta\cdot\Delta(2\sqrt{3}-(M-1)\Delta)\Pr\left(|U-\hat{U}|>\sqrt{3}/M\right)\right. \\ &\left.+\sum_{i=3}^{M}\int_{\sqrt{3}/i}^{\sqrt{3}/(i-1)} d\Delta\cdot\Delta(2\sqrt{3}-(i-1)\Delta)\Pr\left(|U-\hat{U}|>\sqrt{3}/(i-1)\right)\right) \\ &= \frac{\sqrt{3}}{M^4}(5M+1)\sum_{n=2}^{M} Q\left(\sqrt{\frac{\mathcal{E}}{N_0}\frac{n}{n-1}}\right) \\ &+\sqrt{3}\sum_{i=2}^{M-1}\left(\frac{5i-4}{(i-1)^4}-\frac{5i+1}{i^4}\right)\sum_{n=2}^{i} Q\left(\sqrt{\frac{\mathcal{E}}{N_0}\frac{n}{n-1}}\right) \end{aligned} \tag{2.29}$$

for any suitably large M. All bounds are plotted in comparison to the proposed transmission strategies in Section 2.3.

Relationships with classical conjectures on optimal signal sets

It is worth pointing out that certain classical and more recent results on the validity of conjectures on optimal signal sets are strongly related to the problem at hand and could provide tighter numerical lower-bounds on the reconstruction fidelity. In Merhav's bounding technique for the parameter modulation-estimation problem he relies on zero-rate lower-bounds on the probability of error (e.g. in [13, eq. 21]) in characterizing the tail-function of the estimation error at discrete values of its argument. For coherent detection on AWGN channels, it was long conjectured that the regular simplex was an optimal signal set for M-ary signaling in $M-1$ dimensions (i.e. without a bandwidth constraint). This was disproved by Steiner in [50] for the so-called *Strong Simplex Conjecture* which corresponds to the average energy constraint used here. The so-called *Weak Simplex Conjecture* is the classical conjecture [51] for equal-energy signaling which still has not been disproved and is valid for $M = 2, 3$. It is largely considered to be true for all M, and from a numerical perspective, was shown to be valid for $M \leq 8$ in [52]. From a numerical perspective, the use of the constructive techniques in [52] for finding optimal signal sets could be used instead of Shannon's lower bound in (2.29). Although this will not provide an asymptotic difference, it could lead to tighter bounds for low signal-to-noise ratios. For the equal-energy case, it may be sufficient to use the error probability of the regular simplex in (2.29), at least if we limit the sum to $M \leq 8$. Even if the Weak Simplex Conjecture is false, it is highly unlikely that any other signal set will provide a noticeable numerical difference in (2.29).

The equivalent equal-energy conjecture for non-coherent detection [53] also remains unproven. But it is reasonable for numerical purposes to use the error probability of orthogonal modulation with non-coherent detection as an approximate lower-bound. Using [53, eq. 28] instead of Shannon's lower bound in (2.29) we obtain

$$D_{M4}(\mathcal{E}, M, N_0) \geq \frac{\sqrt{3}}{M^3}(5M+1)P_M + \sqrt{3}\sum_{i=2}^{M-1}\left(\frac{5i-4}{(i-1)^3} - \frac{5i+1}{i^3}\right)P_i \tag{2.30}$$

where

$$P_i = \sum_{n=1}^{i-1}(-1)^{n+1}\binom{i-1}{n}\frac{1}{n+1}\exp\left[-\frac{n}{n+1}\frac{\mathcal{E}}{N_0}\right] \tag{2.31}$$

which, strictly speaking, is only a true bound for equal-energy signaling and $M = 2$, subject to the validity of the classical conjecture. Note that (2.30) will have the same asymptotic behavior as (2.29).

Comments on variable-energy signaling

It is reasonable to expect that the use of variable-energy signaling (even orthogonal) can help close the 1.76dB asymptotic gap between (2.14) and (2.29) and the 3dB gap between (2.15) and (2.25). This is because with equal-energy signaling, erroneous decisions can lead to distortions at the peak or on the order of a bit with equal probability. A more judicious choice of energy distribution across the signal set would choose the energy difference between points according to their pairwise distortion. High distortion error events would then be less likely than low distortion error events.

2.2 More General Wireless Channels

Consider a general multi-channel wireless model instead of the AWGN channel studied in Section 2.1 where the channel amplitude and phase correspond to that of a multi-dimensional Ricean channel with a ratio of the non-line-of-sight amplitude total signal amplitude α. Let L be the total number of statistically independent observations or diversity order of the transmitted signals and let $L' \leq L$ be the number of observations over which the average received energy is spread. To a first-order approximation, L' represents the number of coherence bandwidths and L/L' would represent the number of receive antennas. For example, $L = 4$, $L' = 2$ would correspond to a dual-antenna receiver with two coherence bandwidths. In this case the output signal in the data phase of round i on channel l (generalizing (2.1)) becomes

$$\mathbf{Y}'_{d,l} = \sqrt{\mathcal{E}_{\mathrm{D},i}/L'}\left(\sqrt{(1-\alpha)}\mathrm{e}^{j\Phi_{i,l}} + \sqrt{\alpha}h_{i,l}\right)\mathbf{S}_m + \mathbf{Z}_l, l = 0, \cdots, L-1 \tag{2.32}$$

where $\mathrm{h_i} \sim N_{\mathbf{C}}(0,1)$ and α is a constant defined in the range $[0,1]$.

For this channel model, only the statistics of the mis-detected acknowledged error event is unchanged and is as given by (2.6). The probability of an uncorrectable error becomes

$$\begin{aligned}
&\Pr(E_{\mathrm{e}\to\mathrm{c},i}) \\
&= \Pr\left(\sum_{l=0}^{L-1} |\sqrt{(1-\alpha)\mathcal{E}_{\mathrm{C},i}/L'}\mathrm{e}^{j\Phi_{i,l}} + \sqrt{\alpha\mathcal{E}_{\mathrm{C},i}/L'}h_{i,l} + z_{c,l}|^2 \leq \lambda L\mathcal{E}_{\mathrm{C},i/L'}\right) \\
&= 1 - \mathrm{Q}_L\left(\sqrt{\frac{2L(1-\alpha)\mathcal{E}_{\mathrm{C},i}}{\alpha\mathcal{E}_{\mathrm{C},i} + L'N_0}}, \sqrt{\frac{2L\lambda(1-\alpha)\mathcal{E}_{\mathrm{C},i}}{\alpha\mathcal{E}_{\mathrm{C},i} + L'N_0}}\right).
\end{aligned} \tag{2.33}$$

The error probabilities $\Pr(E_1)$ and $\Pr(E_2)$ corresponding to the first and second rounds, respectively are derived using an adaptation of [48, eq:12.1-

22], which is given by

$$P_M(j) = 1 - \int_0^\infty \left(1 - e^{-v(1+\alpha\gamma)} \sum_{k=0}^{jL-1} \frac{(v(1+\alpha\gamma))^k}{k!}\right)^{M-1} \left[v\left(\frac{1+\alpha\gamma}{\gamma(1-\alpha)}\right)\right]^{\frac{jL-1}{2}} e^{-v-\frac{\gamma(1-\alpha)}{(1+\alpha\gamma)}} I_{jL-1}\left(2\sqrt{\frac{v\gamma(1-\alpha)}{1+\alpha\gamma}}\right) \quad (2.34)$$

where j is the round index, I_n is the modified Bessel function of order n, $v = \frac{u}{2\mathcal{E}(N_0+\alpha\mathcal{E})}$ and $\gamma = \mathcal{E}/L'N_0$. u is the first decision variable with a non-central chi-square distribution having $2L$ degrees of freedom and non-centrality parameter $s^2 = \mathcal{E}(1-\alpha)$. Note that above probability reduces to [48, eq:12.1-22] for $\alpha = 0$. In the fading channel case, the protocol provides a more significant improvement when going from one to two rounds, due to the added diversity. Here it should be expected that the use of more than two rounds could be even more beneficial, unlike the AWGN case. The use of many rounds, however, will incur a non-coherent combining loss, despite the added diversity.

The upper bound on the reconstruction error given in Section 2.1 by (2.2) is adapted to the current model and by substituting (2.34) and (2.33) we obtain the following bound on the distortion at the end of the second round.

$$\begin{aligned} D(\mathcal{E}, N_0, 2, \lambda) &\leq 2^{-2B}(1-P_e) + 2P_e \\ &\leq 2^{-2B} + 2\left[P_M(1)\Pr(E_{\mathrm{e}\to\mathrm{c},1}) + P_M(2)\right] \end{aligned} \quad (2.35)$$

In the upcoming section, we provide numerical evaluation results of the upper bound given above for different values of α for 0.5 and 0.1 since it is not possible to give an analytical result and discuss the improvement to be gained in two rounds through comparing (2.35) versus the distortion to be achieved in a single round without feedback, i.e. $D \leq 2^{-2B} + 2P_M(1)$.

2.2.1 Lower-bounds on Distortion

We consider the same two lower bounds on performance considered in the previous sections. Merhav's bounding technique must be computed numerically in this case. as the upper bound introduced above and the other one is presented in an analytical form. Merhav's results were derived for Rayleigh fading which is generalized here to channels with a line-of-sight component and more degrees-of-freedom. Secondly we adapt the classical bound from Goblick [4] for a fading channel. Both of these techniques assume that the channel is known to the receiver and the distortion is averaged over all realizations of the random channel coefficients.

Merhav's bound (2.29) is

$$\overline{D}_{M3}(\mathcal{E}, M, N_0) \geq \mathbb{E}_a D_{M3}(a\mathcal{E}, M, N_0) \quad (2.36)$$

where $a = \sum_{i=0}^{L-1} |\sqrt{1-\alpha} + \sqrt{\alpha} h_{i,l}|^2$ is a non-central chi-square distributed random variable with the non-centrality parameter $(1-\alpha)L$, $2L$ degrees of freedom and with the variance of the $2L$ underlying Gaussian random variables given by $\sigma^2 = \alpha/2$. Its p.d.f. is given below.

$$f(a) = \frac{1}{\alpha}\left(\frac{a}{(1-\alpha)L}\right)^{\frac{L-1}{2}} \exp\left(-\frac{a+(1-\alpha)L}{\alpha}\right) I_{L-1}\left(2\frac{\sqrt{a(1-\alpha)L}}{\alpha}\right) \tag{2.37}$$

The behavior of the lower-bound (2.36) will be presented numerically in the upcoming section.

The wireless adaptation of the Goblick bound given by (1.1) tries to capture the scenario considered in the achievable scheme above, namely that a finite number of channel of realizations (or block-fading model) is exploited by the transmission strategy. To this end, we consider observations comprising N signaling dimensions split into R blocks of size N/R. Let $\mathbf{x}_i$ be the codeword in block i and constrain its energy as $\mathbb{E}||\mathbf{x}_i||^2 \leq \mathcal{E}/R$. Each block witnesses an independent and identically distributed fading amplitude. We show in Appendix 6.1.1 that the distortion is bounded below by

$$D \geq (1 + 4\alpha\mathcal{E}/RN_0)^{-LR} \exp\left\{-\frac{2(1-\alpha)L\mathcal{E}/N_0}{1+4\alpha\mathcal{E}/RN_0}\right\} \tag{2.38}$$

2.3 Numerical Results

In this section, we present numerical evaluation results for the bounds in Sections 2.1 and 2.2. In Figure (2.1) we show the bound given by (2.15) for two rounds and different values of B from 2 to 10. The convex hull of these curves should be compared with the Goblick-bound given by (2.25) which is valid for systems with feedback. The curves labeled as the single-round scheme without feedback represent (2.14). The convex hull of these curves should be compared with the Merhav bounds which are valid only without feedback. Note that, in Figure (2.1) Merhav bound 1, 2 and 3 represent the lower bounds given by equations (2.27), (2.28) and (2.29) , respectively. Firstly we see the significant effect of using the novel feedback protocol with respect to the reconstruction fidelity. The latter clearly provides an improvement in terms of distortion or approximately 3 dB in energy efficiency. We do not quite see the predicted 3dB gap (around 4.5 dB for 14-bits) in energy-efficiency with respect to the outer-bound with a known channel, even with a very high-resolution quantization level. Tighter bounding techniques for the case with feedback in addition to variable-energy schemes should therefore be considered for future work. The tightest of the Merhav bounds is clearly (2.29) but also does not quite predict the 1.7 dB asymptotic gap. Although not shown, numerical analysis also confirmed the asymptotic result given in Section 2.1 by (2.16) regarding the use of twice as much energy in the second round in comparison to the first.

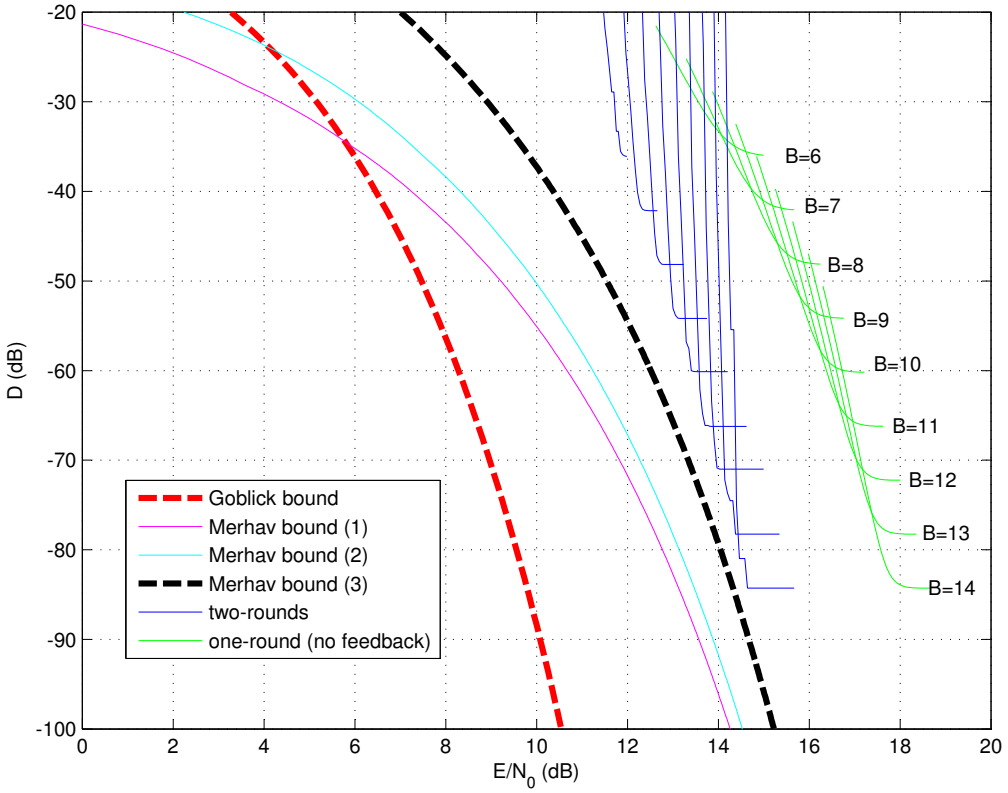

Figure 2.1: Numerical evaluation of the upper and lower bounds on distortion for different values of B in an AWGN channel.

The upper-bound in (2.35) is depicted in Figures (2.2), (2.3) and (2.4) for several values of B for the cases $\alpha = 0.1$ and $\alpha = 0.5$ and both high ($L = 4$) and low diversity orders $L = 1$. In all cases we see a very significant effect ($\geq$10dB in energy-efficiency) in using a two-round feedback protocol compared to a one-shot transmission, and this even in the case of a strong line-of-sight component ($\alpha = 0.1$). Bound types of lower-bounds are looser in the case of the fading channels, and especially in the high-diversity case (Figure (2.4)). This can be attributed to the non-coherent combining loss which is not captured by the bounds which assume known channels. This motivates the search for better lower-bounds assuming unknown channels in their formulation.

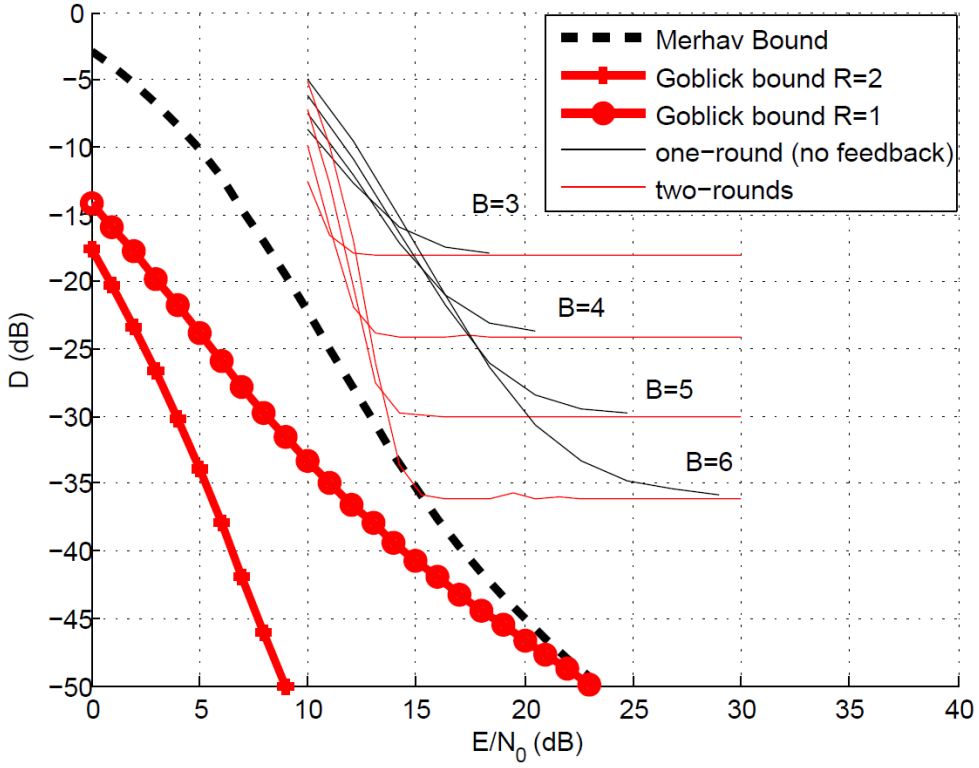

Figure 2.2: Numerical evaluation of the distortion for B from 3 to 6 in a wireless channel for $\alpha = 0.1, L = 1$

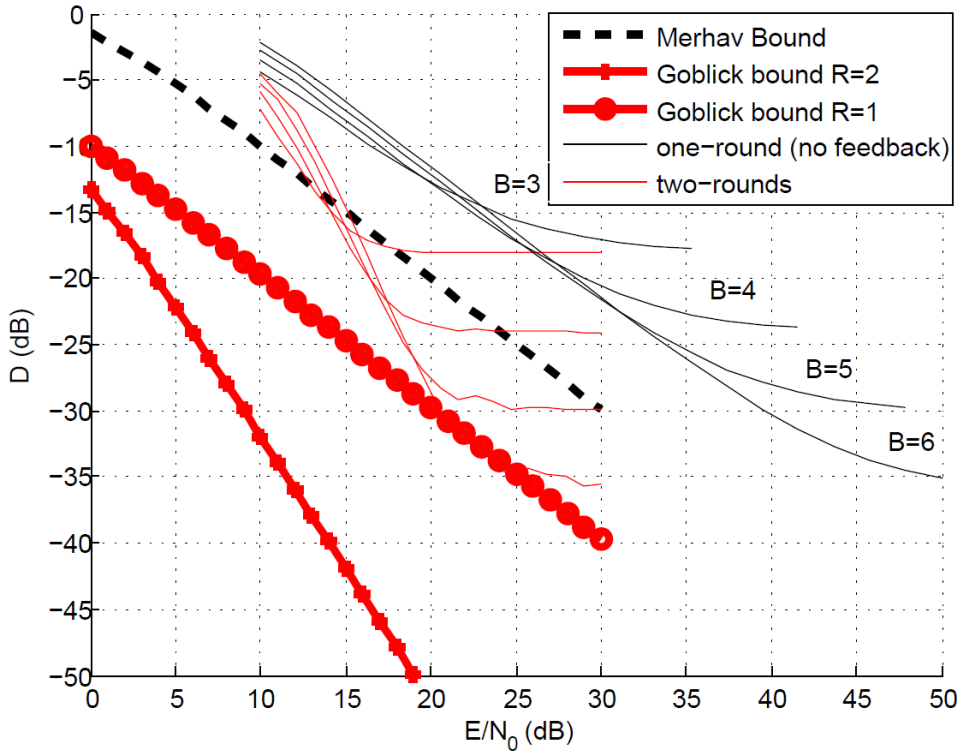

Figure 2.3: Numerical evaluation of the distortion for B from 3 to 6 in a wireless channel for $\alpha = 0.5, L = 1$

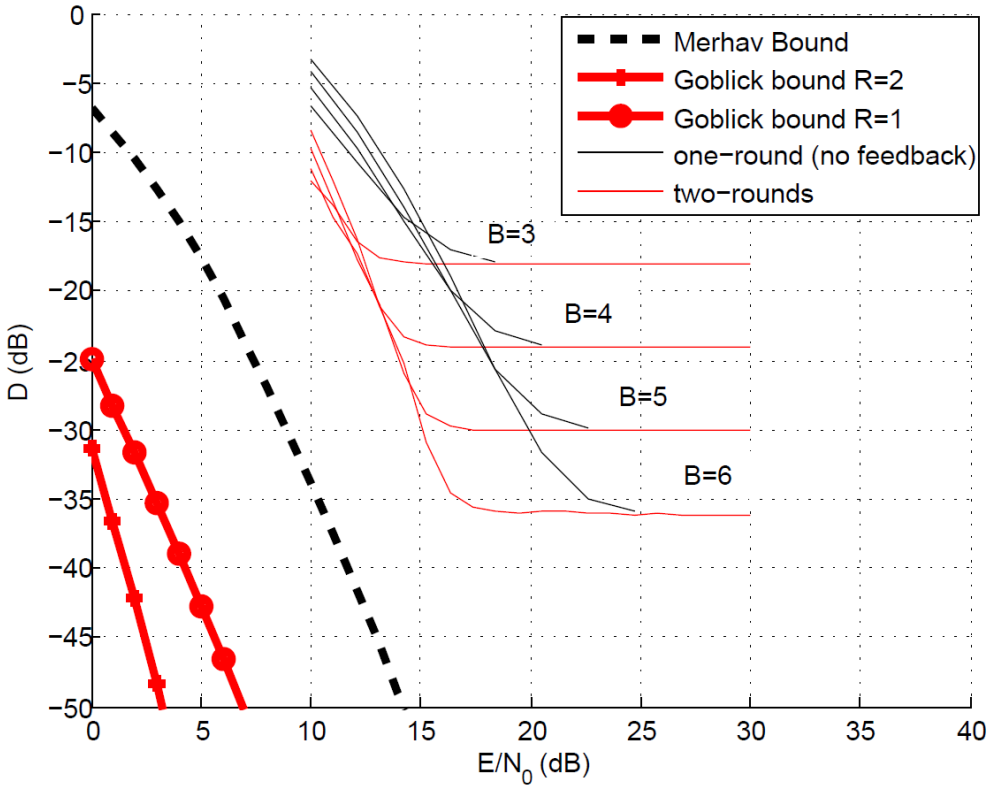

Figure 2.4: Numerical evaluation of the derived bounds for B from 3 to 6 in a wireless channel for $\alpha = 0.5, L = 4$

Chapter 3

Transmission of Correlated Dual-Source over a MAC

In this chapter, we consider a simple transmission strategy for a network of sensors able to mesure a physical phenomenon from different locations. Furthermore, we envisage a scenario where sensors operate under tight energy constraints over a wireless transmission medium which motivates the use of low-latency coding method. The multi-sensor scenario reflected in Figure (1.4) is an important generalization which is considered here. In particular, we are interested in the case where two correlated random variables are transmitted over multiple-access channels, where the information of the sources are sent through an AWGN channel. The main issue is how to do the encoding with respect to the performance to be achieved as a function of the required energy upon reconstruction. The key element in the multi-sensor scenario being to exploit is the correlation, which is assumed to be known, both at the transmitter and receiver. We focus our attention on the case where unitary samples of the source are transmitted sporadically due to slow time-variation, and consequently we cannot perform vector quantization. Moreover, we aim to determine the operating regimes for such a multiple-access system in terms of the role correlation plays in determining the energy efficiency.

In this chapter, we introduce three different lower bounds on the reconstruction error of estimating the source vectors based on different ranges in which the correlation coefficient between the two sources is defined, right after we describe the system model of the addressed problem in Section 3.1. In Sections 3.3, 3.3.1 and 3.3.2, we present new results which aim to show the benefit of feedback regarding optimality, yet with minimal latency through

a two-way protocol and its asymptotic performance of reconstruction error is analyzed for two correlated continuous sources. We conclude the chapter with the numerical evaluation of the derived bounds. All the derivations can be found in detail in Appendix 6.2.

3.1 Model Description

3.1.1 Channel model

Let us begin with the description of the system model for the addressed problem. The considered system for the multiple-access is depicted in Figure (3.1) where we note that the encoders can make use of an ideal feedback link. The received signal $\mathbf{Y} = \{Y_i; i = 1, ..., N\}$ and the energy constraints are given as

$$Y_i = X_{1,i}e^{i\phi_{1,i}} + X_{2,i}e^{j\phi_{2,i}} + Z_{1,i} + Z_{2,i} \tag{3.1}$$

$$\frac{1}{K}\sum_{i=1}^{N} E[|X_{m,i}|^2] \leq \mathcal{E}_m \tag{3.2}$$

for $m = 1, 2$ and $i, j = 1, ..., N$, respectively. K is the dimensionality of the source vectors and is assumed to be finite (i.e. it cannot grow without bound with N). The criteria to satisfy is chosen as the squared-error distortion measure, which is defined by $d(u_m, \hat{u}_m) = (u_m - \hat{u}_m)^2$. $\phi_m = \{\phi_{m,i}; i = 1, ..., N\}$ denotes the random phases which are assumed to be unknown both to the transmitter and the receiver. The encoding functions are arbitrary mappings, $(U_m, Y_1, Y_2, \cdots, Y_{i-1}) \rightarrow X_{m,i}$ for each channel input in the case of causal feedback, and $U_m \rightarrow X_{m,i}$ without feedback. Interested reader is

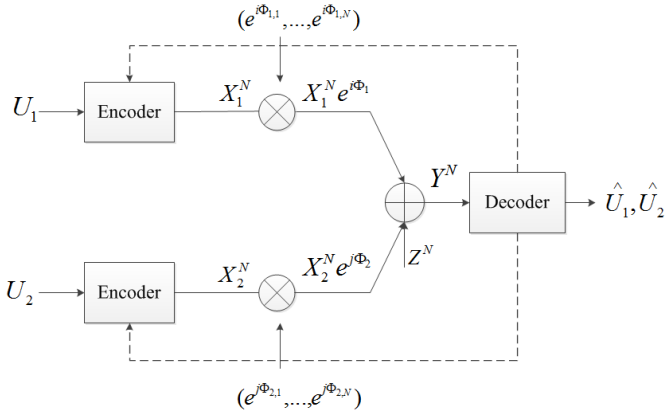

Figure 3.1: Correlated sources over GMAC with feedback.

encouraged to see [54, Section 9] for the results of the parallel channel.

3.1.2 Source model

Here, we give the description of the source model which is used for both the lower bounds on the reconstruction error in estimating the source messages presented in Section 3.2 and the upper bounds derived for the achievable scheme described and analyzed in Sections 3.3 and 3.3.2. The correlational relationship between the sources $\mathbf{U}_1, \mathbf{U}_2$ dimension of K is defined through the following expression

$$\mathbf{U}_2 = \rho \mathbf{U}_1 + \sqrt{1-\rho^2}\mathbf{U}_2' \tag{3.3}$$

where we denote the first source by $\mathbf{U}_1$ and the second source by $\mathbf{U}_2$. $\mathbf{U}_2'$ here is an auxiliary random vector. Note that the first source $\mathbf{U}_1$ and the auxiliary vector $\mathbf{U}_2'$ are independent of each other. For the distributions of the two sources, two different types will be considered. In the first case, $\mathbf{U}_1$ is defined to be uniformly distributed over $(-\sqrt{3}, \sqrt{3})$ and the second source $\mathbf{U}_2$ is defined to have a contaminated uniform distribution with above given equality (3.3), based on $\mathbf{U}_1$ and $\mathbf{U}_2'$ which is also uniform on $(-\sqrt{3}, \sqrt{3})$. So, we have one uniform and one near-uniform source having covariance equal to the correlation coefficient ρ between them. Secondly, in order to cover a more general case, correlated sources $\mathbf{U}_1$ and $\mathbf{U}_2$ are defined to be standard normal random variables, guaranteed by the auxiliary random variable $\mathbf{U}_2'$ is also normally distributed with zero mean and unit variance.

3.1.3 Discussion

In order to highlight the essence of the behaviour of the general case, we consider first the special case of a single source $\mathbf{U}$ dimension of K, whose message is sent over a Gaussian channel by being split into two parts through two different codebooks. Let us call the encoded parts of $\mathbf{U}$ as $\mathbf{X}_1$ and $\mathbf{X}_2$. The estimate $\hat{\mathbf{U}}$ is received after $\mathbf{X}_1$ and $\mathbf{X}_2$ are merged again before being decoded. In the following, $I(\mathbf{U}; \hat{\mathbf{U}})$ is derived using two different expansions and the corresponding distortion D is lower bounded.

$$I(\mathbf{U}; \hat{\mathbf{U}}) \leq N \log\left(1 + \frac{K\mathcal{E}}{NN_0}\right) \tag{3.4}$$

and also

$$I(\mathbf{U}; \hat{\mathbf{U}}) \geq h(\mathbf{U}) - h(\mathbf{U} - \hat{\mathbf{U}}) \tag{3.5}$$

which varies based on the source distribution, since the entropy is directly related to the distribution type. The derivations of (3.4) and (3.5) are provided in Appendix 6.2.1. Combining above given two expansions, we obtain Shannon's lower-bound on distortion as

$$D \geq C_d(1 + \frac{K\mathcal{E}}{NN_0})^{-\frac{2N}{K}} \tag{3.6}$$

which predicts that the energy used by the two transmitters can be accumulated where

$$C_d = \begin{cases} 1 & \text{Gaussian,} \\ \frac{6}{\pi e} & \text{Uniform.} \end{cases} \tag{3.7}$$

Asymptotically in N, (3.6) yields $D \geq C_d e^{-\frac{2\mathcal{E}}{N_0}}$. In the upcoming section 3.2, it is shown that benefiting from the correlation between the sources, it is possible to achieve the behaviour of (3.6) and also the energy efficiency with two highly correlated sources.

3.2 Distortion Bounds in a Multiple-Access Channel

After the detailed description of the system model, we introduce outer bounds on reconstruction error of each source in a multiple-access channel. In order to avoid the repetitions as giving the derivations of the outer bounds, we will use the notation m to represent one of the sources and m' will be used to indicate the other source.

Throughout the section, the two different expansions of a mutual information (one of which is based on the output signal and the other one is based on the sources) are derived and equated in order to obtain a lower bound on the distortion level. For that reason, the first expansions on the output signals are applicable to both sources. Naturally, the second expansions vary depending on the source number and distribution. Furthermore, we note that the bounds are valid for both the use of feedback-based encoders and those without feedback.

3.2.1 Lower Bound I

In order to obtain a lower bound on the reconstruction error in estimating $\mathbf{U}_1, \mathbf{U}_2$, we derive a relatively simple mutual information between the m^{th} source U_m and the output signal Y through two different expansions, which depends on the sum energy and turns out to be appropriate for the cases of high correlation between the sources. Two different expansions of $I(\mathbf{U}_m; \mathbf{Y})$ are derived first of which is based on the output signal where the second expansion depends on the sources. The two expansions of $I(\mathbf{U}_m; \mathbf{Y})$ are given by

$$I(\mathbf{U}_m; \mathbf{Y}) \leq N \log\left(1 + \frac{K(\mathcal{E}_m + \mathcal{E}_{m'})}{NN_0}\right), \tag{3.8}$$

$$I(\mathbf{U}_m; \mathbf{Y}) \geq h(\mathbf{U}_m) - h(\mathbf{U}_m - \hat{\mathbf{U}}_m), \tag{3.9}$$

respectively. The derivations of both expansions given above can be found in Appendix 6.2.2 together with the source entropies for $m = 1, 2$ and both

source distributions. Equating the two expansions of the same mutual information provides the below given bound on distortion level for the m^{th} source

$$D_{I,m} \geq C_{I,m}\left(1+\frac{K(\mathcal{E}_m+\mathcal{E}_{m'})}{NN_0}\right)^{-\frac{2N}{K}} \tag{3.10}$$

where

$$C_{I,m}=\begin{cases}1 & \text{if } m=1,2 \text{ for Gaussian}\\ \frac{6}{\pi e} & \text{if } m=1,2 \text{ for Uniform}\end{cases} \tag{3.11}$$

Asymptotically in N, (3.10) is obtained as

$$D_{I,m} \geq C_{I,m}e^{-\frac{2(\mathcal{E}_m+\mathcal{E}_{m'})}{N_0}}. \tag{3.12}$$

3.2.2 Lower Bound II

The main difference between this case and the previous one treated high correlation is the mutual information term to be used in order to come up with a bound on the distortion level corresponding each source. Hence the mutual information between the source $\mathbf{U}_m$ and the output signal $\mathbf{Y}$ will be expanded through two different ways when the information of the other source $\mathbf{U}_{m'}$ is given, so that the output signal expansion yields dependent on the individual energy. The aim is to obtain a different bound when the sources are not strongly correlated since $\mathbf{U}_m$ does not have the information of $\mathbf{U}_{m'}$ due to correlation. The two expansions of $I(\mathbf{U}_m;\mathbf{Y}|\mathbf{U}_{m'})$ are given as

$$I(\mathbf{U}_m;\mathbf{Y}|\mathbf{U}_{m'},\Phi_m,\Phi_{m'}) \leq N\log\left(1+\frac{K\mathcal{E}_m}{NN_0}\right), \tag{3.13}$$

$$I(\mathbf{U}_m;\mathbf{Y}|\mathbf{U}_{m'},\Phi_m,\Phi_{m'}) \geq h(\mathbf{U}_m|\mathbf{U}_{m'})-h(\mathbf{U}_m-\hat{\mathbf{U}}_m). \tag{3.14}$$

The derivations of (3.13) and (3.14) are given in Appendix 6.2.3. The general form of the distortion bound is obtained as $D_{II,m} \geq C_{II,m}\left(1+\frac{KE_m}{NN_0}\right)^{-\frac{2N}{K}}$ and asymptotically in N it becomes

$$D_{II,m} \geq C_{II,m}e^{-\frac{2\mathcal{E}_m}{N_0}}, \tag{3.15}$$

where $C_{II,m}$ is a constant depends on the source given as

$$C_{II,m}=\begin{cases}(1-\rho^2) & \text{if } m=1,2 \text{ for Gaussian}\\ \frac{36(1-\rho^2)}{\pi^2e^2} & \text{if } m=1, \text{ for Uniform}\\ \frac{6(1-\rho^2)}{\pi e} & \text{if } m=2 \text{ for Uniform}\end{cases} \tag{3.16}$$

3.2.3 Lower Bound III

In addition to the lower bounds I and II, the product distortion term $D_{III} = D_1 D_2$ is bounded as given in the following form

$$D_{III} \geq C_{III} \exp\left(-\frac{2(\mathcal{E}_m + \mathcal{E}_{m'})}{N_0}\right), \tag{3.17}$$

where

$$C_{III,m} = \begin{cases} 1-\rho^2, & \text{for Gaussian} \\ \frac{36(1-\rho^2)}{e^2\pi^2}, & \text{for Uniform} \end{cases} \tag{3.18}$$

The derivation of the bound (3.17) given above can be found in Appendix 6.2.4. Combining all three bounds (3.12), (3.15) and (3.17) introduced above, we obtain the following overall bound for the uniform case first and second source

$$D_1 \geq \begin{cases} D_{I,1} & \text{if } \frac{6(1-\rho^2)}{\pi e} \leq \min(D_2, e^{-\frac{2\mathcal{E}_2}{N_0}}), \\ D_{II,1} & \text{if } D_2 \geq e^{-\frac{2\mathcal{E}_2}{N_0}} \text{ and } \frac{6(1-\rho^2)}{\pi e} \geq e^{-\frac{2\mathcal{E}_2}{N_0}}, \\ D_{III}/D_2 & \text{if } \frac{6(1-\rho^2)}{\pi e} \geq \min(D_2, e^{-\frac{2\mathcal{E}_2}{N_0}}), \end{cases} \tag{3.19}$$

$$D_2 \geq \begin{cases} D_{I,2} & \text{if } 1-\rho^2 \leq \min((\pi e D_1)/6, e^{-\frac{2\mathcal{E}_1}{N_0}}), \\ D_{II,2} & \text{if } D_1 \geq \frac{6}{\pi e} e^{-\frac{2\mathcal{E}_1}{N_0}} \text{ and } 1-\rho^2 \geq e^{-\frac{2\mathcal{E}_1}{N_0}}, \\ D_{III}/D_1 & \text{if } 1-\rho^2 \geq \min((\pi e D_1)/6, e^{-\frac{2\mathcal{E}_1}{N_0}}), \end{cases} \tag{3.20}$$

respectively. And we have following overall bound for the Gaussian case through combining all three bounds (3.12), (3.15) and (3.17) introduced above, we obtain the following overall bound

$$D_m \geq \begin{cases} D_{I,m} & \text{if } 1-\rho^2 \leq \min(D_{m'}, e^{-\frac{2\mathcal{E}_{m'}}{N_0}}), \\ D_{II,m} & \text{if } D_{m'} \geq e^{-\frac{2\mathcal{E}_{m'}}{N_0}} \text{ and } 1-\rho^2 \geq e^{-\frac{2\mathcal{E}_{m'}}{N_0}}, \\ D_{III}/D_{m'} & \text{if } 1-\rho^2 \geq \min(D_{m'}, e^{-\frac{2\mathcal{E}_{m'}}{N_0}}). \end{cases} \tag{3.21}$$

The bounds given above predict that energy accumulation cannot be achieved when the distortion resulting from the estimation of one source realization using the other (i.e. $1-\rho^2$) is more than the point-to-point distortion (Goblick bound $e^{-2\mathcal{E}/N_0}$, [4]) incurred during transmission.

3.3 Two-Way Protocol with Correlated Analog Sources

As in the original work [1] and its non-coherent version studied in [55], the protocol comprises a data phase and a control phase, which can be repeated

up to two rounds. The total energy to be used by protocol is fixed and we will denote the energy used in the data phase of the i^{th} round by the j^{th} source by $\mathcal{E}_{\mathrm{D},i,j}$, where $i, j = 1, 2$. In the same way, $\mathcal{E}_{\mathrm{C},i,j}$ denotes the energy used in the control phase of the i^{th} round by the j^{th} source. The energy in the control and data phases of the i^{th} round are defined as the sum energy on both sources. The quantized source sample of the j^{th} source is encoded into 2^B messages with dimension N.

In the data phase, the first source sends its message $\mathbf{m}_1(U_1)$ to the receiver with energy $\mathcal{E}_{\mathrm{D},1,1}$. The receiver detects $\hat{m}_1$ and feeds it back. And the second source sends $\mathbf{m}_2(U_2)$ with energy $\mathcal{E}_{\mathrm{D},1,2}$. The energy in the control phase of the i^{th} round is defined as $\mathcal{E}_{\mathrm{C},i} = \mathcal{E}_{\mathrm{C},i,1} + \mathcal{E}_{\mathrm{C},i,2}$ and the total energy in the data phase is $\mathcal{E}_{\mathrm{D},i} = \mathcal{E}_{\mathrm{D},i,1} + \mathcal{E}_{\mathrm{D},i,2}$. This encoding rule allows the second source to exploit the correlation of its sample with that of its peer and the energy used is chosen according to the likelihood of the estimate fed back from the receiver. After the estimation and feedback of $\hat{m}_2$, data phase of the first round ends and the encoders enter the control phase to inform the receiver about the correctness of its decision, as in the single source case. For that, each source sends ACK/NACK signals regarding its own message to the decoder. According to the control signals, either the protocol halts or goes on another round to do the retransmission of the message which were not acknowledged in the control phase. For the second data phase, the destination instructs the sources to retransmit and re-detect its message.

The output signal based on the N dimensional observation of the j^{th} source in the data phase is given as

$$\mathbf{Y}_d = \sqrt{\mathcal{E}_{\mathrm{D},1,j}} \mathrm{e}^{j\Phi_j} \mathbf{S}_{m_j} + \mathbf{Z}_j. \tag{3.22}$$

We assume the random phases Φ_j to be distributed uniformly on $[0, 2\pi)$, the channel noise $\mathbf{Z}_j$ to have zero mean and equal autocorrelation $N_0\mathbf{I}_{N\times N}$ for $j = 1, 2$ and $\mathbf{S}_{m_j}$ are the N-dimensional messages, where $m = 1, 2, \cdots, 2^{B_j}$ and $j = 1, 2$. We have a detector of the form for the j^{th} source as $e_j = I\left(|y_{c,j}|^2 > \lambda_j \mathcal{E}_{\mathrm{C},1,j}\right)$ with $y_{c,j} = \mathbf{Y_{c,j}}^H \mathbf{S}_{c,j}$ λ_1 and λ_2 are threshold values to be optimized and included within the interval $[0, 1)$. For simplification, we will assume λ_1 and λ_2 to be equal to the same value λ. We denote the error events in the first round and on the j^{th}source with $E_{1,j}$. Let $e_{1,j}$ and $c_{1,j}$ denote erroneous and correct decoding in the first round on U_j, respectively. Accordingly $E_{c\to e,1}$ and $E_{e\to c,1}$ are used to denote a mis-detected acknowledged error and an uncorrectable error, respectively. The probability of an uncorrectable error in the first round is taken as the sum of the probability of errors of each source as $\Pr(E_{e\to c,1}) = \sum_{j=1}^{2} \Pr(E_{e\to c,1,j})$.

The probability of an uncorrectable error $E_{e\to c}$ for U_j is given by

$$\begin{aligned}\Pr(E_{e\to c,1,j}) &= \Pr(|\sqrt{\mathcal{E}_{\mathrm{C},1,j}} + z_{c,j}|^2 \leq \lambda\mathcal{E}_{\mathrm{C},1,j}) \\ &= 1 - Q_1\left(\sqrt{\frac{\mathcal{E}_{\mathrm{C},1,j}}{N_0/2}}, \sqrt{\frac{\lambda\mathcal{E}_{\mathrm{C},1,j}}{N_0/2}}\right) \\ &\overset{(a)}{\leq} 1/2\exp\left(-\frac{(\sqrt{\lambda}-1)^2\mathcal{E}_{\mathrm{C},1,j}}{N_0}\right). \end{aligned} \tag{3.23}$$

using the recent bound on the $Q_1(\alpha,\beta)$ given in [47, eq:4] in step (a). The total probability of a mis-detected acknowledged error to occur in the first round is obtained in the same way by; $\Pr(E_{c\to e,1}) = \sum_{j=1}^{2}\Pr(E_{c\to e,1,j})$. And the probability of a mis-detected acknowledged error $E_{c\to e}$ for U_j is

$$\Pr(E_{c\to e,1,j}) = \exp\left\{-\frac{\lambda\mathcal{E}_{\mathrm{C},1,j}}{N_0}\right\}. \tag{3.24}$$

- Detection Rule

The receiver chooses

$$(\hat{\mathbf{m_1}}, \hat{\mathbf{m_2}}) \sim \underset{(\hat{\mathbf{m_1}},\hat{\mathbf{m_2}})s.t.(\hat{\mathbf{m_1}},\hat{\mathbf{m_2}})\in J_m}{\operatorname{argmax}} |\mathbf{U}_{\mathbf{m}}^{(1)}|^2 \tag{3.25}$$

in the first round, whereas the detection rule is cumulatively given by

$$(\hat{\mathbf{m_1}}, \hat{\mathbf{m_2}}) \sim \underset{(\hat{\mathbf{m_1}},\hat{\mathbf{m_2}})s.t.(\hat{\mathbf{m_1}},\hat{\mathbf{m_2}})\in J_m}{\operatorname{argmax}} |\mathbf{U}_{\mathbf{m}}^{(1)}|^2 + |\mathbf{U}_{\mathbf{m}}^{(2)}|^2 \tag{3.26}$$

for the second round where $|\mathbf{U}_{\mathbf{m}}^{(1)}|^2 = |\mathbf{U}_{\mathbf{m_1}}^{(1)}|^2 + |\mathbf{U}_{\mathbf{m_2}}^{(1)}|^2$ and $|\mathbf{U}_{\mathbf{m}}^{(2)}|^2 = |\mathbf{U}_{\mathbf{m_1}}^{(2)}|^2 + |\mathbf{U}_{\mathbf{m_2}}^{(2)}|^2$. As defining the error probabilities per round/source, in the upcoming subsections, we will make use of the rule defined above.

3.3.1 Asymptotic Performance of Uniform Sources

The structure of the sources is defined as in (3.3) where U_1 and U_2' are independent of each other and uniformly distributed over $(-\sqrt{3},\sqrt{3})$ and the second source U_2 is defined as $U_2 = \rho U_1 + \sqrt{1-\rho^2}U_2'$ based on U_1 and an auxiliary random vector U_2' which is also uniform on $(-\sqrt{3},\sqrt{3})$. Depending on the value of ρ, the distribution of the second source U_2 can be either a triangular distribution or a contaminated uniform distribution. In the case of a high correlation, i.e. $\sqrt{1-\rho^2} < \theta 2^{-B}$ where θ is an arbitrary constant, the effect of the auxiliary random variable U_2' will be very small. On the contrary, for a low correlation between U_1 and U_2, U_2' will have a significant effect so the second source will have a triangular distribution as a sum of the two uniform random vectors. We will focus on the extreme

case of a very high correlation between the two sources. So, here we have one uniform and one almost uniform (contaminated uniform) source having covariance equal to the correlation coefficient ρ between them.

The source messages are quantized as depicted in Figure (3.2), where each tail of the distribution is considered as one quantization bin and the interior part, which is composed by the remaining $2^B - 2$ bins, is uniformly quantized. Note that for a full correlation between the sources the 'contamination' in the source distribution vanishes and the shape given by Figure (3.2) becomes a rectangular.

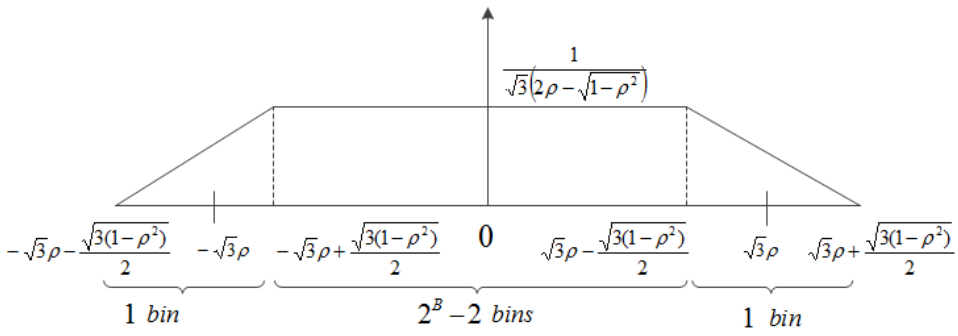

Figure 3.2: Pictorial representation of quantization process for the defined distribution with the allocation of the quantization bins

At the end of the second round, the protocol is terminated with distortion bounded as

$$D = D_q(1 - P_e) + D_e P_e \leq D_q + D_{e,1}P_{e,1} + D_{e,2}P_{e,2} \tag{3.27}$$

where P_e is the total probability of error which consists of $P_{e,1}$ and $P_{e,2}$. $P_{e,1}$ and $P_{e,2}$ indicate the probability of error on one of the sources and both sources, respectively. Both probabilities include the uncorrectable error in the first round. $P_{e,1}$ is defined by

$$P_{e,1} = \left\lceil 2^B\sqrt{1-\rho^2} \right\rceil \Pr(E_{e\to c,1})P_2(1) + \left\lceil 2^B\sqrt{1-\rho^2} \right\rceil P_2(2) \tag{3.28}$$

On the other hand for the case where both sources to be in error at the end of the first or the second round, the probability of error is achieved as

$$P_{e,2} = \left\lceil 2^B\sqrt{1-\rho^2} \right\rceil 2^B \Pr(E_{e\to c,1})^2 P_2(2) + \left\lceil 2^B\sqrt{1-\rho^2} \right\rceil 2^B P_2(4) \tag{3.29}$$

where

$$P_2(L,\gamma) = \frac{1}{2^{2L-1}} e^{-\gamma} \sum_{n=0}^{L-1} \left(\frac{1}{n!} \sum_{k=0}^{L-1-n} \binom{2L-1}{k} \right) \gamma^n$$

in round L given by the formula [48, eq:12.1-24] where γ represents the SNR. Explicitly, in the first round for only one source being in error, the error probability is obtained by $P_2(1)$ whereas $P_2(2)$ gives the probability for both sources being in error. Accordingly $P_2(2)$ and $P_2(4)$ represent the probabilities in the second round. Further detail on the derivation of the error probabilities (3.28) and (3.29) can be found in Appendix 6.2.5.

D_q represents the distortion caused by the quantization process and D_e corresponds to the MSE distortion for the case where an error was made. Splitting the distortion for the erroneous case, where $D_{e,1}$ denotes the distortion for one source in error and in the same way $D_{e,2}$ denotes the case when both sources incorrectly decoded. Let us denote the estimation error by e, so that its variance $E[u-\hat{u}|l \; in \; error]^2$ for $l = 0$ yields the quantization distortion given by

$$D_q \leq (2^B - 2)^{-2} \left(12 + \frac{1-\rho^2}{\rho^2} - \frac{4\sqrt{3(1-\rho^2)}}{\rho}\right) + \frac{3(1-\rho^2)^{3/2}}{8\rho^3}. \quad (3.30)$$

$D_{e,1}$ is defined and bounded as follows

$$\begin{aligned} D_{e,1} &= E\left[(u_m - \hat{u}_m)^2 \,|u_m \; in \; error\right] \\ &\leq 6\left(2^{-2B+2} + 5(1-\rho^2) + 2^{-B+3}\sqrt{1-\rho^2}\right) \end{aligned} \quad (3.31)$$

for the m^{th} source where $m = 1, 2$. Note that for $m = 2$ above given expression (3.31) becomes an equality. Finally, for the worst case when both sources are in error we have the following expansion and it is bounded as given by

$$\begin{aligned} D_{e,2} &= \sum_{m=1}^{2} E\left[(u_m - \hat{u}_m)^2 \,|u_m \; in \; error\right] \\ &\leq 14 + 12\rho^2 + 3(1-\rho^2)/4 + 6\rho\sqrt{1-\rho^2} \end{aligned} \quad (3.32)$$

Through combining (3.28), (3.29), (3.30), (3.31), (3.32) with (3.27), we get the following bound on distortion as

$$\begin{aligned} D \leq K_1 D_q &+ \left(K_2\sqrt{1-\rho^2}e^{B\ln 2} + K_3\epsilon(\rho)\right) e^{(B-3)\ln 2 - \frac{\mathcal{E}_{\mathrm{D},1} + \mathcal{E}_{\mathrm{C},1}(\sqrt{\lambda}-1)^2}{2N_0}} D_{e,2} \\ &+ \left(K_4\sqrt{1-\rho^2}e^{B\ln 2} + K_5\epsilon(\rho)\right) e^{-\frac{\mathcal{E}_{\mathrm{D},1} + 2\mathcal{E}_{\mathrm{C},1}(\sqrt{\lambda}-1)^2}{4N_0}} D_{e,1} \\ &+ \left(K_6\sqrt{1-\rho^2}e^{B\ln 2} + K_7\epsilon(\rho)\right) e^{(B-7)\ln 2 - \frac{\mathcal{E}_{\mathrm{D},1} + \mathcal{E}_{\mathrm{D},2}}{2N_0}} D_{e,2} \\ &+ \left(K_8\sqrt{1-\rho^2}e^{B\ln 2} + K_9\epsilon(\rho)\right) e^{-\frac{\mathcal{E}_{\mathrm{D},1} + \mathcal{E}_{\mathrm{D},2}}{4N_0}} D_{e,1} \end{aligned} \quad (3.33)$$

where K_1, K_4, K_5 are $O(1)$, K_2, K_3 are $O(\mathcal{E}_{\mathrm{D},1})$, K_6, K_7, K_8, K_9 are $O((\mathcal{E}_{\mathrm{D},1}+\mathcal{E}_{\mathrm{D},2})^3)$ with $\epsilon(\rho) \in [0,1)$ which arose from the ceiling functions in (3.28) and (3.29).

For a high level of correlation between the sources we set the relations of the energies as $\mathcal{E}_{C,1} = \frac{\mathcal{E}_{D,2}}{(1-\sqrt{\lambda})^2}$ and $\mathcal{E}_{D,2} = (2-\mu)\mathcal{E}_{D,1}$ where μ is an arbitrary constant satisfying $\mu \in (0,2)$. And the asymptotic bound for a high correlation level becomes

$$D_{high} \leq e^{-\frac{\mathcal{E}_{\mathrm{D},1}(1-\mu/3)}{N_0}} \beta(\mathcal{E}_{\mathrm{D},1}, \rho) \tag{3.34}$$

where

$$\beta(\mathcal{E}_{\mathrm{D},1}, \rho) = \left(\frac{96 + \frac{3}{\rho^2} e^{-\frac{\mathcal{E}_{\mathrm{D},1}}{2N_0}}}{14 + \left(\frac{1}{2} e^{-\frac{\mathcal{E}_{\mathrm{D},1}}{2N_0}} + 2\rho^2 \right)^2} \right)^{2/3}$$

which arose from the distortion terms together with the ceiling functions.To simplify the calculations the energy used by a source on a particular phase is assumed to be half of the energy on the corresponding round, e.g. $\mathcal{E}_{D,1} = 2\mathcal{E}_{D,1,1} = 2\mathcal{E}_{D,1,2}$. Note that the exponential behaviour observed in (3.34) is the same as a single source yields in [55]. Furthermore, there is a difference of factor $1/2$ between the exponentials of (3.34) and the information theoretic bounds (3.12), (3.15) and (3.6).

The average energy $\mathcal{E}$ used by the protocol given by (6.27) in Appendix 6.2.6 can be made arbitrarily close to $\mathcal{E}_{\mathrm{D},1}$ with vanishing $P_{e,1}$ and $P_{e,2}$, guaranteed by the interval in which $\epsilon(\rho)$ is defined.

3.3.2 Asymptotic Performance of Gaussian Sources

The structure of the sources is defined as in (3.3) where U_1 and U_2' are independent of each other and normally distributed with zero mean and unit variance. Here U_2' is used as an auxiliary random variable to define the relationship between the two sources U_1 and U_2 with the joint probability density function given below

$$f(u_1, u_2) = \frac{1}{2\pi\sqrt{1-\rho^2}} \exp\left[-\frac{u_1^2 - 2\rho u_1 u_2 + u_2^2}{2(1-\rho^2)} \right] \tag{3.35}$$

for $-\infty < u_1 < \infty$ and $\infty < u_2 < \infty$. The definition of U_2 ensures that the covariance between the sources equals the correlation coefficient ρ.

- Quantization

The messages m_1 and m_2 will be discretized through uniform quantization, i.e. the bins are located equidistantly from each other and for each source the

reconstruction points $x_{j,n}$ are the midpoints of the intervals $I_{j,n}$ which define each of the bins for the j^{th} source with $n = 2, ..., 2^B - 1$. The quantization intervals corresponding to the tails of the bell curve ($I_{j,1}$ and $I_{j,2^B}$ for $j = 1, 2$) are considered as one bin for each side as shown in Figure (3.3). The rest of the partitioning is made for each source as $I_{j,n} = [-\Delta + \frac{\Delta(n)}{2^{B-1}-1}, -\Delta + \frac{\Delta(n+1)}{2^{B-1}-1}[$, with $\Delta = 2\sqrt{B \ln 2}$. Let us set the quantization levels for each source as $x_{j,1} = -\Delta$ and $x_{j,2^B} = \Delta$.

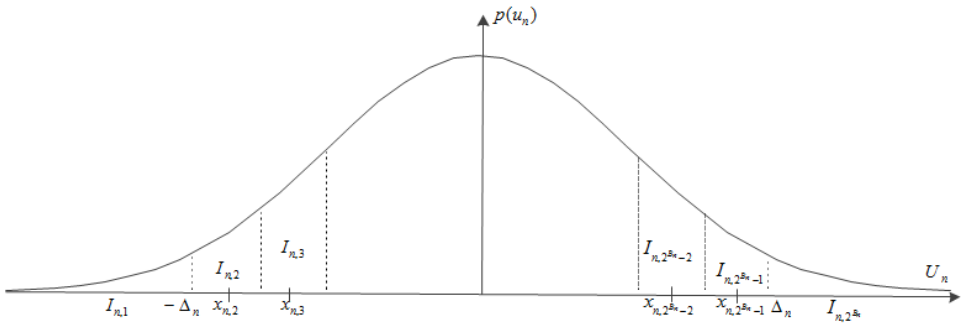

Figure 3.3: Uniform Quantization of U_j

Definition (m, n) is called a compatible pair if $|\rho U_1 - U_2| < \theta$ is satisfied for $\forall u_1, u_2 \in B$ where θ is an arbitrary constant.

This definition assures that, during the quantization process, the correlation between the two sources would not allow the second source to fall in a bin further than a certain distance. J_m represents the set that n is assumed to be contained. Outside of this set, the pair (m, n) becomes incompatible with the corresponding probability of error $(1 - \Pr(|U_2'| < \theta\sqrt{1-\rho^2}))$. In this case, the probability of having an error can be composed by three different events; both sources to be detected wrong, $\hat{u}_1$ detected correctly as $\hat{u}_2$ detected wrong or vice versa. These three events are summarized in two cases as only one source to be in error or both. The overall distortion at the end of the second round is defined as $D = D_q(1 - P_e) + D_e P_e$ and bounded by

$$\begin{aligned} D &\leq D_q + (1 - \Pr(|U_2'| > \theta\sqrt{1-\rho^2}))\,(D_{e,c,1}P_{e,c,1} + D_{e,c,2}P_{e,c,2}) \\ &\quad + \Pr(|U_2'| > \theta\sqrt{1-\rho^2})D_{e,ic,1}P_{e,ic,1} + \Pr(|U_2'| > \theta\sqrt{1-\rho^2})D_{e,ic,2}P_{e,ic,2} \\ &\overset{(a)}{\leq} D_q + D_{e,c,1}P_{e,c,1} + D_{e,c,2}P_{e,c,2} + \Pr(|U_2'| > \theta\sqrt{1-\rho^2})\,(D_{e,ic,1} + D_{e,ic,2}P_{e,ic,2}) \end{aligned} \tag{3.36}$$

where ic and c in the subscripts represent the incompatible and compatible pairs, respectively. $P_{e,ic,j}$ is the error probability of j incompatible sources

being in error whereas $P_{e,c,j}$ represents the error probability of those which are compatible. $D_{e,ic,j}$ and $D_{e,c,j}$ denote the corresponding distortions for each case, respectively. Note that, error probabilities and the corresponding distortion levels for the case of both sources being in error are assumed to be equivalent, i.e. $P_{e,c,2} = P_{e,ic,2} = P_{e,2}$ and $D_{e,c,2} = D_{e,ic,2} = D_{e,2}$. It should be also noted that in step (a) of eq. (3.36), the probability of error only one incompatible source to be in error is upper bounded by 1.

$P_{e,1}$ and $P_{e,2}$ are defined by

$$P_{e,1} \leq \left\lceil 2^B \theta \sqrt{1-\rho^2} \right\rceil \Pr(E_{e\to c,1}) P_2(1, \frac{\mathcal{E}_{\mathrm{D},1}}{2}) + \left\lceil 2^B \theta \sqrt{1-\rho^2} \right\rceil P_2(2, \frac{\mathcal{E}_{\mathrm{D},1} + \mathcal{E}_{\mathrm{D},2}}{2}) \quad (3.37)$$

$$P_{e,2} \leq \left\lceil 2^B \theta \sqrt{1-\rho^2} \right\rceil 2^B \Pr(E_{e\to c,1})^2 P_2(2, \mathcal{E}_{\mathrm{D},1}) + \left\lceil 2^B \theta \sqrt{1-\rho^2} \right\rceil 2^B P_2(4, \mathcal{E}_{\mathrm{D},1} + \mathcal{E}_{\mathrm{D},2}) \quad (3.38)$$

$\Pr(E_{e\to c,1})$, error probability of an uncorrectable error to occur in the first round, is defined as $\sum_{j=1}^{2} \Pr(|\sqrt{\mathcal{E}_{\mathrm{C},1,j}} + z_{c,j}|^2 \leq \lambda \mathcal{E}_{\mathrm{C},1,j})$.

Quantization distortion D_q is defined by

$$D_q = \sum_{m=1}^{2^B} \sum_{n=1}^{2^B} \int_{I_{1,m}} \int_{I_{2,n}} \left[(u_1 - \hat{u}_1(m))^2 + (u_2 - \hat{u}_2(n))^2 \right] f(u_1, u_2) du_2 du_1 \quad (3.39)$$

which can be upper bounded by $K_1 e^{-2B \ln 2}$ through substituting the value of Δ. In order to emphasize the exponential term the rest of the factors are given by the coefficient K_1 which represents $O(B)$. Basically, the range within $[-\Delta, \Delta]$ is uniformly quantized whereas the tails are bounded as Q functions. In the same way, for the distortion term $D_{e,2}$, which is caused by the channel when both sources are in error regardless of being compatible or incompatible, is defined as given below.

$$D_{e,2} < 2\left(4\Delta^2 \Pr(|u_j| < \Delta)\right) + 2\left(\int_{\Delta}^{\infty} (u_j + \Delta)^2 f(u_j) du_j + \int_{-\infty}^{-\Delta} (u_j - \Delta)^2 f(u_j) du_j\right) \quad (3.40)$$

We used uniform quantization for the area between the quantization levels under the bell curve and the tails are bounded using an approriate bound on Q functions. The distortion caused by one source to be in error are given below for compatible and incompatible pairs

$$D_{e,c,1} < \sum_{n=1}^{2^B} \int_{I_{j,n}} (u_j - \hat{u}_j(n))^2 f(u_j) du_j + |2\theta^2 \sqrt{1-\rho^2}|^2, \quad (3.41)$$

$$D_{e,ic,1} < \sum_{n=1}^{2^B} \int_{I_{j,n}} (u_j - \hat{u}_j(n))^2 f(u_j) du_j + \int_{u_2'=\theta}^{\infty} \left(\theta\sqrt{1-\rho^2} + \sqrt{1-\rho^2}u_2'\right)^2 f(u_2'||U_2'| > \theta\sqrt{1-\rho^2}) d_{u_2'}, \quad (3.42)$$

respectively. But basically, regardless of being compatible both $D_{e,c,1}$ and $D_{e,ic,1}$ contain one source which is correctly decoded. Therefore both distortion terms include D_q for one of the sources. The inner part under the bell-curve, i.e. the range between the quantization levels, and the tails are treated separately also for the case of 1 source being in error conditioned to be inside (for $D_{e,c,1}$) or outside (for $D_{e,ic,1}$) of the compatible zone ($|\rho U_1 - U_2| < \theta$). For further detail in the derivations of the bounds above, see 6.2.7.

The overall distortion at the end of the second round (3.36) is obtained by substituting error probabilities (3.37) and (3.38) with corresponding distortion terms and given in the explicit form as follows

$$\begin{aligned} D \leq\ & K_1 D_q + K_2 D_{e,ic,1} e^{-\frac{\theta^2(1-\rho^2)}{2}} \\ & + \left(K_3\theta\sqrt{1-\rho^2}e^{B\ln 2} + K_4\epsilon(\rho)\right) D_{e,2} e^{(B-3)\ln 2 - \frac{\mathcal{E}_{\mathrm{D},1}+\mathcal{E}_{\mathrm{C},1}(\sqrt{\lambda}-1)^2}{2N_0}} \\ & + \left(K_5\theta\sqrt{1-\rho^2}e^{B\ln 2} + K_6\epsilon(\rho)\right) D_{e,c,1} e^{-\frac{\mathcal{E}_{\mathrm{D},1}+2\mathcal{E}_{\mathrm{C},1}(\sqrt{\lambda}-1)^2}{4N_0}} \\ & + \left(K_7\theta\sqrt{1-\rho^2}e^{B\ln 2} + K_8\epsilon(\rho)\right) D_{e,2} e^{(B-7)\ln 2 - \frac{\mathcal{E}_{\mathrm{D},1}+\mathcal{E}_{\mathrm{D},2}}{2N_0}} \\ & + \left(K_9\theta\sqrt{1-\rho^2}e^{B\ln 2} + K_{10}\epsilon(\rho)\right) D_{e,c,1} e^{-\frac{\mathcal{E}_{\mathrm{D},1}+\mathcal{E}_{\mathrm{D},2}}{4N_0}} \\ & + \left(K_{11}\theta\sqrt{1-\rho^2}e^{B\ln 2} + K_{12}\epsilon(\rho)\right) D_{e,2} e^{B\ln 2 - \frac{\theta^2(1-\rho^2)}{2} - \frac{\mathcal{E}_{\mathrm{D},1}+\mathcal{E}_{\mathrm{C},1}(\sqrt{\lambda}-1)^2}{2N_0}} \\ & + \left(K_{13}\theta\sqrt{1-\rho^2}e^{B\ln 2} + K_{14}\epsilon(\rho)\right) D_{e,2} e^{B\ln 2 - \frac{\theta^2(1-\rho^2)}{2} - \frac{\mathcal{E}_{\mathrm{D},1}+\mathcal{E}_{\mathrm{D},2}}{2N_0}} \end{aligned} \quad (3.43)$$

where $K_2 = 1/2$, $K_3, K_4, K_5, K_6, K_{11}$ and , K_{12} are $O(\mathcal{E}_{\mathrm{D},1})$ and the rest of the factors are $O((\mathcal{E}_{\mathrm{D},1} + \mathcal{E}_{\mathrm{D},2})^3)$ with $\epsilon(\rho) \in [0, 1)$. For simplification in calculations, the energy used by a source on a particular phase is assumed to be half of the energy on the corresponding round, e.g. $\mathcal{E}_{D,1} = 2\mathcal{E}_{D,1,1} = 2\mathcal{E}_{D,1,2}$. Equating the order of the exponentials for the case of low correlation, i.e. $\theta > 2\sqrt{\frac{B\ln 2}{(1-\rho^2)}}$, we can set the relations of the energies as $\mathcal{E}_{\mathrm{C},1} = \frac{\mathcal{E}_{\mathrm{D},2}}{2(\sqrt{\lambda}-1)^2}$ and $\mathcal{E}_{D,2} = (2-\mu)\mathcal{E}_{D,1}$ where μ is an arbitrary constant within the interval

$(0, 2)$.

$$D_{low} \leq e^{-\frac{\mathcal{E}_{\mathrm{D},1}(1-\mu/4)}{2N_0}}\gamma(\mathcal{E}_{\mathrm{D},1}, \rho) + e^{-\frac{\mathcal{E}_{\mathrm{D},1}(1-\mu/3)}{2N_0}}\delta(\mathcal{E}_{\mathrm{D},1}, \rho) + e^{-\frac{\mathcal{E}_{\mathrm{D},1}(3-\mu)}{4N_0}}\vartheta(\mathcal{E}_{\mathrm{D},1}, \rho) \quad (3.44)$$

$$D_{high} \leq e^{-\frac{\mathcal{E}_{\mathrm{D},1}(1-\mu/3)}{N_0}}\alpha(\mathcal{E}_{\mathrm{D},1}) + K_6 e^{-\frac{\mathcal{E}_{\mathrm{D},1}(9-2\mu)}{4N_0}} + K_{10}e^{-\frac{\mathcal{E}_{\mathrm{D},1}(7-\mu)}{4N_0}} \quad (3.45)$$

Under this condition, the distortion (3.43) yields the bound (3.44) where γ, ω and ϑ are functions of $\mathcal{E}_{\mathrm{D},1}$ and ρ and arose from $K_3, K_4, K_5, K_6, K_9, K_10$ and K_7, K_8, respectively. On the other hand for the highly correlated sources, we set the relations of the energies as $\mathcal{E}_{C,1} = \frac{\mathcal{E}_{D,2}}{(1-\sqrt{\lambda})^2}$ and $\mathcal{E}_{D,2} = (2-\mu)\mathcal{E}_{D,1}$ where μ is an arbitrary constant satisfying $\mu \in (0, 2)$ and the final bound becomes as given by (3.45) whereas α is a function of $\mathcal{E}_{\mathrm{D},1}$ which arose from K_4, K_8, K_{12}, K_{14} together with the distortion terms and given by $\alpha(\mathcal{E}_{\mathrm{D},1}, \rho) = \left(4\sqrt{\frac{\mathcal{E}_{\mathrm{D},1}}{\pi N_0}} + 16\frac{\mathcal{E}_{\mathrm{D},1}}{N_0}\right)^{-2/3}$. The amount of energy used by the protocol is arbitrarily close to the energy consumed by the first data phase assured by vanishing error probability in this round. The exponential behaviour observed in (3.45) is the same with a single source yields in [55]. Note that there is a difference of factor $1/2$ in the exponentials of the significant term in (3.45) and the information theoretic bound given by (3.12) where both upper and lower bounds represent the case of highly correlated sources.

3.4 Numerical Evaluation for the Dual-Source Case

The numerical evaluation of the distortion bounds for the dual-source case are given by Figure (3.4). In this plot, the red curves represent the outer bounds (3.20) derived in Section 3.2 for different values of B, where we have chosen $1 - \rho^2 = 2^{-2B}$. The blue curves are the upper bound (3.27) on distortion analyzed in Section 3.3. The green curves are drawn for a protocol terminated after the first round which is the case without feedback. We see from the lower-bounds that the energy accumulation remains feasible even at distortions below that of a uniform quantizer with B-bits (the asymptotes of the proposed scheme). In practice, this suggests that the quantizer bin size should be chosen such that the difference in amplitude between the two sources should be on the order of the quantization error (i.e. 1-bit deviation between the sources). We also see that the asymptotic performance does not emerge for small values of B using the derived bounds, necessitating further numerical study of the proposed scheme in this case in order to

better judge the gap from the lower-bounds. Nevertheless, the improvement using feedback is very significant, even for small values of B.

Additionally, in order to make a comparison between the lower bounds only, we present the numerical evaluation of the bounds derived in subsections (3.2.1), (3.2.2) and (3.2.3) for the uniform case. Note that, the lower bound III is evaluated for its squared root for equal distortions per source where the horizontal line in each plot represents 2^{-2B} or equaivalently $(1-\rho^2)$ which is the distortion resulting from the estimation of one source realization using the other. Clearly, increasing B (or equivalently increasing ρ) directly effects the significance moreover the usefulness of the bounds. Lower bound II (low correlation bound) becomes useless as B increases whereas the product bound dominates the high correlation bound in the high SNR regime.

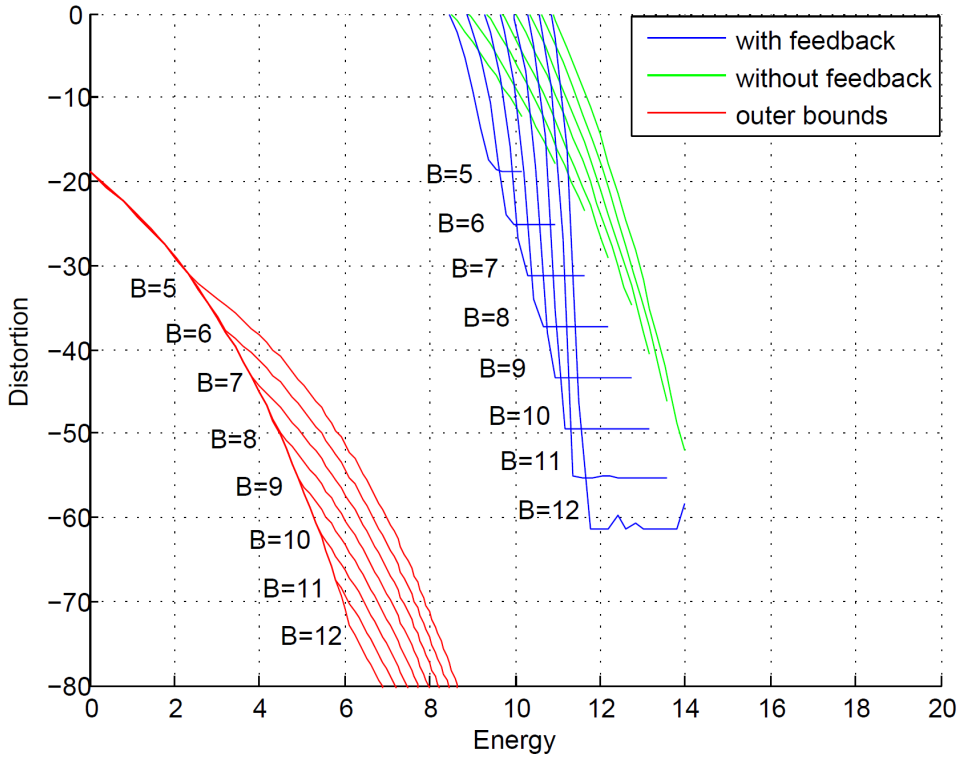

Figure 3.4: Numerical evaluation of the derived upper and lower bounds on distortion for different values of B for uniform/contaminated uniform dual-source case.

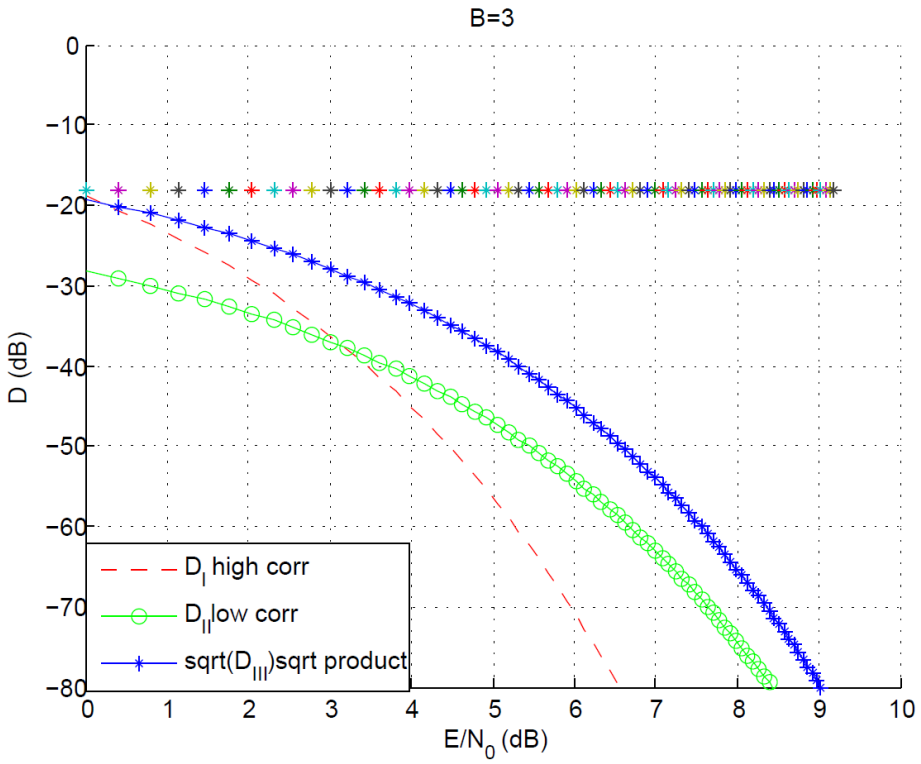

Figure 3.5: Numerical evaluation of the lower bounds I, II and III for $B = 3$.

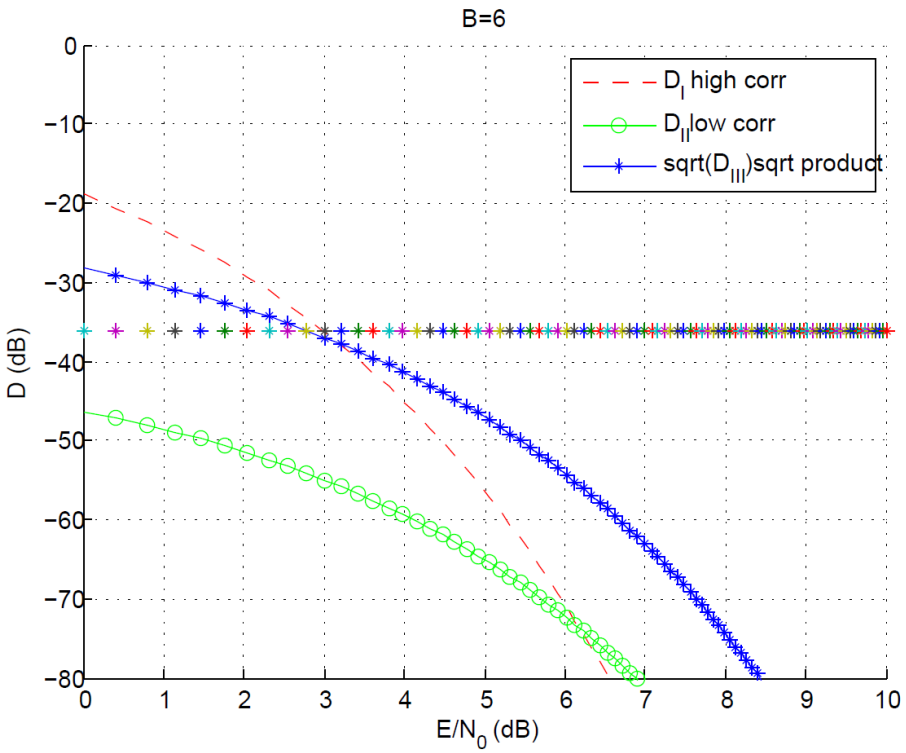

Figure 3.6: Numerical evaluation of the lower bounds I, II and III for $B = 6$.

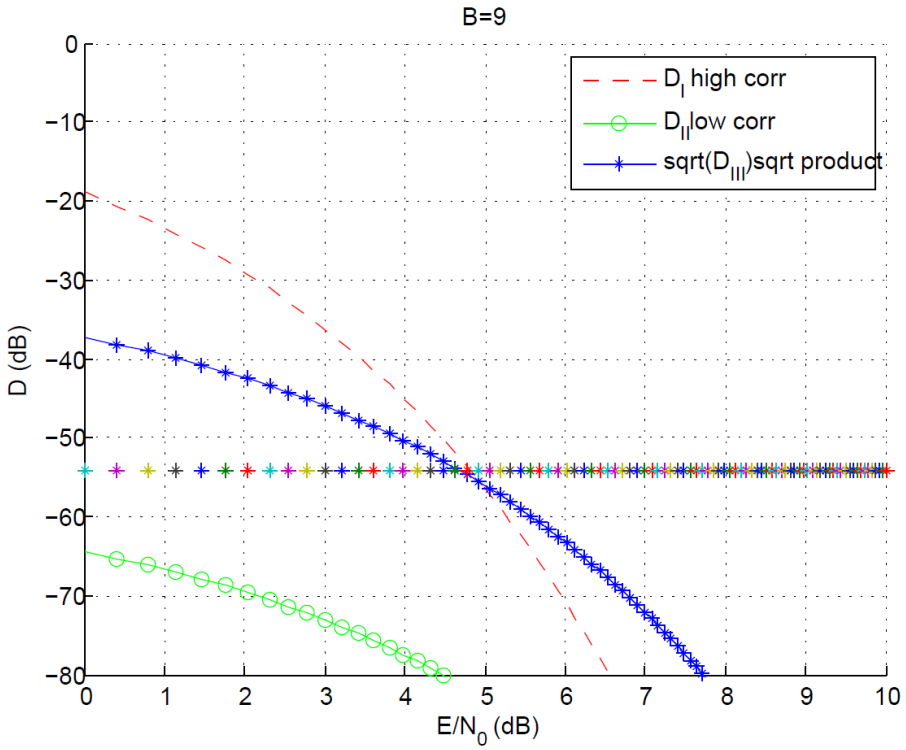

Figure 3.7: Numerical evaluation of the lower bounds I, II and III for $B = 9$.

Chapter 4

Distributed Sensing and Transmission in a MAC

This chapter focuses on the problem of transmitting correlated analog sources over a Gaussian multiple-access channel with a feedback link from the receiver to each encoder. The main results of this chapter are firstly the derivation of lower-bounds governing both the reconstruction error of a single random vector imperfectly measured by a network of sensors and multiple source vectors which are transmitted to a common receiver via an additive white Gaussian noise asynchronous multiple-access channel with a perfect causal feedback link to the encoder connected to each sensor. The bounds are expressed both for a uniform random-vector source with uniformly-distributed observation noise and for a Gaussian source with Gaussian observation noise. Secondly, we extend a retransmission protocol inspired by the classical scheme in [1] applied to the transmission of single and bi-variate analog samples analyzed in Section 2 and 3 to the more general network with M noisy observations of a common random sample. We restrict the second analysis to uniform one-dimensional sources. The simple two-round transmission scheme combines uniform quantization and orthogonal modulation, for which we provide asymptotic upper-bounds on the reconstruction error as a function of the total received energy and observation noise level. Both the upper and lower-bounds show that a trade-off exists between the source SNR and channel SNR indicating the extent to which collaboration to be achieved through energy accumulation.

Finally, we investigate the practical performance of the proposed retransmission protocol through numerical evaluation of the upper-bounds in the non-asymptotic energy regime, which corresponds to using low-order quan-

tization in the sensors. In order to improve the performance of the protocol, we introduce a minor modification in the feedback strategy which allows the error-free performance to be achieved quickly. Comparisons with a one-shot transmission not exploiting feedback are made in order to judge the benefit of the protocol in the non-asymptotic regime for a few network sizes.

The outline of the chapter is as follows: in the following subsection 4.1, we give a description of the general model to explain the problem addressed. It is followed by the derivation of the information-theoretic bounds on the reconstruction error outlined above. In Section 4.4, we provide an M-sensor adaptation of Yamamoto's protocol for a uniformly-distributed source with uniform observation error along with the analysis of its asymptotic performance. In Section 4.5, we present the numerical results for a slightly different protocol and the lower bounds derived in 4.2.

4.1 Problem Definition and Model description

Let us begin with the description of the system which is shown in Figure (4.1). In a similar vein to the source-construction studied in [56, 57], we describe a general model which includes the first source as the mutual element of the whole system and combined with M other sources through a correlational relationship. The construction of the sources is given by the following linear expression.

$$\mathbf{V}_j = \rho\mathbf{U} + \sqrt{1-\rho^2}\mathbf{U}'_j \tag{4.1}$$

Here we denote the M auxiliary random vectors representing the observa-

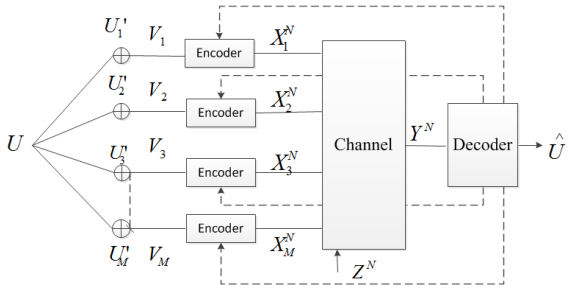

Figure 4.1: Pictorial representation of the described system

tion noise in each sensor by $\mathbf{U}'_j$ and the observation of the mutual source $\mathbf{U}$ by $\mathbf{V}_j$, both dimension of K with $j = 1, 2, ..., M$. Note that the mutual source $\mathbf{U}$ and the observation noise vectors $\mathbf{U}'_j$ are independent of each other. Each realization of $\mathbf{V}_j$ is mapped into $\mathbf{X}_j \triangleq (X_{1,j}, \ldots, X_{N,j})$ which is a representation of an N-dimensional waveform $X_j^N(t)$ using a suitable basis for $t \in [0, T]$ whose power is constrained as $\frac{1}{T}\mathrm{E}\int_0^T |x_j^N(t)|^2 dt \leq KP_j$

or equivalently $\mathrm{E}\sum_{i=1}^{N}[|X_{i,j}|^2] \leq KP_jT = K\mathcal{E}_j$ where $\mathcal{E}_j$ is the energy per dimension of the j^{th} source letter. $\mathbf{X}_j$ is then sent across the channel corrupted by a white complex circularly symmetric Gaussian noise sequence $\mathbf{Z}$, and is received as the output signal $\mathbf{Y}$. The receiver constructs an estimate $\widehat{\mathbf{U}}(\mathbf{Y})$ of $\mathbf{U}$ given $\mathbf{Y}$. The transmitted sequence $\mathbf{X}_j$ is encoded as $X_{i,j} = f_{i,j}(\mathbf{V}_j, Y_1, \cdots, Y_{i-1})$, where the function $f_{i,j}$ is an arbitrary mapping for the j^{th} sensor in dimension i and depends on perfect knowledge of past observations in the case of causal feedback. The latter models an ideal causal feedback path from the receiver. Note that, in case of no feedback the encoding function is given as $X_{i,j} = f_{i,j}(\mathbf{V}_j)$. The dimension of the channel input is denoted by N and can be assumed to be large, whereas K is assumed to be finite and small.

We consider two cases for the distribution of $\mathbf{U}$. In the first case, both the $\mathbf{U}'_j$ and $\mathbf{U}$ are uniformly distributed with zero mean and unit variance, i.e. defined in the range $(-\sqrt{3}, \sqrt{3})$. Depending on the level of correlation, $\mathbf{V}_j$ defined by (4.1) has a contaminated uniform distribution. We will consider the case where $\mathbf{V}_j$, $\mathbf{U}$ and $\mathbf{U}'_j$ are standard normally distributed which is equivalent to having the parameters $\mathcal{N}(0,1)$. The output signal is given in the following by

$$Y_i = \sum_{j=1}^{M} X_{i,j} e^{i\phi_{i,j}} + Z_i, \tag{4.2}$$

for $j = 1, 2, ..., M$ and $i = 1, ..., N$.

The criteria for source-channel code design is chosen as the squared-error distortion measure, which is $d(u_i, \hat{u}_i) = (u_i - \hat{u}_i(y))^2$ for $i = 1, 2, \cdots K$ in estimating U, and the average distortion is defined as

$$D = \frac{1}{K}\mathrm{E}\left[\sum_{i=1}^{K} d(u_i, \hat{u}(\mathbf{y}))\right]. \tag{4.3}$$

$\phi_j = \{\phi_{i,j}; i = 1, ..., N\}$ denotes the random phase sequences which are assumed to be i.i.d. uniform over $[0, 2\pi)$ and unknown to the transmitter and receiver. The latter models an asynchronous network and the fact that a coherent reception model is unrealistic for sporadic information transfer. These assumptions are implicitly relaxed in the lower bounds on the distortion discussed in the following section but are applied in the coding strategy considered in Section 4.4. On another aspect, in a system as in Figure (4.1) one could aim at reconstructing $\mathbf{V}_j$'s as studied in Section 4.3. In that case, the performance measure is defined by the set $\{D_j\}$ corresponds to each $\mathbf{V}_j$ due to the squared-error distance between their estimates; i.e. for a single V_j we get $\frac{1}{K}\mathrm{E}\left[\sum_{i=1}^{K} d(v_{i,j} - \hat{v}_j(\mathbf{y}))\right]$.

4.2 Estimation of U

In order to obtain a bound on the fidelity of estimating the random vector $\mathbf{U}$, we obtain upper and lower bounds on a cut-set mutual information functional $I(\mathbf{U};\mathbf{Y}|\{\mathbf{V}_j\}_S)$ based on a subset $S \subseteq 1,2,\cdots,M$ and its complement S^c. $\{\mathbf{V}_j\}_S$ denotes the subset of $\mathbf{V}_j$'s for $j \in S$. The bounds which are derived based on the source and output signal expansions of the mutual information $I(\mathbf{U};\mathbf{Y}|\{\mathbf{V}_j\}_S)$ are summarized as

$$I(\mathbf{U};\mathbf{Y}|\{\mathbf{V}_j\}_S) \geq -h(\{\mathbf{V}_j\}_S) + h(\{\mathbf{V}_j\}_S|\mathbf{U}) + h(\mathbf{U}) - h(\mathbf{U}-\hat{\mathbf{U}}), \quad (4.4)$$

$$I(\mathbf{U};\mathbf{Y}|\{\mathbf{V}_j\}_S) \leq N \log\left(1 + \frac{K\sum_{j\in S^c}\mathcal{E}_j}{NN_0}\right), \quad (4.5)$$

respectively. The derivations of the bounds given above can be found in detail in Appendix 6.3.1 for both uniform and normal distributions.

Combination of (4.4) and (4.5) allows us to express the distortion level for estimating the mutual random vector $\mathbf{U}$ as

$$D \geq \max_{|S|} C_D \frac{1-\rho^2}{1+(|S|-1)\rho^2}\left(1 + \frac{K\sum_{j\in S^c}\mathcal{E}_j}{NN_0}\right)^{-\frac{2N}{K}} \quad (4.6)$$

where C_D is a constant which varies based on the distribution type and defined as

$$C_D = \begin{cases} (\frac{6}{\pi e})^{|S|+1}, & \text{for } U \sim \mathcal{U}(-\sqrt{3},\sqrt{3}) \\ 1, & \text{for } U \sim \mathcal{N}(0,1). \end{cases}$$

The general bound given above by (4.6) includes two parameters; the correlation coefficient ρ and the energy term and is valid for all $0 \leq |S| \leq M$. In the source-channel coding scheme proposed in the following section which targets broadband networks and small amounts of analog information, we are mostly interested in the case where $N \gg K$, or where the channel bandwidth is significantly higher than the source bandwidth. For $N \to \infty$ and $\mathcal{E}_j = \mathcal{E}\ \ \forall j$, (4.6) becomes

$$D \geq \max_{|S|} C_D \frac{1-\rho^2}{1+(|S|-1)\rho^2}\exp\left(-\frac{2(M-|S|)\mathcal{E}}{N_0}\right) \quad (4.7)$$

which can easily be simplified to

$$D \geq \begin{cases} C_D\left(\frac{1-\rho^2}{1+(M-1)\rho^2}\right), & \frac{1+(M-2)\rho^2}{1+(M-1)\rho^2} \geq e^{-\frac{2\mathcal{E}}{N_0}} \\ \ldots & \\ C_D\left(\frac{1-\rho^2}{1+(i-1)\rho^2}\right)e^{-\frac{2(M-i)\mathcal{E}}{N_0}}, & \frac{1+(M-i-1)\rho^2}{1+(M-i)\rho^2} \geq e^{-\frac{2\mathcal{E}}{N_0}} \\ \ldots & \\ C_D\exp\left(-\frac{2M\mathcal{E}}{N_0}\right), & 1-\rho^2 \leq e^{-\frac{2\mathcal{E}}{N_0}}. \end{cases} \quad (4.8)$$

The above result brings to light the effect of collaboration between the sensors which is achieved either through the spatial expansion in the channel or in the source. To see this, we note that the condition for the i^{th} source $\frac{1+(M-i-1)\rho^2}{1+(M-i)\rho^2} \geq e^{-\frac{2\mathcal{E}}{N_0}}$ is equivalent to saying that the distortion in each sensor node induced by the observation process is more significant than the lowest distortion offered by the channel when estimating $\mathbf{V}_j$ (which is $D_c \geq e^{-\frac{2\mathcal{E}}{N_0}}$) in the absence of the signals from the other sensors. Note that this is the classical point-to-point optimal distortion derived in [4]. A comparable trade-off regarding the collaboration effect due to the source or channel can be seen in [32, 33] for the case $K = N$. As mentioned in the introduction, another example is the Gaussian sensor network application [58, sections VI and VII] (again for $K = N$) or the CEO (Central Estimating Officer) problem studied in [26, 27, 59], where estimation fidelity decays linearly with the size of the network in a manner similar to (4.6).

For the case $|S| = M$ (first line of (4.8)), the distortion is simply that of the conditional estimator of $\mathbf{U}$ with prior knowledge of $\mathbf{V}_j$ for $j = 1, \cdots, M$ that is $\mathrm{E}\left\{||\mathbf{U} - \hat{\mathbf{U}}||^2 | \mathbf{V}_j, j = 1, \cdots, M\right\}$. This can be alternatively derived using the results of [44]. Let us now consider the vector channel model $\mathbf{Y} = \sqrt{snr}\mathbf{H}\mathbf{X} + \mathbf{N}$ analyzed in [44], where $\mathbf{X}$ and $\mathbf{Y}$ are the input and output signals, $\mathbf{H}$ is a deterministic matrix and $\mathbf{N}$ represents the channel noise in the described model. The source component of our system (i.e. up to the input of the channel encoder) can be simply considered as a special-case of the estimation problem treated in [44, eq.19] through the following definition for the Gaussian construction,

$$\mathbf{Y}' = \frac{\rho}{\sqrt{1-\rho^2}}\mathbf{H}\mathbf{X} + \mathbf{N}. \tag{4.9}$$

Here in (4.9), our mutual source $\mathbf{U}$ from the model (4.1) is replaced by the vector $\mathbf{X}$, the auxiliary random vector $\mathbf{U}'_j$ in other words the observation noise is represented by the channel noise $\mathbf{N}$, where the output signal $\mathbf{Y}' = \mathbf{Y}/\sqrt{1-\rho^2}$ corresponds to the vector of $\mathbf{V}_j$'s in our model. Attaining the corresponding vectors, we obtain the mean square error in estimating mutual source $\mathbf{U}$ conditioned on a set of $\mathbf{V}_j$'s given above by (4.7) which is no different than estimating $\mathbf{HX}$ in the original work as

$$\mathrm{E}\left\{||\mathbf{U} - \hat{\mathbf{U}}||^2 | \{\mathbf{V}_j\}\right\} = \frac{1-\rho^2}{1+(M-1)\rho^2} \tag{4.10}$$

since $\mathbf{H}$ is an all-one matrix and where $\hat{\mathbf{U}}$ is the conditional mean estimate.

4.3 Estimation of the set of V_j's

Another way of approaching to the multiple-source problem is the estimation of $\mathbf{V}_j$'s instead of the mutual element $\mathbf{U}$. In contrast to the previous section

which provides a lower bound on the best estimator of the common random variable, in this part we provide lower bounds on the sum and product mean squared error of subsets of sources for individual estimators.

4.3.1 Bound on product distortion $\prod_{j=1}^{M} D_j$

Another way of approaching to the multiple-source problem is the estimation of $\mathbf{V}_j$'s instead of the mutual element $\mathbf{U}$. The product distortion $D_1 D_2 ... D_M$ is bounded using two different expansions of $I(\mathbf{V}_j; \mathbf{Y})$ for both uniformly and normally distributed sources, where $\mathbf{V}_j$ is the whole set with $j = 1, 2, ..., M$. The resulting lower bound on $\prod_{j=1}^{M} D_j$ is obtained as

$$\prod_{j=1}^{M} D_j \geq C_p \left(1 + \frac{KM\mathcal{E}}{NN_0}\right)^{-2N/K} \tag{4.11}$$

with

$$C_p = \begin{cases} (1-\rho^2)^M (1 + \frac{M\rho^2}{1-\rho^2}), & \text{for Gaussian} \\ \left(\frac{6(1-\rho^2)}{\pi e}\right)^M, & \text{for Uniform.} \end{cases}$$

where $\mathcal{E}_j = \mathcal{E} \ \ \forall j$. Let $N \to \infty$, the lower bound (4.11) becomes

$$\prod_{j=1}^{M} D_j \geq C_p \exp\left(-\frac{2M\mathcal{E}}{N_0}\right). \tag{4.12}$$

Lower bound (4.12) can be simplified to $D \geq (C_p)^{1/M} \exp\left(-\frac{2\mathcal{E}}{N_0}\right)$ by taking the M^{th} root for equal distortions per source, i.e. $D_j = D \ \ \forall j$, which is the Goblick bound [4] achieved for a point to point channel. The derivations are given in detail in Appendix 6.3.2.

4.3.2 Bound on some subset of V_j's

In addition to the lower bound (4.12) on the product distortion in estimating V_j's introduced in the previous subsection, in this final information theoretic part, we introduce an alternative lower bound on the squared-error distortion in estimating V_j's.The mutual information that is used to obtain the lower bound on the reconstruction error is $I(\mathbf{V}_j; \mathbf{Y} | \{\mathbf{V}_l\}_S)$ where $\{\mathbf{V}_l\}_S$ denotes the set of V_j's (any subset to be chosen) which excludes j, i.e. $\{\mathbf{V}_l \in S, S \subset \{1, ..., M\} - j\}$. First expansion of $I(\mathbf{V}_j; \mathbf{Y} | \{\mathbf{V}_l\}_S)$ based on the output signal proceeds in the same way for both distribution types as follows

$$I(\mathbf{V}_j; \mathbf{Y} | \{\mathbf{V}_l\}_S) \leq N \log\left(1 + \frac{K \sum_{j \in S^c} \mathcal{E}_j}{NN_0}\right). \tag{4.13}$$

Note that the expansion given above is independent of the source distribution. We obtain the following second expansion based on the source entropies as

$$I(\mathbf{V}_j;\mathbf{Y}|\{\mathbf{V}_l\}_S) \geq -h(\{\mathbf{V}_l\}_S)+h(\{\mathbf{V}_l\}_S|\mathbf{V}_j)+h(\mathbf{V}_j)-h(\mathbf{V}_j-\hat{\mathbf{V}}_j). \quad (4.14)$$

The derivations of (4.13) and (4.14) can be found in detail in the Appendix 6.3.3. The two bounds on the same mutual information $I(\mathbf{V}_j;\mathbf{Y}|\{\mathbf{V}_l\}_S)$ given by (4.13) and (4.14) are equated to obtain the following lower-bound on the sum distortion

$$\sum_{j\in S^c} D_j \geq C_{sum}\left(1+\frac{K\sum_{j\in S^c}\mathcal{E}_j}{NN_0}\right)^{-\frac{2N}{K}}. \quad (4.15)$$

where C_{sum} is a constant differs based on the source distribution and given as

$$C_{sum} = \begin{cases} \frac{(1-\rho^2)}{1+(|S|-1)\rho^2}(2-\rho^2+|S|), & \text{for Gaussian} \\ \frac{(1-\rho^2)}{1+(|S|-1)\rho^2}(\frac{6}{\pi e})^{|S|+1}, & \text{for Uniform.} \end{cases}$$

for $S \in [1, M-1]$. Asymptotically in N, we obtain

$$\sum_{j\in S^c} D_j \geq C_{sum}\exp\left(-\frac{2(M-|S|)\mathcal{E}_j}{N_0}\right). \quad (4.16)$$

Note that in this case due to the definition of $\{\mathbf{V}_l\}_S$, the size of the set S cannot exceed $M-1$, which clearly means that unlike the lower bound on the reconstruction error in estimating the mutual source $\mathbf{U}$ given by (4.7)-(4.8), the lower bounds given above by (4.12) and (4.16) always have the exponential behaviour for any values of M. For the special case of $|S|=0$, $\sum_{j\in S^c} D_j$ yields

$$\sum_{j\in S^c} D_j \geq \begin{cases} \exp\left(-\frac{2M\mathcal{E}_j}{N_0}\right), & \text{for Gaussian} \\ \frac{6}{\pi e}\exp\left(-\frac{2M\mathcal{E}_j}{N_0}\right), & \text{for Uniform} \end{cases} \quad (4.17)$$

since we lose the prior knowledge of $\{\mathbf{V}_l\}_S$ which effects the expansion on the source entropies given above by (4.14). The detailed derivation is given in Appendix 6.3.3.

4.4 Achievable Scheme for a network with Uniform sources

The two-way protocol introduced in [55] for a single source and its extension to dual-source studied in detail in [56] is generalized to large networks where the same approach is applied to a scheme with M sources for $M \geq 2$. As

depicted in Figure (4.1), there is one mutual source which is represented by U, and M other auxiliary random variables which are combined in pairs linearly through (4.1) each of which includes U through a correlational relationship and are distributed uniformly included within the range $(-\sqrt{3}, \sqrt{3})$.

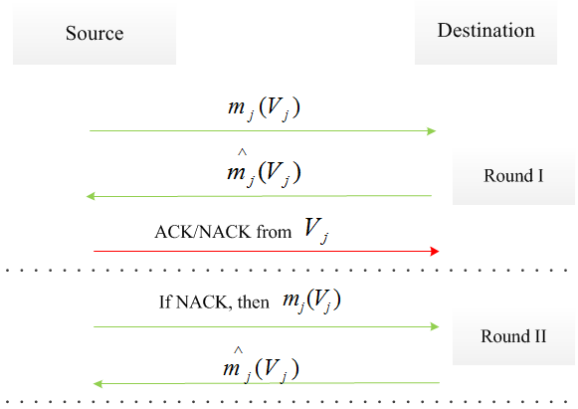

Figure 4.2: Two-round protocol

The protocol consists of two phases which composes one round and proceeds as depicted in Figure (4.2). First phase is called the data phase, in which the first transmission occurs and in return feedback of the messages are received from the decoder by each encoder. The quantization process is depicted in Figure (3.2). We assume that the source sample of the j^{th} source which is uniformly quantized is subsequently encoded into 2^{B_j} messages with dimension N where B_j's are equal to the same value B. Each tail of the distribution is considered as one quantization bin and the interior part, which consists of $2^B - 2$ bins, is uniformly quantized. Note that, for a full correlation between the sources, i.e. $\rho = 1$, the 'contamination' in the source distribution vanishes and the shape given by Figure (3.2) becomes a rectangular. We fix the total energy that is used by protocol and for the sake of simplicity the energy used in one round is allocated equally among V_j's for $j = 1, 2, ..., M$, e.g. for the data phase of the first round the aggregate energy is denoted by $\mathcal{E}_{\mathrm{D},1}$ where $\mathcal{E}_{\mathrm{D},1} = \sum_{j=1}^{M} \mathcal{E}_{\mathrm{D},1,j}$ as $\mathcal{E}_{\mathrm{D},1,j}$ represents the energy on each source. The chosen method is 2^B-ary orthogonal modulation with non-coherent reception. In the data phase, the j^{th}source sends its message $m_j = Q(V_j)$ to the receiver with energy $\mathcal{E}_{\mathrm{D},1,j}$. The aggregated source messages are denoted by $\mathbf{m}$ which is a vector of the messages $(m_1, m_2, ..., m_M)$ with dimension M. Note that, all messages from different sources are mutually orthogonal. The receiver decodes $\hat{m}_j$ and feeds it back. The output signal based on the N dimensional observation of the j^{th} source is given as

$$\mathbf{Y}_{d_j} = \sqrt{\mathcal{E}_{\mathrm{D},1,j}} e^{j\Phi_j} \mathbf{S}_{m_j} + \mathbf{Z}_{d_j}. \tag{4.18}$$

We assume the random phases Φ_j to be distributed uniformly on $[0, 2\pi)$, the channel noise $\mathbf{Z}_{d_j}$ to have zero mean and equal autocorrelation $N_0\mathbf{I}_{N\times N}$ for $j = 1, 2, ..., M$ and $\mathbf{S}_{m_j}$ are the N-dimensional messages, with $m = 1, 2, \cdots, 2^B$. At the receiver end, we consider the following exhaustive search as depicted in Figure (4.3). To decode the first m_1, there are 2^B possibilities whereas $m_{j>1}$ is constrained to $2^B(\frac{2\sqrt{1-\rho^2}}{\rho+\sqrt{1-\rho^2}})$ since it cannot fall outside of the interval $V_1 + \sqrt{1-\rho^2}(U'_j - U'_1)$. The detection rule is given using

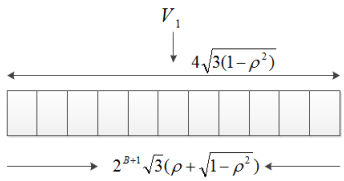

Figure 4.3: Pictorial representation of detection

[48, Chapter 12,eq:12-1-16] considering the following M possible decision variables assuming $(m_1, m_2, ..., m_M)$ is transmitted.

$$\begin{aligned}\mathbf{U}_{\mathbf{m}'} &= \sum_{j=1}^{M} |< \mathbf{Y}_j, \mathbf{S}_{m_j} >|^2 \\ &= \sum_{j:m_j=m'_j} |\sqrt{\mathcal{E}_{D,1,j}} + N_j|^2 + \sum_{j:m_j\neq m'_j} |N_j|^2. \end{aligned} \tag{4.19}$$

Here $< ., . >$ denotes the inner product.

According to (4.19), the receiver chooses $\hat{\mathbf{m}} = \text{argmax}_{\hat{\mathbf{m}'}}\ \mathbf{U}_{\mathbf{m}'}$. After the estimation and feedback of $\hat{m}_j$ to each encoder, data phase of the first round ends and the encoders enter the control phase to inform the receiver about the correctness of its decision by sending an ACK/NACK signal regarding its own message to the decoder. During the control phase the receiver observes $\mathbf{Y}_c$ with $\mathbf{Y}_{c_j} = \sqrt{\mathcal{E}_{\mathrm{C},1,j}}A_j e^{j\Phi_j}\mathbf{S}_{c_j} + \mathbf{Z}_{c_j}$ for j^{th} source where A_j takes the value 0 for an ACK signal and 1 for a NACK and $\mathcal{E}_{\mathrm{C},1,j}$ denotes the energy of the control phase in the first round on one source. So the encoders inform the receiver whether or not its decision was correct via a signal $\sqrt{\mathcal{E}_{\mathrm{C},1,j}}\mathbf{S}_{c_j}$ of energy $\sqrt{\mathcal{E}_{\mathrm{C},1,j}}$ if the decision is incorrect and $\mathbf{0}$ if the decision was correct. The detector, which is basically the receiver's estimate of A_j, is given for the j^{th} source as

$$\hat{A}_j = \mathcal{I}\left(|y_{c,j}|^2 > \lambda\mathcal{E}_{\mathrm{C},1,j}\right) \tag{4.20}$$

with $y_{c,j} = \mathbf{Y}_{c,j}^H\mathbf{S}_{c,j}$ where $\mathcal{I}(\cdot)$ is the indicator function and λ is a threshold to be optimized that is included within the interval $[0, 1)$. $\Pr(E_{e\to c,1}|k\ \ in\ \ error)$ denotes the total probability of uncorrectable error given that k sources are in error in the first round where the probability for a single source is bounded

by the recent bound introduced in [60, eq. 12]

$$\begin{aligned}\Pr(E_{e\to c,1,j}) &= \Pr(|\sqrt{\mathcal{E}_{\mathrm{C},1,j}} + z_{c,j}|^2 \le \lambda\mathcal{E}_{\mathrm{C},1,j}) \\ &= 1 - Q_1\left(\sqrt{\frac{\mathcal{E}_{\mathrm{C},1,j}}{N_0/2}}, \sqrt{\frac{\lambda\mathcal{E}_{\mathrm{C},1,j}}{N_0/2}}\right) \\ &\overset{(a)}{\le} 1/2\exp\left(-\frac{(\sqrt{\lambda}-1)^2\mathcal{E}_{\mathrm{C},1,j}}{N_0}\right). \end{aligned} \tag{4.21}$$

Using the bound given above, the probability yields for k sources

$$\Pr(E_{e\to c,1}|k \;\; in \;\; error) \le \left(\frac{1}{2}\right)^k \exp\left(-\frac{k(\sqrt{\lambda}-1)^2\mathcal{E}_{\mathrm{C},1}}{MN_0}\right) \tag{4.22}$$

where $\mathcal{E}_{\mathrm{C},1,j} = \mathcal{E}_{\mathrm{C},1}/M \quad \forall j$. In the case of at least one NACK out of M control signals is received, the protocol goes on one more round for retransmission, otherwise it is terminated. And the second data phase starts after the sources are instructed by the destination in order to do the retransmission. Note that the scheme could be generalized to more than two rounds.

The probability of error for binary orthogonal signaling $P_2(k)$ is defined in [48, eq:12-1-24] through the following equality

$$P_2(k) = \frac{1}{2^{2k-1}}e^{-\gamma}C_k \tag{4.23}$$

with C_k defined as

$$C_k = \sum_{n=0}^{k-1}\left(\frac{1}{n!}\sum_{l=0}^{k-1-n}\binom{2k-1}{l}\right)\gamma^n \tag{4.24}$$

where γ denotes the SNR. Using (4.23), the union bound on $P_e(\mathbf{m})$, the probability of error at the end of the first round, is given by

$$\begin{aligned} P_e(\mathbf{m}) &\le \sum_{\mathbf{m}\neq\mathbf{m}'} \Pr(\mathbf{U}_{\mathbf{m}} < \mathbf{U}_{\mathbf{m}'}|\mathbf{m}) \\ &= 2^B\left[2^{B+1}\frac{\sqrt{1-\rho^2}}{\rho+\sqrt{1-\rho^2}}\right]^{M-1} P_2(M) \\ &\quad + \sum_{k=1}^{M-1}\binom{M}{k}\left[2^{B+1}\frac{\sqrt{1-\rho^2}}{\rho+\sqrt{1-\rho^2}}\right]^k P_2(k). \end{aligned} \tag{4.25}$$

The decision variables (4.19) are used to bound the conditional probability (4.25). Second round decision variables are represented by $\mathbf{U}^{(2)}_{\mathbf{m}'}$ and given by

$$\mathbf{U}^{(2)}_{\mathbf{m}'} = \mathbf{U}_{\mathbf{m}'} + \sum_{j=1}^{M} |<\mathbf{Y}^{(2)}_j, \mathbf{S}_{m_j}>|^2. \tag{4.26}$$

This is analogous to soft or chase-combining in HARQ mechanisms. As in the first round, the receiver chooses $\hat{\mathbf{m}} = \text{argmax}_{\hat{\mathbf{m}}'} \, \mathbf{U}^{(2)}_{\mathbf{m}'}$ over all possible sequences, thereby disregarding the messages which were hypothesized to be correct after the control phase. Let us consider two different cases of error events as all M sources to be in error and at least one out of M sources to be correctly decoded. We denote the corresponding error probability and distortion term by $P_{e,M}$ and $D_{e,M}$ for the first case. In the same way $P_{e,k}$ and the distortion $D_{e,k}$ are used to represent the case where k corresponds to the number of the sources in error with the values $k = 1, ..., M-1$. $P_{e,k}$ which is the case of any of k sources being in error including the uncorrectable error after the first round, or k being in error at the end of the second round consists of $P_2(2k)$ and $P_2(k)$ from (4.23) is given by

$$
\begin{aligned}
&P_{e,k} \leq \\
&\sum_{\substack{\mathbf{m}' \neq \mathbf{m} \\ d_H(\mathbf{m}', \mathbf{m}) = k}} \Big(\Pr(\mathbf{U}_{\mathbf{m}} < \mathbf{U}_{\mathbf{m}'} | \mathbf{m}) \Pr(E_{e \to c,1} | k \;\; in \;\; error) + \Pr(\mathbf{U}^{(2)}_{\mathbf{m}} < \mathbf{U}^{(2)}_{\mathbf{m}'} | \mathbf{m}) \Big) \\
&\qquad = \binom{M}{k} \left\lceil 2^{B+1} \frac{\sqrt{1-\rho^2}}{\rho + \sqrt{1-\rho^2}} \right\rceil^k \Pr(E_{e \to c,1} | k \;\; in \;\; error) P_2(k) \\
&\qquad\qquad + \binom{M}{k} \left\lceil 2^{B+1} \frac{\sqrt{1-\rho^2}}{\rho + \sqrt{1-\rho^2}} \right\rceil^k P_2(2k) \quad (4.27)
\end{aligned}
$$

where $d_H(\mathbf{x}, \mathbf{y})$ denotes the Hamming distance between two vectors $\mathbf{x}$ and $\mathbf{y}$. $P_{e,M}$ represents all of the M sources being in error after the first or second round. In the same way, $P_2(M)$ and $P_2(2M)$ shape together $P_{e,M}$ as given in the following form.

$$
\begin{aligned}
&P_{e,M} \leq \\
&\sum_{\substack{\mathbf{m}' \neq \mathbf{m} \\ d_H(\mathbf{m}', \mathbf{m}) = M}} \Big(\Pr(\mathbf{U}_{\mathbf{m}} < \mathbf{U}_{\mathbf{m}'} | \mathbf{m}) \Pr(E_{e \to c,1} | M \;\; in \;\; error) + \Pr(\mathbf{U}^{(2)}_{\mathbf{m}} < \mathbf{U}^{(2)}_{\mathbf{m}'} | \mathbf{m}) \Big) \\
&\qquad = 2^B \left\lceil 2^{B+1} \frac{\sqrt{1-\rho^2}}{\rho + \sqrt{1-\rho^2}} \right\rceil^{M-1} \Pr(E_{e \to c,1} | M \;\; in \;\; error) P_2(M) \\
&\qquad\qquad + 2^B \left\lceil 2^{B+1} \frac{\sqrt{1-\rho^2}}{\rho + \sqrt{1-\rho^2}} \right\rceil^{M-1} P_2(2M). \quad (4.28)
\end{aligned}
$$

When the message vector $\mathbf{m}$ is decoded correctly, the reconstruction error D_q is caused solely by the quantization process and the source observation error. Let us denote the estimation error by $e_q = \sum_1^M e_{q,j}$, so that its second moment $E[(u - \hat{u})^2 | l \; in \; error]$ for $l = 0$ yields the quantization distortion

with the following expansion using the chosen estimator $\hat{u} = \frac{1}{M}\sum_{j=1}^{M} \hat{v}_j/\rho$,

$$D_q = E\left[\frac{1}{\rho M}\sum_{j=1}^{M}(\sqrt{1-\rho^2}u'_j + e_{q,j})\right]^2. \tag{4.29}$$

The squared distortion when k out of M sources are decoded in error is calculated through

$$\begin{aligned} D_{e,k} &= E\left[(u-\hat{u})^2 | k \text{ in error}\right] \\ &= E\left[\frac{1}{M}\left(\sum_{\substack{j \text{ s.t.} \\ \hat{v}_j \neq v_j}}(u-\hat{v}_j/\rho) + \sum_{\substack{j \text{ s.t.} \\ \hat{v}_j = v_j}}(u-\hat{v}_j/\rho)\right)\right]^2 \end{aligned} \tag{4.30}$$

for $k = 1, 2, ..., M-1$ by using the chosen estimator and bounded considering the furthest distance between u and its estimate for the cases when $\hat{v}_j$ is correctly and incorrectly decoded. Lastly, $D_{e,M} = E\left[(u-\hat{u}|^2) M \text{ in error}\right]$ is given as

$$D_{e,M} = E\left(\frac{1}{\rho M}\sum_{j=1}^{M}(\rho u - \hat{v}_j)\right)^2. \tag{4.31}$$

See Appendix 6.3.4 for the detailed derivations and resulting bounds. Note that, D_q and $D_{e,k}$ $(1 < k < M)$ are in the exponential order of 2^{-2B} while $D_{e,M}$ is upper bounded by an order of 1. Using the chosen estimator $\hat{u}$ and the definitions given above from (4.27) to (4.31), the protocol terminates with the following distortion at the end of the second round.

$$D(\mathcal{E}, N_0, 2, \lambda) \leq D_q + \sum_{k=1}^{M-1} D_{e,k}P_{e,k} + D_{e,M}P_{e,M}. \tag{4.32}$$

The derivation of the bound (4.32) can be found in detail in Appendix 6.3.4. Substituting $P_{e,k}$ (4.27) and $P_{e,M}$ (4.28) along with their corresponding distortions $D_{e,k}$ (4.30), $D_{e,M}$ (4.31) in addition to the quantization distortion D_q (4.29) into (4.32), we obtain the following form of the upper bound in the distortion at the end of the second round as

$$\begin{aligned} D \leq D_q &+ D_{e,M}\left(K_1\frac{\sqrt{1-\rho^2}}{\rho+\sqrt{1-\rho^2}}e^{(B+1)\ln 2} + K_2\epsilon(\rho)\right)^{M-1} \\ &\qquad e^{(B-2M+2)\ln 2 - \frac{\mathcal{E}_{\mathrm{D},1}+2\mathcal{E}_{\mathrm{C},1}(\sqrt{\lambda}-1)^2}{2N_0}} \\ &+ D_{e,M}\left(K_3\frac{\sqrt{1-\rho^2}}{\rho+\sqrt{1-\rho^2}}e^{(B+1)\ln 2} + K_4\epsilon(\rho)\right)^{M-1} e^{(B-4M+2)\ln 2 - \frac{\mathcal{E}_{\mathrm{D},1}+\mathcal{E}_{\mathrm{D},2}}{2N_0}} \end{aligned}$$

$$+\sum_{k=1}^{M-1} D_{e,k}\binom{M}{k}\left(K_5(k)\frac{\sqrt{1-\rho^2}}{\rho+\sqrt{1-\rho^2}}e^{(B+1)\ln 2}+K_6(k)\epsilon(\rho)\right)^k e^{-\frac{k(\mathcal{E}_{\mathrm{D},1}+2\mathcal{E}_{\mathrm{C},1}(\sqrt{\lambda}-1)^2)}{2MN_0}}$$
$$+\sum_{k=1}^{M-1} D_{e,k}\binom{M}{k}\left(K_7(k)\frac{\sqrt{1-\rho^2}}{\rho+\sqrt{1-\rho^2}}e^{(B+1)\ln 2}+K_8(k)\epsilon(\rho)\right)^k e^{-\frac{k(\mathcal{E}_{\mathrm{D},1}+\mathcal{E}_{\mathrm{D},2})}{2MN_0}} \tag{4.33}$$

where K_1, K_2 are $O((\mathcal{E}_{\mathrm{D},1})^{M-1})$, K_3, K_4 are $O((\mathcal{E}_{\mathrm{D},1}+\mathcal{E}_{\mathrm{D},2})^{M-1})$ whereas $K_5(k)$ and $K_6(k)$ are $O((\mathcal{E}_{\mathrm{D},1})^{k-1})$, $K_7(k)$ and $K_8(k)$ correspond to $O((\mathcal{E}_{\mathrm{D},1}+\mathcal{E}_{\mathrm{D},2})^{k-1})$ with $\epsilon(\rho)\in[0,1)$.

In order to have a vanishing $P_e(\mathbf{m})$ in the first round, we set the relations of the energies as $\mathcal{E}_{C,1}=\frac{\mathcal{E}_{D,2}}{2(1-\sqrt{\lambda})^2}$ and $\mathcal{E}_{D,2}=(2-\mu)\mathcal{E}_{D,1}$ where μ is an arbitrary constant satisfying $\mu\in(0,2)$, so that the average energy used by the protocol can be made arbitrarily close to $\mathcal{E}_{\mathrm{D},1}$ guaranteed by vanishing union error probability $P_e(\mathbf{m})$ given that $k<M$. Further detail regarding the average energy consumed by the two rounds of the protocol can be found in Appendix 6.3.4.

For the case of high correlation, i.e. when $2^{B+1}\sqrt{1-\rho^2}<\theta$ where $\theta\sim O(1)$, we obtain the asymptotic bound with respect to B on distortion as

$$D_{high}\leq\alpha(\rho,M)\exp\left\{-\frac{\mathcal{E}_{\mathrm{D},1}(1-\mu/3)}{N_0}\right\}+\sum_{k=1}^{M-1}\beta(k,\rho,M)\exp\left\{-\frac{(2M+3k-\mu(2M+k))\mathcal{E}_{\mathrm{D},1}}{2MN_0}\right\}. \tag{4.34}$$

Because of the quantizer construction, $1-\rho^2$ is considered as in the same order of 2^{-2B} and consequently should be chosen to behave as $\exp\left\{-\frac{\mathcal{E}_{\mathrm{D},1}}{N_0}\right\}$. As a result we obtain the same collaboration effect as in (4.8) albeit with a factor 2 gap in energy efficiency. The latter may be due to simplifying steps in the outer-bound. Furthermore, we notice that condition for exploiting collaboration between the sources is based on relationship between the observation error variance $(1-\rho^2)$ and the *aggregate energy* as opposed to the individual source energies. The significant term is isolated in the bound given above in order to be emphasized, where

$$\alpha(\rho,M)=\left(\frac{29/2+2\sqrt{3}}{\rho^2M}+\frac{\rho^2M+12\rho^2+12\rho\sqrt{1-\rho^2}+3(1-\rho^2)}{\rho^2M}\right)\left((K_1'+K_2\epsilon(\rho))^{M-1}2^{-2M+2}+(K_3'+K_4\epsilon(\rho))^{M-1}2^{-4M+2}\right) \tag{4.35}$$

which arose from the distortion terms corresponds to K_2, K_4 in (4.33) and β also denotes a function of k, ρ and M which is given by

$$\beta(k,\rho,M) = \frac{9M+16k}{(M^2\rho^2)/3}\binom{M}{k}\left[(K_5'(k)+K_6(k)\epsilon(\rho))^k+(K_7'(k)+K_8(k)\epsilon(\rho))^k)\right] \quad (4.36)$$

arose from the distortion terms corresponds to K_5, K_6, K_7 and K_8 which represents the lower order terms. Note that $K_n'(k) = \theta K_n(k)$ for $n = 1, 3, 5, 7$.

4.5 Practical Adaptation and Numerical Evaluation

4.5.1 Lower Bounds

This part presents the comparison of the lower bounds on the reconstruction error in estimating V_j's as a product (Section 4.3.1) and as a sum (Section 4.3.2) for both uniformly and normally distributed sources.

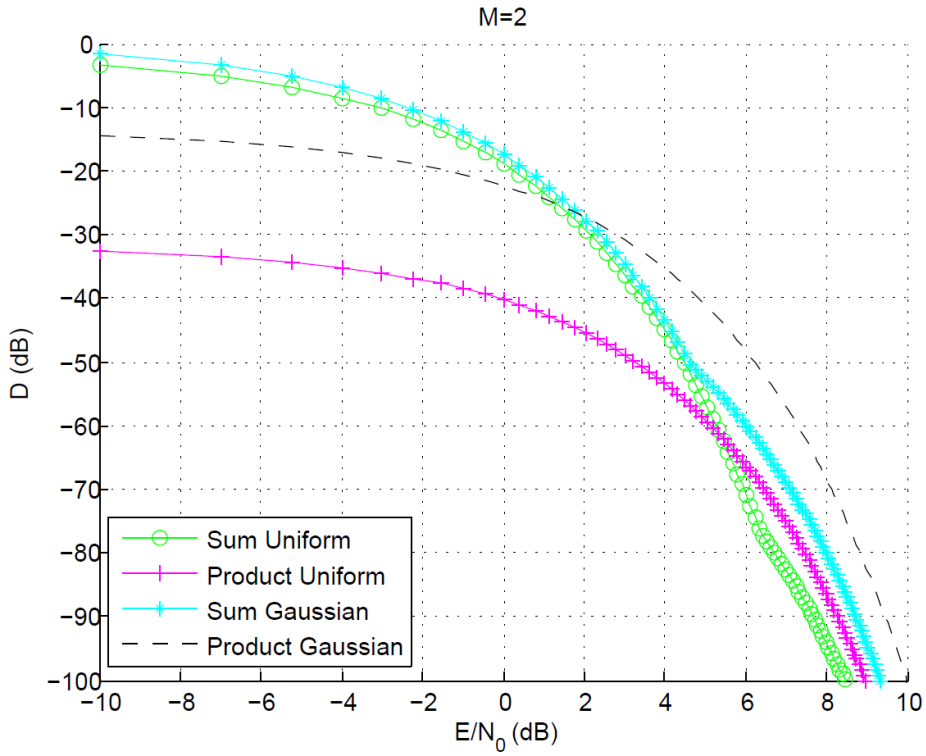

Figure 4.4: Numerical evaluation of the lower bounds (4.12) and (4.16) for $M = 2$ and $B = 5$.

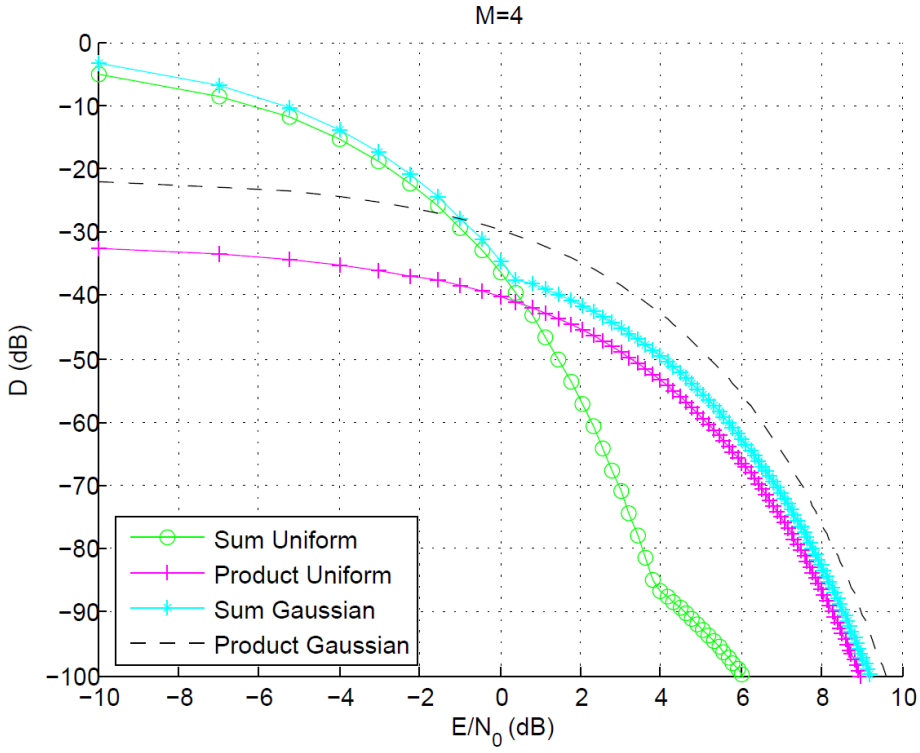

Figure 4.5: Numerical evaluation of the lower bounds (4.12) and (4.16) for $M = 4$ and $B = 5$.

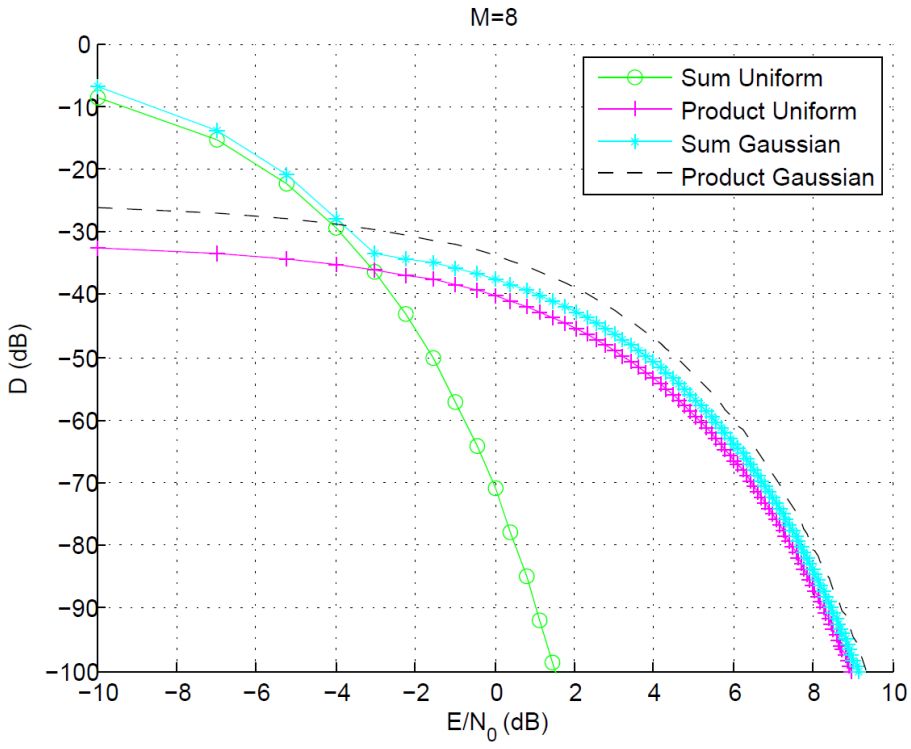

Figure 4.6: Numerical evaluation of the lower bounds (4.12) and (4.16) for $M = 8$ and $B = 5$.

Figures (4.4), (4.5) and (4.6) represent the numerical evaluation of the lower bounds given by (4.12), (4.16) and (4.17) for three different cases of $M = 2, 4, 8$, respectively with $D_j = D$, $\forall j$. Note that the curves labeled as the product bound are drawn for the M^{th} root of (4.12) for equal distortions per source where as the curves labeled as the sum bound are drawn based on the maximization of (4.16) and (4.17) over $|S| = 0, ..., M-1$. For all three cases, it can be clearly seen that the product bound dominates the sum bound for both types of source distributions in the high energy regime.

4.5.2 Achievable Scheme

In this subsection we consider the performance of the protocol described in the previous section with a minor adaptation allowing finer control of the probability of going to the second round. We introduce the condition that the receiver decides to continue with the second round only if it detects L or more errors after the control phase, including the extreme case of $L = M$ which corresponds to detecting errors from all sources. Based on this adaptation, the bound on the distortion to be achieved at the end of the second round given above by (4.32 is modified as follows

$$D'(\mathcal{E}, N_0, 2, \lambda) \leq D_q + \sum_{k=1}^{L-1} D_{e,k} P_{e,k}^{(1)} + \sum_{k=L}^{M-1} D_{e,k} P_{e,k}^{(1)} \Pr(E_{e\to c,1} | k \ \ in \ \ error) + \sum_{k=1}^{M-1} D_{e,k} P_{e,k}^{(2)} + D_{e,M} P_{e,M} \quad (4.37)$$

where $P_{e,k}^{(1)} = \binom{M}{k} \left\lceil 2^{B+1} \frac{\sqrt{1-\rho^2}}{\rho+\sqrt{1-\rho^2}} \right\rceil^k P_2(k)$ and $P_{e,k}^{(2)}$ uses $P_2(2k)$ with the same factor in front which represent the first and second rounds of $P_{e,k}$, respectively. The curves labeled as without feedback represent the case where the protocol halts after the first round of transmission, i.e. after the data phase of the first round. Since there will not be a second round for retransmission, there is no use of the control phase in the first round either. The following upper bound on the distortion at the end of the first round is numerically evaluated and given in Figures from (4.7) to (4.9).

$$D'(\mathcal{E}, N_0, 1, \lambda) \leq D_q + \sum_{k=1}^{M-1} D_{e,k} P_{e,k}^{(1)} + D_{e,M} P_{e,M}^{(1)}. \quad (4.38)$$

where $\binom{M}{k} 2^B \left\lceil 2^{B+1} \frac{\sqrt{1-\rho^2}}{\rho+\sqrt{1-\rho^2}} \right\rceil^k P_2(M)$.

The motivation for this adaptation is to bring the distortion down to D_q as quickly as possible, since as long as a few sources are decoded correctly, D will be proportional to 2^{-2B}. It is only when a significant number of sources

are in error that we make use of the extra energy in the second round to bring the distortion close to D_q. In Figures (4.7)-(4.8) and (4.9) we show the behaviour of the protocol for $M = 2, 4, 8$ and $B = 7$ bits compared to the lower bound on D in (4.7) for uniform statistics on one-dimensional $\mathbf{U}$ and $\mathbf{U}'_j$. The relationship between the correlation coefficient and the number of the quantization bins enabled us to present the curves labeled as the outer bound in Figures (4.7)-(4.8) and (4.9) . The quantization distortion 2^{-2B} is considered in the order of $(1 - \rho^2)$ which is the distortion induced by the observation noise in (4.7). Clearly, increasing B (or equivalently increasing ρ) directly effects the significance of the lower bound. We first see that, as in the single-source [61] and dual correlated source problems [56, 57] we do not quite approach the asymptotic gain of 4.7 dB over the case when only 1 round is used (i.e. one-shot transmission without feedback having exponent $e^{-\frac{\mathcal{E}}{3N_0}}$ as opposed to $e^{-\frac{\mathcal{E}}{N_0}}$). We can, however, obtain somewhere between 2-3 dB for moderate energies. Secondly, we see that increasing M has the effect of allowing for lower distortions around the asymptote, D_q, since the latter decreases linearly with M. However, the energy-efficiency of the protocol does not decrease linearly with M due to the non-coherent combining loss, which can even be seen when going from $M = 4$ to $M = 8$. We note that the lower-bounds do improve linearly with M due to the bounding step (a) in (6.36). It would be worthwhile to derive a lower-bound which does not remove the unknown parameter to determine if this effect is unavoidable. Moreover, if we were to consider spatial-expansion (i.e. increasing M) with fixed total energy, we would have a loss in energy efficiency which increases with M.

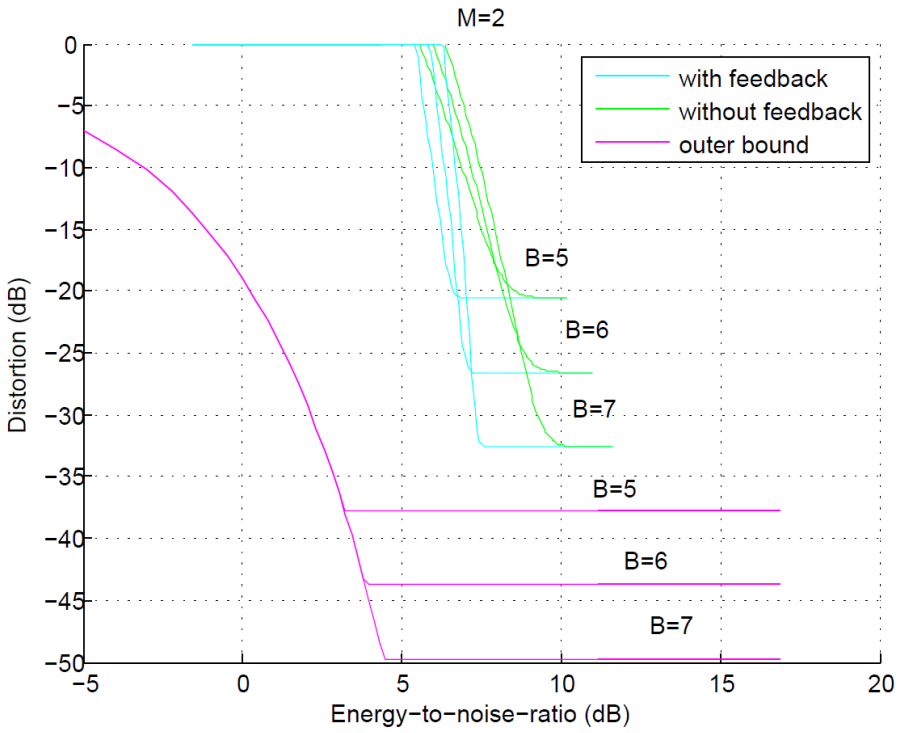

Figure 4.7: Numerical evaluation of the upper bound (4.37) for $M = 2$ and B from 5 to 7.

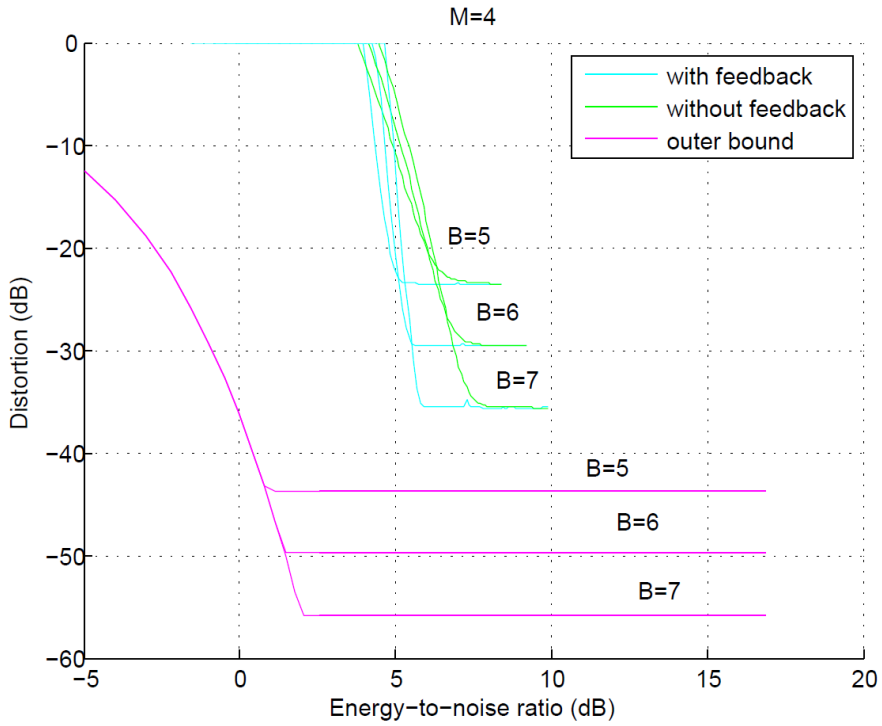

Figure 4.8: Numerical evaluation of the upper bound (4.37) for $M = 4$ and B from 5 to 7.

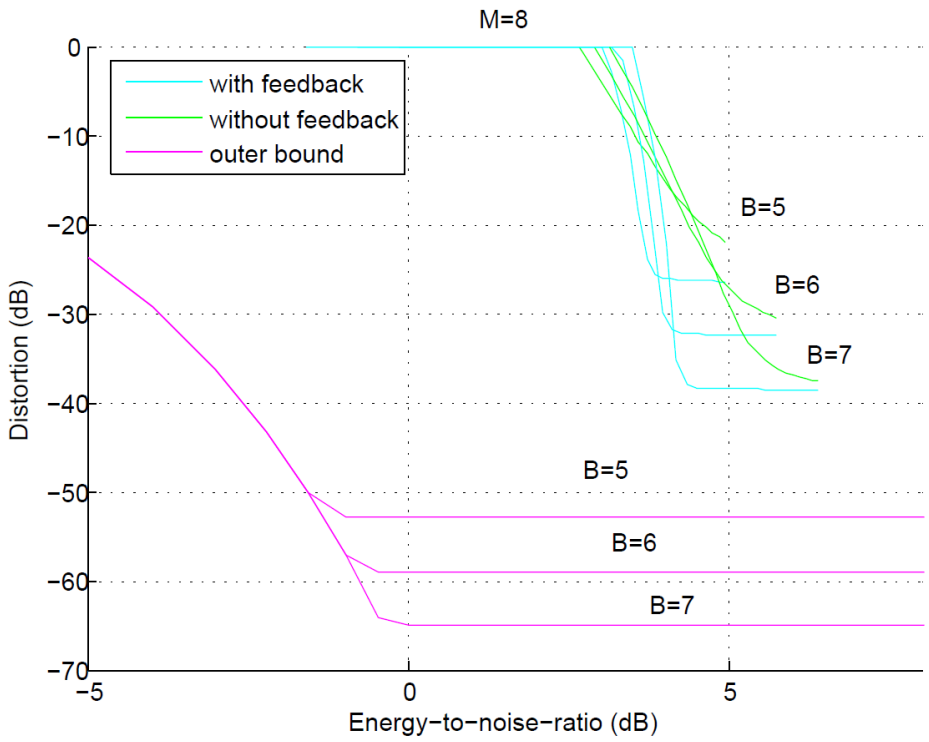

Figure 4.9: Numerical evaluation of the upper bound (4.37) for $M = 8$ and B from 5 to 7.

Chapter 5

Conclusions

Firstly, we introduced a low-latency, two-way protocol for the transmission of a single random variable over a wide-band channel and analyzed its asymptotic behavior with non-coherent detection on both pure line-of-sight and more general fading channels. The protocol and transmission strategy could be used for future energy-limited sensors making use of broadband cellular networks. We showed that the gap between the classical Goblick bound [4] and the bound obtained by our proposed feedback scheme cannot be closed (i.e. an improvement in terms of the asymptotic performance cannot be achieved) by repeating the protocol more than two rounds to less than 3 dB. The improvement over a one-shot transmission is on the order of 3-4 dB and asymptotically 4.7 dB. We have also included a discussion regarding the case of imperfect feedback and its effect on the trade-off between the required energy for the protocol and the reconstruction error in estimating the source message. We showed that in this case, if the energy consumption required by the feedback link is accounted , this reduces the reconstruction fidelity. Additionally, numerical evaluation of Merhav's recent lower-bounds [13] for one-shot transmission are included and the tightest variant using his techniques is determined. Both the bounds and performance evaluation of the feedback protocol have been extended to a multi-channel fading model. The improvement of the feedback protocol over one-shot transmission is even more significant than in the line-of-sight case. We further suggest that tighter bounding techniques which rely on unknown channels should be found for the fading channel. Furthermore, schemes using variable-energy transmission should be considered to close the gap with the lower-bounds.

We proceeded with the derivation of lower bounds on the reconstruction error for the transmission of two correlated analog sources in the presence

of causal feedback. The bounds are specialized to the case of wide-band channels. All our derivations are applied to sum-channel with both uniformly and normally distributed sources. We then introduced a low-latency two-way protocol for the transmission of two correlated random variables over a wide-band channel and analyze its asymptotic behaviour with non-coherent detection for uniform and Gaussian distribution. We show that the transmission of two highly correlated sources can achieve the energy-efficiency of a single source with the same total energy, at least in certain regimes governing the level of correlation. The high correlation case yields the exponential behaviour of the single-source case and benefits from energy accumulation, or the collaboration of the two sources. Low-correlation results insignificantly reduced energy-efficiency.

The final part of the thesis covered an adaptation of two-way low-latency feedback protocol for minimal distortion studied in Sections 2 and 3 to a large network scenario with multiple sources. Specifically, we have provided lower-bounds on the reconstruction error of arbitrary multi-sensor transmission strategies which can serve in a subsequent step to determine the optimality of particular multiple-access and encoding strategies. To this end, we have proposed one such collaborative strategy exploiting correlation between sensors. Asymptotic upper-bounds on the reconstruction error have been provided for the proposed protocol. Both the upper and lower-bounds show that collaboration can be achieved through energy accumulation and bring to light a trade-off in source and channel SNR allowing it to occur. The practical performance of the proposed retransmission protocol was investigated through numerical evaluation of the upper-bounds in the non-asymptotic energy regime, which corresponds to using low-order quantization in the sensors. The performance of the protocol was improved through the introduction of a minor modification in the feedback strategy which allows the error-free performance to be achieved quickly. Comparisons with a one-shot transmission not exploiting feedback show that gains with one round of feedback are on the order to 2-3 dB in comparison to a feedback-less system and are often to within 5 dB from the lower-bound. It is further shown that an increase in the size of the network brings benefit in terms of performance, but that the gain in terms of energy efficiency diminishes quickly at finite energies due to a non-coherent combining loss.

Chapter 6

Appendix

6.1 Appendix for Point-to-point Channel

6.1.1 Wireless Adaptation of the Goblick Bound

In order to come up with a lower bound the distortion level of the wireless channel with feedback, we begin with the model $Y_{r,i} = \sqrt{h_r}X_{r,i} + Z_{r,i}$, $i = 1, \cdots, N/R$, $r = 1, \cdots, R$. We start with two different expansions of the mutual information $I(\mathbf{U}; \mathbf{Y} | \{\mathbf{H}_r = h_r, r = 1, \cdots, R\})$ which are equated and given as follows.

$$
\begin{aligned}
&I(\mathbf{U}; \mathbf{Y} | \{\mathbf{H}_r = h_r\}) = h(\mathbf{U}|\{\mathbf{H}_r = h_r\}) - h(\mathbf{U} - \hat{\mathbf{U}}(\{\mathbf{H}_r = h_r\}) | \mathbf{Y}, \{\mathbf{H}_r = h_r\}) \\
&\overset{(a)}{=} h(\mathbf{U}) - h(\mathbf{U} - \hat{\mathbf{U}}(\{\mathbf{H}_r = h_r\}) | \mathbf{Y}, \{\mathbf{H}_r = h_r\}, \hat{\mathbf{U}}(\{\mathbf{H}_r = h_r\})) \\
&\geq h(\mathbf{U}) - h(\mathbf{U} - \hat{\mathbf{U}}(\{\mathbf{H}_r = h_r\})) \\
&= \frac{1}{2}\log 2\pi e - \frac{1}{2}\log(2\pi e D(h)) \\
&= \frac{1}{2}\log(1/D(h))
\end{aligned} \tag{6.1}
$$

where $D(h)$ represents $D\left(\{\mathbf{H}_r = h_r\}\right)$.

$$
\begin{aligned}
&I(\mathbf{U};\mathbf{Y}|\left\{\mathbf{H}_r = h_r\right\}) = h(\mathbf{Y}|\left\{\mathbf{H}_r = h_r\right\}) - h(\mathbf{Y}|\mathbf{U},\{\mathbf{H}_r = h_r\}) \\
&= \sum_{r=1}^{R}\sum_{i=1}^{N/R} h(Y_{r,i}|Y_r^{i-1}, Y_1^N, \cdots, Y_{r-1}^N, \{\mathbf{H}_r = h_r\}) \\
&- \sum_{r=1}^{R}\sum_{i=1}^{N/R} h(Y_{r,i}|Y_r^{i-1}, Y_1^N, \cdots, Y_{r-1}^N, \mathbf{U}, \{\mathbf{H}_r = h_r\}) \\
&= \sum_{r=1}^{R}\sum_{i=1}^{N/R} h(Y_{r,i}|Y_r^{i-1}, Y_1^N, \cdots, Y_{r-1}^N, \{\mathbf{H}_r = h_r\}) \\
&- \sum_{r=1}^{R}\sum_{i=1}^{N/R} h(Y_{r,i}|Y_r^{i-1}, Y_1^N, \cdots, Y_{r-1}^N, \mathbf{U}, \mathbf{X}, \{\mathbf{H}_r = h_r\}) \\
&= \sum_{r=1}^{R}\sum_{i=1}^{N/R} h(X_{r,i}\sqrt{h_r} + Z_{r,i}|Y_r^{i-1}, Y_1^N, \cdots, Y_{r-1}^N, \{\mathbf{H}_r = h_r\}) \\
&- \sum_{r=1}^{R}\sum_{i=1}^{N/R} h(Z_{r,i}) \\
&\leq \sum_{r=1}^{R}\sum_{i=1}^{N/R} \log 2\pi e\left(N_0 + E_{r,i}|h_r|^2\right) - \sum_{r=1}^{R}\sum_{i=1}^{N/R} \log 2\pi e N_0 \\
&\overset{(b)}{=} \sum_{r=1}^{R} \frac{N}{R} \log\left(1 + \frac{R}{N}\frac{E_r|h_r|^2}{N_0}\right) \\
&\leq \sum_{r=1}^{R} \frac{E_r|h_r|^2}{N_0}.
\end{aligned} \tag{6.2}
$$

In step (a) given the independence between $\mathbf{U}$ and $\{\mathbf{H}_r = h_r\}$, the conditional entropy equals the entropy of the source. And in step (b) we used the following property $\log(1+x) \leq x$. Equating the two expansions (6.1) and (6.2) yields

$$D(h) \geq e^{-2\sum_{r=1}^{R} E_r|h_r|^2/N_0} \tag{6.3}$$

which can be re-written as $D(h) \geq e^{-2\frac{\mathcal{E}}{RN_0}\sum_{r=1}^{R}|h_r|^2}$ with $E_r = \mathcal{E}/R \quad \forall r$. Let us define the right-hand side of the inequality as the moment generating function of $|h|^2$ with $t = -2\mathcal{E}/N_0$.

$$M_{|h|^2}(t) = \prod_{r=1}^{R}\left(1 + 4\alpha\mathcal{E}/RN_0\right)^{-L} \exp\left\{-\frac{2(1-\alpha)L\mathcal{E}/RN_0}{1 + 4\alpha\mathcal{E}/RN_0}\right\} \tag{6.4}$$

The final form of the lower bound (6.3) is given in Section 2.2.1 by (2.38).

6.2 Appendix for Dual-Source Case Derivations

6.2.1 Appendix I

Hereafter, we give the derivation of $I(\mathbf{U};\hat{\mathbf{U}})$ in two different expansions in order to bound the reconstruction error, first of which is based on the sources and given as

$$\begin{aligned} I(\mathbf{U};\hat{\mathbf{U}}) &= h(\mathbf{U}) - h(\mathbf{U}|\hat{\mathbf{U}}) \\ &\geq h(\mathbf{U}) - h(\mathbf{U}-\hat{\mathbf{U}}) \end{aligned} \tag{6.5}$$

where $h(\mathbf{U}) = K\log 2\sqrt{3}$ for a uniform source and $h(\mathbf{U}) = \frac{K}{2}\log 2\pi e$ for a standard normal U. Second part of (6.5) is mutual for both distirbutions since we bound it by the Gaussian entropy as follows

$$\begin{aligned} h(\mathbf{U}-\hat{\mathbf{U}}) &= \sum_{i=1}^{K} h(U_i - \hat{U}_i) \\ &\leq \sum_{i=1}^{K} \frac{1}{2}\log(\mathbb{E}[(U_i-\hat{U}_i)^2]) \\ &\leq \frac{K}{2}\log(2\pi e D). \end{aligned} \tag{6.6}$$

Consequently, substituting corresponding source entropies into (6.5) we get

$$I(\mathbf{U};\hat{\mathbf{U}}) \geq \begin{cases} \frac{K}{2}\log(1/D) & \text{for Gaussian} \\ \frac{K}{2}\log\left(\frac{6}{\pi e}\frac{1}{D}\right) & \text{for Uniform} \end{cases} \tag{6.7}$$

Secondly, the same mutual information is expanded based on the output signals as follows

$$\begin{aligned} I(\mathbf{U};\hat{\mathbf{U}}) &\leq I(\mathbf{X}_1,\mathbf{X}_2;\mathbf{Y}|\mathbf{\Phi}) \\ &= h(\mathbf{Y}|\mathbf{\Phi}) - h(\mathbf{Y}|\mathbf{X}_1,\mathbf{X}_2,\mathbf{\Phi}) \\ &\leq \sum_{i=1}^{N} h(Y_i|\mathbf{\Phi}) - h(\mathbf{Z}) \\ &\leq N\left(\sum_{i=1}^{N}\log(\mathbb{E}[Y_i^2]) - \log(NN_0)\right) \\ &= N\log\left(1+\frac{K\mathcal{E}}{NN_0}\right) \end{aligned} \tag{6.8}$$

which is applicable to both distributions. Equating the two different expressions of $I(\mathbf{U};\hat{\mathbf{U}})$ yields the lower bound (3.6).

6.2.2 Appendix II-Lower Bound I

The mutual information $I(\mathbf{U}_m;\mathbf{Y})$ is derived through two different expansions where the first expansion is

$$\begin{aligned}
I(\mathbf{U}_m;\mathbf{Y}) &\leq I(\mathbf{U}_m;\mathbf{Y},\Phi_m,\Phi_{m'}) \\
&= h(\mathbf{Y}|\Phi_m,\Phi_{m'}) - h(\mathbf{Y}|\mathbf{U}_m,\Phi_m,\Phi_{m'}) \\
&= \sum_{i=1}^{N} h(Y_i|Y^{i-1},\Phi_m,\Phi_{m'}) - \sum_{i=1}^{N} h(Y_i|Y^{i-1},\mathbf{U}_m,\Phi_m,\Phi_{m'}) \\
&\overset{(a)}{\leq} \sum_{i=1}^{N} h(Y_i|Y^{i-1},\Phi_m,\Phi_{m'}) \\
&- \sum_{i=1}^{N} h(Y_i|Y^{i-1},\mathbf{U}_m,\mathbf{X}_m e^{j\phi_m},\mathbf{X}_{m'} e^{i\phi_{m'}},\Phi_m,\Phi_{m'}) \\
&= \sum_{i=1}^{N} h(Y_i|Y^{i-1},\Phi_m,\Phi_{m'}) - \sum_{i=1}^{N} h(Z_i) \\
&\leq \sum_{i=1}^{N} \log\left(1+\frac{\mathcal{E}_{m,i}+\mathcal{E}_{m',i}}{NN_0}\right) \\
&\leq N\log\left(1+\frac{\sum_{i=1}^{N}(\mathcal{E}_{m,i}+\mathcal{E}_{m',i})}{NN_0}\right) \\
&\leq N\log\left(1+\frac{K(\mathcal{E}_{m,i}+\mathcal{E}_{m',i})}{NN_0}\right). \qquad (6.9)
\end{aligned}$$

where in step (a), $\mathbf{X}_m e^{j\phi_m}$ is introduced due conditioning on $(Y^{i-1},\mathbf{U}_m,\Phi_m)$ in the case of a feedback link between the decoder and the encoder and simply $(\mathbf{U}_m,\Phi_m)$ when no feedback is present. $\mathbf{X}_{m'}e^{i\phi_{m'}}$ can added since conditioning reduces differential entropy. For the second expansion of the same mutual information we have

$$\begin{aligned}
I(\mathbf{U}_m;\mathbf{Y}) &= h(\mathbf{U}_m) - h(\mathbf{U}_m-\hat{\mathbf{U}}_m|\mathbf{Y}) \\
&\geq h(\mathbf{U}_m) - h(\mathbf{U}_m-\hat{\mathbf{U}}_m). \qquad (6.10)
\end{aligned}$$

The required entropies for $m=1,2$ in the Uniform case, we have

$$h(\mathbf{U}_1) = K\log 2\sqrt{3}, \qquad (6.11)$$

$$\begin{aligned}
h(\mathbf{U}_2) &= h(\rho\mathbf{U}_1+\sqrt{1-\rho^2}\mathbf{U}_2') \\
&\geq \frac{K}{2}\log\left(2^{\frac{2}{K}(K\log|\rho|+h(\mathbf{U}_1)} + 2^{\frac{2}{K}h(\sqrt{1-\rho^2}\mathbf{U}_2'}\right) \\
&= \frac{K}{2}\log\left(2^{\frac{2}{K}K\log|\rho|2\sqrt{3}} + 2^{\frac{2}{K}K\log 2\sqrt{3|1-\rho^2|}}\right) \\
&= K\log 2\sqrt{3}. \qquad (6.12)
\end{aligned}$$

The source entropy of a Gaussian source is independent of the source number.

$$h(\mathbf{U}_m) = \frac{K}{2} \log 2\pi e. \tag{6.13}$$

The final term required to derive the second expansion of (6.10), which is common for both distributions, is given by

$$\begin{aligned} h(\mathbf{U}_m - \hat{\mathbf{U}}_m) &\leq \sum_{j=1}^{K} h(U_{m,j} - \hat{U}_{m,j}) \\ &\leq \frac{K}{2} \log \left(2\pi e \frac{1}{K} \sum_{j=1}^{K} \mathbb{E}[(U_{m,j} - \hat{U}_{m,j})^2] \right) \\ &\leq K \log \left(\sqrt{2\pi e D_m} \right). \end{aligned} \tag{6.14}$$

Substituting (6.11) and (6.14) for $m = 1$ into (6.10), yields the second expansion of the desired mutual information for the first source. In the same way, (6.11) and (6.14) with $m = 2$ is substituted into (6.10) for the second source U_2. Finally, combining (6.13) and (6.14) and applying it to (6.10) results in

$$I(\mathbf{U}_m; \mathbf{Y}) \geq \begin{cases} \frac{K}{2} \log(1/D_m) & \text{for Gaussian} \\ \frac{K}{2} \log \left(\frac{6}{\pi e} \frac{1}{D_m} \right) & \text{for Uniform} \end{cases} \tag{6.15}$$

.

6.2.3 Appendix III- Lower Bound II

First expansion on the output signals is independent of the source distribution.

$$
\begin{aligned}
&I(\mathbf{U}_m;\mathbf{Y}|\mathbf{U}_{m'}) \leq I(\mathbf{U}_m;\mathbf{Y}|\mathbf{U}_{m'},\Phi_m,\Phi_{m'})\\
&= h(\mathbf{Y}|\mathbf{U}_{m'},\Phi_m,\Phi_{m'}) - h(\mathbf{Y}|\mathbf{U}_m,\mathbf{U}_{m'},\Phi_m,\Phi_{m'})\\
&= \sum_{i=1}^{N} h(Y_i|Y^{i-1},\mathbf{U}_{m'},\Phi_m,\Phi_{m'}) - \sum_{i=1}^{N} h(Y_i|Y^{i-1},\mathbf{U}_m,\mathbf{U}_{m'},\Phi_m,\Phi_{m'})\\
&\overset{(b)}{=} \sum_{i=1}^{N} h(Y_i|Y^{i-1},\mathbf{U}_{m'},\mathbf{X}_{m'}e^{i\phi_{m'}},\Phi_m,\Phi_{m'})\\
&- \sum_{i=1}^{N} h(Y_i|Y^{i-1},\mathbf{U}_m,\mathbf{U}_{m'},\mathbf{X}_m e^{j\phi_m},\mathbf{X}_{m'}e^{i\phi_{m'}},\Phi_m,\Phi_{m'})\\
&\overset{(c)}{=} \sum_{i=1}^{N} h(X_{m,i}e^{j\phi_{m,i}} + Z_i|Y^{i-1},\mathbf{U}_{m'},\Phi_m,\Phi_{m'}) - \sum_{i=1}^{N} h(Z_i)\\
&\leq \sum_{i=1}^{N} h(X_{m,i}e^{j\phi_{m,i}} + Z_i) - \sum_{i=1}^{N} h(Z_i)\\
&\leq N\log\left(\sum_{i=1}^{N}\log(Var(X_{m,i}e^{j\phi_{m,i}} + Z_i)) - \log(Var(\mathbf{Z}))\right)\\
&= N\log\left(1+\frac{K\mathcal{E}_m}{NN_0}\right). \qquad (6.16)
\end{aligned}
$$

In the first part of step (b), $\mathbf{X}_{m'}e^{i\phi_{m'}}$ comes from conditioning on $(Y^{i-1},\mathbf{U}_{m'},\Phi_{m'})$ in the case of feedback and from conditioning on $(\mathbf{U}_{m'},\Phi_{m'})$ when no feedback is present. Similarly the second half of step (b) stems from conditioning on $(Y^{i-1},\mathbf{U}_m,\mathbf{U}_{m'},\Phi_m,\Phi_{m'})$. And in (c), $\mathbf{X}_{m'}e^{i\phi_{m'}}$ is subtracted from the output signal, which provides $\mathbf{X}_m e^{j\phi_m}$ together with the noise term in the next step. For the second expansion based on the sources, we have for the Uniform case

$$
\begin{aligned}
I(\mathbf{U}_m;\mathbf{Y}|\mathbf{U}_{m'}) &= h(\mathbf{U}_m|\mathbf{U}_{m'}) - h(\mathbf{U}_m|\mathbf{U}_{m'},\mathbf{Y})\\
&= h(\mathbf{U}_m|\mathbf{U}_{m'}) - h(\mathbf{U}_m-\hat{\mathbf{U}}_m|\mathbf{U}_{m'},\mathbf{Y})\\
&\geq h(\mathbf{U}_m|\mathbf{U}_{m'}) - h(\mathbf{U}_m-\hat{\mathbf{U}}_m). \qquad (6.17)
\end{aligned}
$$

The conditional entropy $h(\mathbf{U}_m|\mathbf{U}_{m'})$ is obtained for $m = 1, 2$

$$\begin{aligned} h(\mathbf{U}_1|\mathbf{U}_2) &= -I(\mathbf{U}_1;\mathbf{U}_2) + h(\mathbf{U}_1) \\ &= -h(\mathbf{U}_2) + h(\mathbf{U}_2|\mathbf{U}_1) + h(\mathbf{U}_1) \\ &\overset{(d)}{\geq} -\frac{K}{2}\log 2\pi e + K\log 2\sqrt{3|1-\rho^2|} + K\log 2\sqrt{3} \\ &= K\log\left(\frac{12\sqrt{|1-\rho^2|}}{\sqrt{2\pi e}}\right) \end{aligned} \tag{6.18}$$

$$\begin{aligned} h(\mathbf{U}_2|\mathbf{U}_1) &= h(\rho\mathbf{U}_1 + \sqrt{1-\rho^2}\mathbf{U}_{2'}|\mathbf{U}_1) \\ &= h(\sqrt{1-\rho^2}\mathbf{U}_{2'}) \\ &= K\log 2\sqrt{3|1-\rho^2|} \end{aligned} \tag{6.19}$$

,respectively. In step (d) of (6.18), the entropy of $\mathbf{U}_2$ is bounded by the entropy of a standard gaussian random vector. The conditional entropy of one source given the other is obtained as

$$\begin{aligned} h(\mathbf{U}_1|\mathbf{U}_2) &= -I(\mathbf{U}_1;\mathbf{U}_2) + h(\mathbf{U}_1) \\ &\overset{(e)}{=} -h(\mathbf{U}_2) + h(\mathbf{U}_2|\mathbf{U}_1) + h(\mathbf{U}_1) \\ &= h(\mathbf{U}_2|\mathbf{U}_1) \\ &= \frac{K}{2}\log(1-\rho^2)2\pi e \end{aligned} \tag{6.20}$$

where in the step (e), we used the equality of the entropies between two standard normal random vectors. Consequently, the second expansion of $I(\mathbf{U}_m;\mathbf{Y}|\mathbf{U}_{m'})$ on the source entropies can be summarized as

$$I(\mathbf{U}_m;\mathbf{Y}|\mathbf{U}_{m'}) \geq \begin{cases} \frac{K}{2}\log\left(\frac{(1-\rho^2)}{D_m}\right) & \text{for Gaussian and } m = 1,2 \\ \frac{K}{2}\log\left(\frac{36(1-\rho^2)}{\pi^2 e^2}\frac{1}{D_1}\right) & \text{for Uniform and } m = 1 \\ \frac{K}{2}\log\left(\frac{6(1-\rho^2)}{\pi e}\frac{1}{D_2}\right) & \text{for Uniform and } m = 2 \end{cases} \tag{6.21}$$

.

6.2.4 Appendix IV- Lower Bound III

The mutual information $I(\mathbf{U}_m, \mathbf{U}_{m'}; \mathbf{Y})$ is obtained as

$$\begin{aligned} I(\mathbf{U}_m, \mathbf{U}_{m'}; \mathbf{Y}) &\leq I(\mathbf{U}_m, \mathbf{U}_{m'}; \mathbf{Y}|\mathbf{\Phi}) \\ &= h(\mathbf{Y}|\mathbf{\Phi}) - h(\mathbf{Y}|\mathbf{U}_m, \mathbf{U}_{m'}, \mathbf{\Phi}) \\ &= h(\mathbf{Y}|\mathbf{\Phi}) - \sum_{i=1}^{N} h(Y_i|Y^{i-1}, \mathbf{U}_m, \mathbf{U}_{m'}, \mathbf{\Phi}) \\ &\overset{(e)}{\leq} \sum_{i=1}^{N} h(Y_i|\mathbf{\Phi}) - \sum_{i=1}^{N} h(Y_i|Y^{i-1}, \mathbf{U}_m, \mathbf{X}_m, \mathbf{U}_{m'}, \mathbf{X}_{m'}, \mathbf{\Phi}) \\ &= \sum_{i=1}^{N} h(Y_i|\mathbf{\Phi}) - \sum_{i=1}^{N} h(Z_i). \end{aligned} \tag{6.22}$$

Note that, in (e) the additional terms in the second differential entropy stem from conditioning on $(Y^{i-1}, \mathbf{U}_m, \mathbf{U}_{m'}, \Phi_m, \Phi_{m'})$ in the case of feedback and $(\mathbf{U}_m, \mathbf{U}_{m'}, \Phi_m, \Phi_{m'})$ when no feedback is present. The variance of the received signal Y_i becomes $\sum_{i=1}^{N} Var(Y_i) = K(\mathcal{E}_m + \mathcal{E}_{m'}) + NN_0$ and the desired mutual information is obtained as

$$I(\mathbf{U}_m, \mathbf{U}_{m'}; \mathbf{Y}|\mathbf{\Phi}) \leq N \log(1 + \frac{K(\mathcal{E}_m + \mathcal{E}_{m'})}{NN_0}). \tag{6.23}$$

We also have for the uniform contaminated uniform construction the following expansion

$$\begin{aligned} I(\mathbf{U}_m, \mathbf{U}_{m'}; \mathbf{Y}) &\geq I(\mathbf{U}_m, \mathbf{U}_{m'}; \hat{\mathbf{U}}_m, \hat{\mathbf{U}}_{m'}) \\ &\geq h(\mathbf{U}_m, \mathbf{U}_{m'}) - h(\mathbf{U}_m - \hat{\mathbf{U}}_m) - h(\mathbf{U}_{m'} - \hat{\mathbf{U}}_{m'}) \\ &\geq \frac{K}{2} \log 144(1-\rho^2) - \frac{K}{2} \log(2\pi e)^2 D_p \\ &= \frac{K}{2} \log \left(\frac{36(1-\rho^2)}{\pi^2 e^2 D_p} \right) \end{aligned} \tag{6.24}$$

where $D_p = D_1 D_2$. On the other hand, for the Gaussian case, we get

$$\begin{aligned} &I(\mathbf{U}_m, \mathbf{U}_{m'}; \mathbf{Y}) \geq I(\mathbf{U}_m, \mathbf{U}_{m'}; \hat{\mathbf{U}}_m, \hat{\mathbf{U}}_{m'}) \\ &\geq h(\mathbf{U}_m, \mathbf{U}_{m'}) - h(\mathbf{U}_m - \hat{\mathbf{U}}_m) - h(\mathbf{U}_{m'} - \hat{\mathbf{U}}_{m'}) \\ &\geq \frac{K}{2} \log(2\pi e)^2 (1-\rho^2) - \frac{K}{2} \log(2\pi e)^2 D_m D_{m'} \\ &= \frac{K}{2} \log \left(\frac{(1-\rho^2)}{D_p} \right). \end{aligned} \tag{6.25}$$

6.2.5 Appendix V- Probability of Error for the Achievable Scheme Dual-Source Case

The probability of the error is bounded by

$$\begin{aligned}
P_e &= \Pr(E_{1,1}, E_{1,2}^c)\Pr(E_{e\to c,1,1}) + \Pr(E_{1,1}^c, E_{1,2})\Pr(E_{e\to c,1,2}) \\
&+ \Pr(E_{1,1}, E_{1,2})\Pr(E_{e\to c,1,1})\Pr(E_{e\to c,1,2}) \\
&+ \{\Pr(E_{1,1}, E_{1,2})(1 - \Pr(E_{e\to c,1,1})\Pr(E_{e\to c,1,2})) \\
&+ \Pr(E_{1,1}, E_{1,2}^c)(1 - \Pr(E_{e\to c,1,1})) \\
&+ \Pr(E_{1,1}^c, E_{1,2})(1 - \Pr(E_{e\to c,1,2}))\}\Pr(E_2|E_1) \\
&+ (1 - \Pr(E_{1,1}, E_{1,2}))\Pr(E_{c\to e,1,1})\Pr(E_{c\to e,1,2})\Pr(E_2|E_1^c) \\
&\overset{(a)}{=} \Pr(E_{e\to c,1,j})\{\Pr(E_{1,1}, E_{1,2}^c) + \Pr(E_{1,1}^c, E_{1,2})\} \\
&+ \Pr(E_{e\to c,1,j})^2\Pr(E_{1,1}, E_{1,2}) \\
&+ \Pr(E_2|E_1)\{\Pr(E_{1,1}, E_{1,2})(1 - \Pr(E_{e\to c,1,j})^2) + (\Pr(E_{1,1}, E_{1,2}^c) \\
&+ \Pr(E_{1,1}^c, E_{1,2}))(1 - \Pr(E_{e\to c,1,j}))\} \\
&+ \Pr(E_2|E_1^c)[\Pr(E_{1,1}^c, E_{1,2}^c)\Pr(E_{c\to e,1,j})^2] \\
&\overset{(b)}{\leq} \Pr(E_{e\to c,1,j})\{\Pr(E_{1,1}, E_{1,2}^c) + \Pr(E_{1,1}^c, E_{1,2})\} \\
&+ \Pr(E_{e\to c,1,j})^2\Pr(E_{1,1}, E_{1,2}) \\
&+ \Pr(E_2|E_1)\{\Pr(E_{1,1}, E_{1,2}) + \Pr(E_{1,1}, E_{1,2}^c) + \Pr(E_{1,1}^c, E_{1,2})\} \\
&+ \Pr(E_2|E_1^c)\Pr(E_{1,1}^c, E_{1,2}^c) \\
&\overset{(c)}{=} \Pr(E_{e\to c,1,j})P_{e,1,1} + \Pr(E_{e\to c,1,j})^2 P_{e,2,1} + \Pr(E_2)
\end{aligned} \tag{6.26}$$

In step (a) the probability of an uncorrectable $\Pr(E_{e\to c,1,j})$ and mis-detected acknowledged error $\Pr(E_{e\to c,1,j})$ are assumed to be equal for both sources whereas in (b) the probability of being decoded correctly, i.e. $(1-\Pr(E_{e\to c,1,j}))$, and the mis-detection is upper bounded by 1. In the final step (c), the probability of only one source and both of the sources to be in error in the first round is denoted by $P_{e,1,1}$ and $P_{e,2,1}$, respectively.

6.2.6 Appendix VI- Average Energy

The protocol uses the average energy given by

$$\begin{aligned}
\mathcal{E} &= \mathcal{E}_{\mathrm{D},1,1} + \mathcal{E}_{\mathrm{D},1,2} + \mathcal{E}_{\mathrm{C},1,1}\Pr(E_{1,1}, E_{1,2}^c) + \mathcal{E}_{\mathrm{C},1,2}\Pr(E_{1,1}^c, E_{1,2}) \\
&+ (\mathcal{E}_{\mathrm{C},1,1} + \mathcal{E}_{\mathrm{C},1,2})\Pr(E_{1,1}, E_{1,2}) \\
&+ \mathcal{E}_{\mathrm{D},2}\left\{\Pr(E_{1,1}, E_{1,2}^c) + \Pr(E_{1,1}^c, E_{1,2}) + \Pr(E_{1,1}, E_{1,2})\right\} \\
&\leq \mathcal{E}_{\mathrm{D},1} + \left(\frac{\mathcal{E}_{\mathrm{C},1}}{2} + \mathcal{E}_{\mathrm{D},2}\right)\{\Pr(E_{1,1}, E_{1,2}^c) + \Pr(E_{1,1}^c, E_{1,2})\} \\
&+ (\mathcal{E}_{\mathrm{C},1} + \mathcal{E}_{\mathrm{D},2})\Pr(E_{1,1}, E_{1,2})
\end{aligned} \tag{6.27}$$

6.2.7 Appendix VII- Distortion Terms for the Dual-Source Case

The distortion caused by quantization process D_q, by channel itself when both sources are in error $D_{e,2}$ are given by

$$\begin{aligned}
D_q &= \sum_{m=1}^{2^B}\sum_{n=1}^{2^B}\int_{I_{1,m}}\int_{I_{2,n}}\left[(u_1-\hat{u}_1(m))^2+(u_2-\hat{u}_2(n))^2\right]f(u_1,u_2)du_2du_1\\
&=\sum_{m=1}^{2^B}\int_{I_{1,m}}(u_1-\hat{u}_1(m))^2\sum_{n=1}^{2^B}\int_{I_{2,n}}f(u_1,u_2)du_2du_1\\
&+\sum_{n=1}^{2^B}\int_{I_{2,n}}(u_2-\hat{u}_2(n))^2\sum_{m=1}^{2^B}\int_{I_{1,m}}f(u_1,u_2)du_1du_2\\
&=\sum_{m=1}^{2^B}\int_{I_{1,m}}(u_1-\hat{u}_1(m))^2f(u_1)du_1+\sum_{n=1}^{2^B}\int_{I_{2,n}}(u_2-\hat{u}_2(n))^2f(u_2)du_2\\
&=\int_{\Delta}^{\infty}(u_1-\Delta)^2f(u_1)du_1+\int_{\Delta}^{\infty}(u_2-\Delta)^2f(u_2)du_2\\
&+\int_{-\infty}^{-\Delta}(u_1+\Delta)^2f(u_1)du_1+\int_{-\infty}^{-\Delta}(u_2+\Delta)^2f(u_2)du_2\\
&+\sum_{m=2}^{2^B-1}\int_{I_{1,m}}(u_1-\hat{u}_1(m))^2f(u_1)du_1+\sum_{n=2}^{2^B-1}\int_{I_{2,n}}(u_2-\hat{u}_2(n))^2f(u_2)du_2\\
&\leq 4\left(e^{-\Delta^2/2}\left(\frac{\Delta}{\sqrt{2\pi}}+\frac{1+\Delta^2}{2}\right)\right)+\frac{2\Delta^2}{(2^B-2)^2}\\
&\overset{(a)}{\leq} K_1e^{-2B\ln 2},
\end{aligned}\tag{6.28}$$

$$\begin{aligned}
D_{e,2} &< 2\left(4\Delta^2\Pr(|u_j|<\Delta)+\int_{\Delta}^{\infty}(u_j+\Delta)^2f(u_j)du_j\right.\\
&\left.+\int_{-\infty}^{-\Delta}(u_j-\Delta)^2f(u_j)du_j\right)\\
&\leq 4\left(2\Delta^2(1-e^{-\Delta^2/2})+e^{-\Delta^2/2}(\Delta\sqrt{2/\pi}+1)+\Delta^2e^{-\Delta^2/2}\right.\\
&\left.+2\Delta\left(\frac{1}{\sqrt{2\pi}}+\frac{1-\Delta}{2}e^{-\Delta^2/2}\right)\right)\\
&=(32B\ln 2+4\sqrt{2B\ln 2/\pi})+4e^{-2B\ln 2}(1-4B\ln 2+2\sqrt{2B\ln 2/\pi})
\end{aligned}\tag{6.29}$$

respectively. Note that in step(a) of (6.28) the value of Δ is substituted and to emphasize the exponential term the rest of the factors are given by the coefficient K_1 which represents $O(B)$. In the same way, for the

distortion caused by channel when both sources are in error regardless of being compatible or incompatible, above bound on $D_{e,2}$ is obtained. The reconstruction error expressions when only one source is in error are derived for compatible and incompatible pairs, respectively.

$$\begin{aligned}
D_{e,c,1} &< \sum_{n=1}^{2^{B_j}} \int_{I_{j,n}} (u_j - \hat{u}_j(n))^2 f(u_j) du_j + |2\theta^2\sqrt{1-\rho^2}|^2 \\
&= \int_{\Delta}^{\infty} (u_j - \Delta)^2 f(u_j) du_j + \int_{-\infty}^{-\Delta} (u_j + \Delta)^2 f(u_j) du_j \\
&+ \sum_{n=2}^{2^B-1} \int_{I_{j,n}} (u_j - \hat{u}_j(n))^2 f(u_j) du_j + 4\theta^2(1-\rho^2) \\
&\leq 2e^{-\Delta^2/2} \left(\frac{\Delta}{\sqrt{2\pi}} + \frac{1+\Delta^2}{2} \right) + \frac{\Delta^2}{(2^B-2)^2} + 4\theta^2(1-\rho^2) \\
&\overset{(b)}{\leq} K_1 e^{-2B\ln 2}/2 + 4\theta^2(1-\rho^2),
\end{aligned} \tag{6.30}$$

$$\begin{aligned}
D_{e,ic,1} &< \sum_{n=1}^{2^B} \int_{I_{j,n}} (u_j - \hat{u}_j(n))^2 f(u_j) du_j \\
&+ \int_{u_2'=\theta}^{\infty} \left(\theta\sqrt{1-\rho^2} + \sqrt{1-\rho^2} u_2' \right)^2 f(u_2' | |U_2'| > \theta\sqrt{1-\rho^2}) d_{u_2'} \\
&= \int_{\Delta}^{\infty} (u_j - \Delta)^2 f(u_j) du_j + \int_{-\infty}^{-\Delta} (u_j + \Delta)^2 f(u_j) du_j \\
&+ \sum_{n=2}^{2^B-1} \int_{I_{j,n}} (u_j - \hat{u}_j(n))^2 f(u_j) du_j + 3\theta^2(1-\rho^2) + (1-\rho^2) \\
&\leq 2e^{-\Delta^2/2} \left(\frac{\Delta}{\sqrt{2\pi}} + \frac{1+\Delta^2}{2} \right) + \frac{\Delta^2}{(2^B-2)^2} + 3\theta^2(1-\rho^2) + (1-\rho^2) \\
&\overset{(c)}{\leq} K_1 e^{-2B\ln 2}/2 + 3\theta^2(1-\rho^2) + (1-\rho^2).
\end{aligned} \tag{6.31}$$

Given the symmetry of the normal distribution $D_{e,c,1}$ and $D_{e,ic,1}$ are derived and given in a general form for both sources where $j = 1, 2$. To simplify the calculations, the quantization levels and the number of quantization bins are assumed also to be equal to each other. Thus, the quantization distortion (6.28) can be bounded by $D_q \leq K_1 e^{-2B\ln 2}$. Accordingly, both $D_{e,c,1}$ and $D_{e,ic,1}$ compose the quantization distortion on one source since they represent one correctly and one incorrectly decoded, this is why in steps (b) and (c) the upper bound on D_q derived in (6.28) is used for the source which is decoded correctly.

6.3 Appendix for Multiple-Source Case Derivations

6.3.1 Appendix VIII- Estimation of U

The first expansion of $I(\mathbf{U};\mathbf{Y}|\{\mathbf{V}_j\}_S)$ based on the sources, we have two different derivations for the two distribution types.

$$\begin{aligned} I(\mathbf{U};\mathbf{Y}|\{\mathbf{V}_j\}_S) &= h(\mathbf{U}|\{\mathbf{V}_j\}_S) - h(\mathbf{U}|\mathbf{Y},\{\mathbf{V}_j\}_S) \\ &= -I(\mathbf{U};\{\mathbf{V}_j\}_S) + h(\mathbf{U}) - h(\mathbf{U}-\hat{\mathbf{U}}|\mathbf{Y},\{\mathbf{V}_j\}_S) \\ &\geq -h(\{\mathbf{V}_j\}_S) + h(\{\mathbf{V}_j\}_S|\mathbf{U}) + h(\mathbf{U}) - h(\mathbf{U}-\hat{\mathbf{U}}). \quad (6.32) \end{aligned}$$

For the case where $\mathbf{U}$ and whole set of $\mathbf{U}_j$'s are uniformly distributed, the above expansion (6.32) becomes

$$\begin{aligned} I(\mathbf{U};\mathbf{Y}|\{\mathbf{V}_j\}_S) &\geq -\frac{K}{2}\log\left((2\pi e)^{|S|}(1-\rho^2)^{|S|}(1+\frac{|S|\rho^2}{1-\rho^2})\right) \\ &\quad + |S|K\log(2\sqrt{3(1-\rho^2)}) + K\log 2\sqrt{3} - \frac{K}{2}\log(2\pi eD) \\ &= \frac{K}{2}\log\left(\left(\frac{6}{\pi e}\right)^{|S|+1}\frac{1}{(1+\frac{|S|\rho^2}{1-\rho^2})D}\right) \quad (6.33) \end{aligned}$$

whereas the same expansion yields for the Gaussian case

$$\begin{aligned} I(\mathbf{U};\mathbf{Y}|\{\mathbf{V}_j\}_S) &\geq -\frac{K}{2}\log\left((2\pi e)^{|S|}(1-\rho^2)^{|S|}(1+\frac{|S|\rho^2}{1-\rho^2})\right) \\ &\quad + \frac{|S|K}{2}\log(1-\rho^2)2\pi e + \frac{K}{2}\log(2\pi e) - \frac{K}{2}\log(2\pi eD) \\ &= \frac{K}{2}\log\left(\frac{1}{(1+\frac{|S|\rho^2}{1-\rho^2})D}\right) \quad (6.34) \end{aligned}$$

where $|S|$ denotes the size of the set $\mathbf{V}_j$ and using the following bound on entropy $h(\mathbf{U}-\hat{\mathbf{U}})$

$$\begin{aligned} h(\mathbf{U}-\hat{\mathbf{U}}) &\leq \sum_{j=1}^{K} h(U_j-\hat{U}_j) \\ &\leq \frac{K}{2}\log\left(\frac{2\pi e}{K}\sum_{j=1}^{K}\mathbb{E}[(U_j-\hat{U}_j)^2]\right) \\ &\leq K\log\left(\sqrt{2\pi eD}\right). \quad (6.35) \end{aligned}$$

The second expansion of (6.32) based on the output signals is given by

$$
\begin{aligned}
I(\mathbf{U};\mathbf{Y}|\{\mathbf{V}_j\}_S) &\overset{(a)}{\leq} I(\mathbf{U};\mathbf{Y}|\{\mathbf{V}_j\}_S,\Phi) \\
&= h(\mathbf{Y}|\{\mathbf{V}_j\}_S,\Phi) - h(\mathbf{Y}|\mathbf{U},\{\mathbf{V}_j\}_S,\Phi) \\
&= \sum_{i=1}^{N} h(Y_i|Y^{i-1},\{\mathbf{V}_j\}_S,\Phi) - \sum_{i=1}^{N} h(Y_i|Y^{i-1},\{\mathbf{V}_j\}_S,\mathbf{U},\Phi) \\
&\overset{(b)}{\leq} \sum_{i=1}^{N} h(Y_i|Y^{i-1},\{\mathbf{V}_j\}_S,\{X_j^i e^{i\phi_j}\}_S,\Phi) \\
&\quad - \sum_{i=1}^{N} h(Y_i|Y^{i-1},\{\mathbf{V}_j\}_S,\mathbf{U},\{X_j^i e^{i\phi_j}\}_S,\{X_j^i e^{i\phi_j}\}_{S^c},\Phi) \\
&= \sum_{i=1}^{N} h(Y_i - \sum_{j\in S} X_{i,j} e^{i\phi_{i,j}}|Y^{i-1},\{\mathbf{V}_j\}_S,\{X_j^i e^{i\phi_j}\}_S,\Phi) \\
&\quad - \sum_{i=1}^{N} h(Y_i - \sum_{j\in S} X_{i,j} e^{i\phi_{i,j}} - \sum_{j\in S^c} X_{i,j} e^{i\phi_{i,j}}| \\
&\quad Y^{i-1},\{\mathbf{V}_j\}_S,\mathbf{U},\{X_j^i e^{i\phi_j}\}_S,\{X_j^i e^{i\phi_j}\}_{S^c},\Phi) \\
&= \sum_{i=1}^{N} h(\sum_{j\in S^c} X_{i,j} e^{i\phi_{i,j}} + Z_i|Y^{i-1},\{\mathbf{V}_j\}_S,\{X_j^i e^{i\phi_j}\}_S,\Phi) \\
&\quad - \sum_{i=1}^{N} h(Z_i) \\
&\leq \sum_{i=1}^{N} \log\left(1 + \frac{\sum_{j\in S^c} \mathcal{E}_{i,j}}{N_0}\right) \\
&\leq N \log\left(1 + \frac{\sum_{i=1}^{N}\sum_{j\in S^c} \mathcal{E}_j}{NN_0}\right) \\
&\leq N \log\left(1 + \frac{K\sum_{j\in S^c} \mathcal{E}_j}{NN_0}\right) \qquad (6.36)
\end{aligned}
$$

where (a) is a result of the fact that $\mathbf{U}$ and Φ are independent conditioned on $\{\mathbf{V}_j\}_S$. In the both terms of step (b), we introduce $\{X_j^i e^{i\phi_j}\}_S$ which comes for free due to the feedback in the system, i.e. conditioning on $(Y^{i-1},\{\mathbf{V}_j\}_S,\Phi)$ and simply $(\{\mathbf{V}_j\}_S,\Phi)$ when no feedback is present. $\{X_j^i e^{i\phi_j}\}_{S^c}$ can be added in the same step since conditioning reduces entropy.

6.3.2 Appendix IX- Bound on product Distortion $\prod_{j=1}^{M} D_j$

For the first expansion based on the output signals, we have

$$
\begin{aligned}
&I(\{\mathbf{V}_j\};\mathbf{Y}) \overset{(a)}{\leq} I(\{\mathbf{V}_j\};\mathbf{Y}|\Phi)\\
&= h(\mathbf{Y}|\Phi) - h(\mathbf{Y}|\{\mathbf{V}_j\},\Phi)\\
&= \sum_{i=1}^{N} h(Y_i|Y^{i-1},\Phi) - \sum_{i=1}^{N} h(Y_i|Y^{i-1},\{\mathbf{V}_j\},\Phi)\\
&\overset{(b)}{=} \sum_{i=1}^{N} h(Y_i|Y^{i-1},\Phi) - \sum_{i=1}^{N} h(Y_i|Y^{i-1},\{\mathbf{V}_j\},\{X_j^i e^{i\phi_j}\},\Phi)\\
&= \sum_{i=1}^{N} h(\sum_{j=1}^{M} X_{i,j}e^{i\phi_{i,j}} + Z_i|Y^{i-1},\Phi)\\
&- \sum_{i=1}^{N} h(Y_i - \sum_{j=1}^{M} X_{i,j}e^{i\phi_{i,j}}|Y^{i-1},\{\mathbf{V}_j\},\{X_j^i e^{i\phi_j}\},\Phi)\\
&= \sum_{i=1}^{N} h(\sum_{j=1}^{M} X_{i,j}e^{i\phi_{i,j}} + Z_i|Y^{i-1},\Phi) - \sum_{i=1}^{N} h(Z_i)\\
&\leq \sum_{i=1}^{N} \log\left(1 + \frac{\sum_{j=1}^{M}\mathcal{E}_{i,j}}{NN_0}\right)\\
&\leq N\log\left(1 + \frac{\sum_{i=1}^{N}\sum_{j=1}^{M}\mathcal{E}_{i,j}}{NN_0}\right)\\
&\leq N\log\left(1 + \frac{KM\mathcal{E}}{NN_0}\right)
\end{aligned}
\tag{6.37}
$$

where (a) is a result of the fact that $\mathbf{V}_j$ and Φ are independent and (b) results from the feedback in the system which allows us to introduce $\{X_j^i e^{i\phi_j}\}$ without having any effect on the equality due to conditioning on $(Y^{i-1},\{\mathbf{V}_j\},\Phi)$ and simply $(\{\mathbf{V}_j\},\Phi)$ when no feedback is present. On the other hand, the second expansion of $I(\{\mathbf{V}_j\};\mathbf{Y})$ is derived for normally distributed $\mathbf{V}_j$'s as

$$
\begin{aligned}
&I(\{\mathbf{V}_j\};\mathbf{Y}) = h(\{\mathbf{V}_j\}) - h(\{\mathbf{V}_j\}|\mathbf{Y})\\
&= h(\{\mathbf{V}_j\}) - h(\{\mathbf{V}_j - \hat{\mathbf{V}}_j\}|\mathbf{Y})\\
&\geq h(\{\mathbf{V}_j\}) - h(\{\mathbf{V}_j - \hat{\mathbf{V}}_j\})\\
&\geq \frac{K}{2}\log\left((1-\rho^2)^M(2\pi e)^M(1+\frac{M\rho^2}{1-\rho^2})\right) - \frac{K}{2}\log\left((2\pi e)^M\prod_{j=1}^{M} D_j\right)\\
&= \frac{K}{2}\log\left(\frac{(1-\rho^2)^M(1+\frac{M\rho^2}{1-\rho^2})}{\prod_{j=1}^{M} D_j}\right)
\end{aligned}
\tag{6.38}
$$

which yields

$$
\begin{aligned}
&I(\{\mathbf{V}_j\};\mathbf{Y}) = h(\{\mathbf{V}_j\}) - h(\{\mathbf{V}_j\}|\mathbf{Y}) \\
&= h(\{\mathbf{V}_j\}) - h(\{\mathbf{V}_j - \hat{\mathbf{V}}_j\}|\mathbf{Y}) \\
&\geq h(\{\mathbf{V}_j\}) - h(\{\mathbf{V}_j - \hat{\mathbf{V}}_j\}) \\
&= h(\{\rho\mathbf{U}\mathbf{1} + \sqrt{1-\rho^2}\mathbf{U'}_j\}) - h(\{\mathbf{V}_j - \hat{\mathbf{V}}_j\}) \\
&\geq h(\{\rho\mathbf{U}\mathbf{1} + \sqrt{1-\rho^2}\mathbf{U'}_j\}|\rho\mathbf{U}\mathbf{1}) - h(\{\mathbf{V}_j - \hat{\mathbf{V}}_j\}) \\
&= h(\{\sqrt{1-\rho^2}\mathbf{U'}_j\}) - h(\{\mathbf{V}_j - \hat{\mathbf{V}}_j\}) \\
&\geq \frac{KM}{2}\log\Big(12(1-\rho^2)\Big) - \frac{K}{2}\log\left((2\pi e)^M \prod_{j=1}^{M} D_j\right) \\
&= \frac{K}{2}\log\left(\Big(6(1-\rho^2)\pi e\Big)^M \frac{1}{\prod_{j=1}^{M} D_j}\right)
\end{aligned}
\tag{6.39}
$$

for the uniform case.

6.3.3 Appendix X- Estimation of the set of V_j's

The first expansion of $I(\mathbf{V}_j;\mathbf{Y}|\{\mathbf{V}_l\}_S)$ on the output signals is given as

$$
\begin{aligned}
&I(\mathbf{V}_j;\mathbf{Y}|\{\mathbf{V}_l\}_S) \overset{(a)}{\leq} I(\mathbf{V}_j;\mathbf{Y}|\{\mathbf{V}_l\}_S,\Phi) \\
&= h(\mathbf{Y}|\{\mathbf{V}_l\}_S,\Phi) - h(\mathbf{Y}|\mathbf{V}_j,\{\mathbf{V}_l\}_S,\Phi) \\
&= \sum_{i=1}^{N} h(Y_i|Y^{i-1},\{\mathbf{V}_l\}_S,\Phi) - \sum_{i=1}^{N} h(Y_i|Y^{i-1},\mathbf{V}_j,\{\mathbf{V}_l\}_S,\Phi) \\
&\overset{(b)}{\leq} \sum_{i=1}^{N} h(Y_i|Y^{i-1},\{\mathbf{V}_l\}_S,\{X_j^i e^{i\phi_j}\}_S,\Phi) \\
&- \sum_{i=1}^{N} h(Y_i|Y^{i-1},\mathbf{V}_j,\{\mathbf{V}_l\}_S,\{X_j^i e^{i\phi_j}\}_{S^c},\{X_j^i e^{i\phi_j}\}_S,\Phi) \\
&\overset{(c)}{=} \sum_{i=1}^{N} h(Y_i - \sum_{j\in S} X_{i,j}e^{i\phi_{i,j}}|Y^{i-1},\{\mathbf{V}_l\}_S,\{X_j^i e^{i\phi_j}\}_S,\Phi) \\
&- \sum_{i=1}^{N} h(Y_i - \sum_{j\in S^c} X_{i,j}e^{i\phi_{i,j}} - \sum_{j\in S} X_{i,j}e^{i\phi_{i,j}}| \\
&\qquad Y^{i-1},\{\mathbf{V}_j\}_{S^c},\{\mathbf{V}_l\}_S,\{X_j^i e^{i\phi_j}\}_{S^c},\{X_j^i e^{i\phi_j}\}_S,\Phi)
\end{aligned}
$$

$$
\begin{aligned}
&\overset{(d)}{\leq} \sum_{i=1}^{N} h(\sum_{j\in S^c} X_{i,j}e^{i\phi_{i,j}} + Z_i|Y^{i-1}, \{\mathbf{V}_l\}_S, \{X_j^i e^{i\phi_j}\}_S, \Phi) - \sum_{i=1}^{N} h(Z_i) \\
&\leq \sum_{i=1}^{N} \log\left(1 + \frac{\sum_{j\in S^c}\mathcal{E}_{i,j}}{NN_0}\right) \\
&\leq N\log\left(1 + \frac{\sum_{i=1}^{N}\sum_{j\in S^c}\mathcal{E}_{i,j}}{NN_0}\right) \\
&\leq N\log\left(1 + \frac{K\sum_{j\in S^c}\mathcal{E}_j}{NN_0}\right) \qquad (6.40)
\end{aligned}
$$

where (a) is a result of the fact that $\mathbf{V}_j$ and Φ are independent conditioned on $\{\mathbf{V}_l\}_S$.. In step (b), $\{X_j^i e^{i\phi_j}\}_S$ comes from conditioning on $(Y^{i-1}, \{\mathbf{V}_l\}, \Phi)$ in the case of feedback and from conditioning on $(\{\mathbf{V}_j\}, \Phi)$ when no feedback is present. In (c), $\sum_{j\in S} X_{i,j}e^{i\phi_{i,j}}$ is subtracted from the output signal which yields $\sum_{j\in S^c} X_{i,j}e^{i\phi_{i,j}}$ together with the noise term in the following step (d). For $S \in [1, M-1]$, the second expansion is obtained for the Gaussian sources as

$$
\begin{aligned}
&I(\mathbf{V}_j; \mathbf{Y}|\{\mathbf{V}_l\}_S) = h(\mathbf{V}_j|\{\mathbf{V}_l\}_S) - h(\mathbf{V}_j|\mathbf{Y}, \{\mathbf{V}_l\}_S) \\
&= -I(\mathbf{V}_j; \{\mathbf{V}_l\}_S) + h(\mathbf{V}_j) - h(\mathbf{V}_j - \hat{\mathbf{V}}_j|\mathbf{Y}, \{\mathbf{V}_l\}_S) \\
&\geq -h(\{\mathbf{V}_l\}_S) + h(\{\mathbf{V}_l\}_S|\mathbf{V}_j) + h(\mathbf{V}_j) - h(\mathbf{V}_j - \hat{\mathbf{V}}_j) \\
&= -\frac{K}{2}\log\left((2\pi e)^{|S|}(1-\rho^2)^{|S|}\left(1 + \frac{|S|\rho^2}{1-\rho^2}\right)\right) \\
&+ \frac{K}{2}\log\left((2\pi e)^{|S|}(1-\rho^2)^{|S|}(2-\rho^2+|S|)\right) \\
&+ \frac{K}{2}\log(2\pi e) - \frac{K}{2}\log(2\pi e D) \\
&= \frac{K}{2}\log\left(\frac{1}{D}\frac{(1-\rho^2)(2-\rho^2+|S|)}{1+(|S|-1)\rho^2}\right). \qquad (6.41)
\end{aligned}
$$

whereas for the uniform case, same mutual information yields

$$
\begin{aligned}
&I(\mathbf{V}_j; \mathbf{Y}|\{\mathbf{V}_l\}_S) = h(\mathbf{V}_j|\{\mathbf{V}_l\}_S) - h(\mathbf{V}_j|\mathbf{Y}, \{\mathbf{V}_l\}_S) \\
&= -I(\mathbf{V}_j; \{\mathbf{V}_l\}_S) + h(\mathbf{V}_j) - h(\mathbf{V}_j - \hat{\mathbf{V}}_j|\mathbf{Y}, \{\mathbf{V}_l\}_S) \\
&\overset{(a)}{\geq} -h(\{\mathbf{V}_l\}_S) + h(\{\mathbf{V}_l\}_S|\mathbf{V}_j) + h(\mathbf{V}_j) - h(\mathbf{V}_j - \hat{\mathbf{V}}_j)
\end{aligned}
$$

$$
\begin{aligned}
&\geq -h(\{\mathbf{V}_l\}_S) + h(\{\mathbf{V}_l\}_S|\rho\mathbf{U} + \sqrt{1-\rho^2}\mathbf{U'}_j, \mathbf{U}) \\
&+ \frac{K}{2}\log\left(2^{\frac{K}{2}h(\rho\mathbf{U})} + 2^{\frac{K}{2}h(\sqrt{1-\rho^2}\mathbf{U'}_j)}\right) - h(\mathbf{V}_j - \hat{\mathbf{V}}_j) \\
&= -h(\{\mathbf{V}_l\}_S) + h(\{\sqrt{1-\rho^2}\mathbf{U'}_l\}_S|\rho\mathbf{U} + \sqrt{1-\rho^2}\mathbf{U'}_j, \mathbf{U}) \\
&+ \frac{K}{2}\log\left(2^{\frac{K}{2}h(\rho\mathbf{U})} + 2^{\frac{K}{2}h(\sqrt{1-\rho^2}\mathbf{U'}_j)}\right) - h(\mathbf{V}_j - \hat{\mathbf{V}}_j) \\
&\overset{(b)}{=} -h(\{\mathbf{V}_l\}_S) + h(\{\sqrt{1-\rho^2}\mathbf{U'}_l\}_S) + \frac{K}{2}\log\left(2^{\frac{K}{2}h(\rho\mathbf{U})} + 2^{\frac{K}{2}h(\sqrt{1-\rho^2}\mathbf{U'}_j)}\right) \\
&- h(\mathbf{V}_j - \hat{\mathbf{V}}_j) \\
&\geq -\frac{K}{2}\log\left((2\pi e)^{|S|}(1-\rho^2)^{|S|}(1 + \frac{|S|\rho^2}{1-\rho^2})\right) + \frac{K}{2}\log(12(1-\rho^2))^{|S|} \\
&+ \frac{K}{2}\log(12) - \frac{K}{2}\log(2\pi eD) \\
&= \frac{K}{2}\log\left((\frac{6}{\pi e})^{|S|+1}\frac{1}{D(1+\frac{|S|\rho^2}{1-\rho^2})}\right)
\end{aligned} \tag{6.42}
$$

(a) is caused by the independence between $\mathbf{U}'_j$ and $\mathbf{V}_j$ and in step (b) the conditioning is dropped due to the independence among $\mathbf{U}$ and $\mathbf{U}'_j$'s included within the set S. Equating (6.40) and (6.42) yields the lower bound given by (4.16) for uniformly distributed sources and setting (6.41) equal to (6.42) brings out the Gaussian case of the same bound. For the special case of $|S| = 0$, since we lose the condition of $I(\mathbf{V}_j; \mathbf{Y}|\{\mathbf{V}_l\}_S)$, the first expansion of $I(\mathbf{V}_j; \mathbf{Y})$ is given as

$$
\begin{aligned}
I(\mathbf{V}_j; \mathbf{Y}) &= h(\mathbf{V}_j) - h(\mathbf{V}_j|\mathbf{Y}) \\
&= h(\mathbf{V}_j) - h(\mathbf{V}_j - \hat{\mathbf{V}}_j|\mathbf{Y}) \\
&\geq h(\mathbf{V}_j) - h(\mathbf{V}_j - \hat{\mathbf{V}}_j).
\end{aligned} \tag{6.43}
$$

with

$$
\begin{aligned}
h(\mathbf{V}_j - \hat{\mathbf{V}}_j) &\leq \sum_{j=1}^{K} h(V_{j,i} - \hat{V}_{j,i}) \\
&\leq \frac{K}{2}\log\left(\frac{2\pi e}{K}\sum_{j=1}^{K}\mathbb{E}[(V_{j,i} - \hat{V}_{j,i})^2]\right) \\
&\leq K\log\left(\sqrt{2\pi eD_j}\right).
\end{aligned} \tag{6.44}
$$

The source entropies are given by $h(\mathbf{V}_j) = K \log \sqrt{2\pi e}$ and

$$\begin{aligned} h(\mathbf{V}_j) &= h(\rho \mathbf{U} + \sqrt{1-\rho^2}\mathbf{U}'_j) \\ &\geq \frac{K}{2} \log \left(2^{\frac{2}{K}(K \log |\rho| + h(\mathbf{U})} + 2^{\frac{2}{K} h(\sqrt{1-\rho^2}\mathbf{U}'_j} \right) \\ &= \frac{K}{2} \log \left(2^{\frac{2}{K} K \log |\rho| 2\sqrt{3}} + 2^{\frac{2}{K} K \log 2\sqrt{3|1-\rho^2|}} \right) \\ &= K \log 2\sqrt{3}. \end{aligned} \tag{6.45}$$

for normally and uniformly distributed sources, respectively. Subsituting $h(\mathbf{V}_j)$ and $h(\mathbf{V}_j - \hat{\mathbf{V}}_j)$ into $I(\mathbf{V}_j; \mathbf{Y})$, we obtain

$$I(\mathbf{V}_j; \mathbf{Y}) \geq \begin{cases} \frac{K}{2} \log(1/D_j) & \text{for Gaussian} \\ \frac{K}{2} \log \left(\frac{6}{\pi e} \frac{1}{D_j} \right) & \text{for Uniform.} \end{cases} \tag{6.46}$$

S being an empty set also changes the expansion on the output signals as follows.

$$\begin{aligned} & I(\mathbf{V}_j; \mathbf{Y}) \leq I(\mathbf{V}_j; \mathbf{Y}|\Phi) \\ & = h(\mathbf{Y}|\Phi) - h(\mathbf{Y}|\mathbf{V}_j, \Phi) \\ & = \sum_{i=1}^{N} h(Y_i|Y^{i-1}, \Phi) - \sum_{i=1}^{N} h(Y_i|Y^{i-1}, \mathbf{V}_j, \Phi) \\ & \leq \sum_{i=1}^{N} h(Y_i|Y^{i-1}, \Phi) - \sum_{i=1}^{N} h(Y_i|Y^{i-1}, \mathbf{V}_j, \{X_j^i e^{i\phi_j}\}_{S^c}, \Phi) \\ & = \sum_{i=1}^{N} h(Y_i|Y^{i-1}, \Phi) - \sum_{i=1}^{N} h(Y_i - \sum_{j \in S^c} X_{i,j} e^{i\phi_{i,j}} | Y^{i-1}, \mathbf{V}_j, \{X_j^i e^{i\phi_j}\}_{S^c}, \Phi) \\ & \leq \sum_{i=1}^{N} h(\sum_{j \in S^c} X_{i,j} e^{i\phi_{i,j}} + Z_i | Y^{i-1}, \Phi) - \sum_{i=1}^{N} h(Z_i) \\ & \leq N \log \left(1 + \frac{K \sum_{j \in S^c} \mathcal{E}_j}{N N_0} \right). \end{aligned} \tag{6.47}$$

Through setting (6.46) and (6.47) equal, we obtain the lower bound given by (4.17) in Section 4.3.2.

6.3.4 Appendix XI- Derivation of the Bounds on Distortion and the Average Energy of the Protocol

Hereafter we give the derivations of the distortion terms D_q (4.29), $D_{e,k}$ (4.30), $D_{e,M}$ (4.31) and $D(\mathcal{E}, N_0, 2, \lambda)$ (4.32) together with the average energy consumed by the protocol in more detail. The quantization distortion $D_q = E[(u - \hat{u})^2 | l \ in \ error]$ for $l = 0$ where l denotes the number of

the sources decoded incorrectly. Since the chosen estimator is defined as $\hat{u} = \frac{1}{M}\sum_{j=1}^{M} \hat{v}_j/\rho$, we get

$$\begin{aligned} D_q &= E[(u - \frac{1}{M}\sum_{j=1}^{M} \hat{v}_j/\rho)^2] \\ &\overset{(a)}{=} E\left(\frac{1}{\rho M}\sum_{j=1}^{M}(\sqrt{1-\rho^2}u'_j + e_{q,j})\right)^2 \\ &= \frac{1-\rho^2}{\rho^2 M} Var(u'_j) + \frac{1}{\rho^2 M} Var(e_q) + \frac{2\sqrt{1-\rho^2}}{\rho^2 M^2}\sum E[u'_j e_{q,j}] \\ &\overset{(b)}{\leq} \frac{1-\rho^2}{\rho^2 M} + \frac{\sqrt{3}}{\rho^2 M}\left(2^{-2B+1} + \sqrt{3}(1-\rho^2)/2\right) + \frac{2^{-B+1}(1-\rho^2)}{\rho^2} \end{aligned} \tag{6.48}$$

where $e_q = \frac{1}{\rho M}\sum_{j=1}^{M} e_{q,j}$ and in step (a) we substituted the definition of $\hat{v}_j$ as $\rho u + \sqrt{1-\rho^2}u'_j + e_{q,j}$. In step (b) the variances and the covariance of u'_j and e_q are substituted. The derivations of $D_{e,k}$ and $D_{e,M}$ proceed similarly with a difference of conditioning in the expectation. $D_{e,k}$ is bounded through the peak distortion between u and its estimate for the possible cases when v_j is correctly and incorrectly decoded, i.e. for $\hat{v}_j = v_j$ and $\hat{v}_j \neq v_j$, respectively.

$$\begin{aligned} D_{e,k} &= E\left[(u-\hat{u})^2 | k \; in \; error\right] \\ &= E\left[\frac{1}{M}\left(\sum_{\substack{j \; s.t. \\ \hat{v}_j \neq v_j}} (u - \hat{v}_j/\rho) + \sum_{\substack{j \; s.t. \\ \hat{v}_j = v_j}} (u - \hat{v}_j/\rho)\right)\right]^2 \\ &= E\left[\frac{1}{\rho^2 M^2}\left(\sum_{\substack{j \; s.t. \\ \hat{v}_j \neq v_j}} (\rho u - \hat{v}_j) + \sum_{\substack{j \; s.t. \\ \hat{v}_j = v_j}} (\rho u - \hat{v}_j)\right)^2\right] \\ &\overset{(a)}{=} \frac{k}{\rho^2 M^2} E\left[(\rho u - \hat{v}_j)^2 | \hat{v}_j \neq v_j\right] + \frac{M-k}{\rho^2 M^2} E\left[(\rho u - \hat{v}_j)^2 | \hat{v}_j = v_j\right] \\ &\leq \frac{3(M+8k)(1-\rho^2) + 2^{-B+2}((M+2k)\sqrt{1-\rho^2} + M2^{-B})}{M^2\rho^2/3}. \end{aligned} \tag{6.49}$$

In step (a), the distortion terms for correct and incorrect decoding are weighed by the corresponding numbers which are $M-k$ and k, respectively.

Finally for $D_{e,M}$ we have

$$\begin{aligned}
D_{e,M} &= E\left[(u-\hat{u})^2 | M \text{ in error}\right] \\
&\overset{(a)}{=} E\left[\frac{1}{\rho M}\sum_{j=1}^{M}(\rho u - \hat{v}_j) | M \text{ in error}\right]^2 \\
&= E\left[\frac{1}{\rho^2 M^2}\sum_{j=1}^{M}\rho^2 u^2\right] + E\left[\frac{1}{\rho^2 M^2}\sum_{j=1}^{M}\hat{v}_j^2\right] \\
&+ E\left[\frac{2}{\rho^2 M^2}\sum_{j<j'}(\rho u - \hat{v}_j)(\rho u - \hat{v}_{j'})\right] \\
&= E\left[u^2\right] + \frac{1}{\rho^2 M}E\left[\hat{v}_j^2\right] \\
&\leq 1 + \frac{1}{\rho^2 M}\left(2\rho\sqrt{3} + \sqrt{3(1-\rho^2)}\right)^2 \\
&= 1 + \frac{12}{M} + \frac{12\sqrt{1-\rho^2}}{\rho M} + \frac{3(1-\rho^2)}{\rho^2 M}. \qquad (6.50)
\end{aligned}$$

In step (a), the definition of the estimator $\hat{u} = \frac{1}{M}\sum_{j=1}^{M}\hat{v}_j/\rho$ is substituted.

$D(\mathcal{E}, N_0, 2, \lambda)$, the distortion achieved at the end of the second round of the protocol which consumes the average energy $\mathcal{E}$ is defined and bounded as

$$\begin{aligned}
&D(\mathcal{E}, N_0, 2, \lambda) = D_q(1-P_e) + \sum_{k=1}^{M-1} D_{e,k}P_{e,k}^{(1)}\Pr(E_{e\to c,1}|k \text{ in error}) \\
&+ D_{e,M}P_{e,M}^{(1)}\Pr(E_{e\to c,1}|M \text{ in error}) \\
&+ \Pr(E_1)\sum_{k=1}^{M-1} D_{e,k}P_{e,k}^{(2)}(E_1)(1-\Pr(E_{e\to c,1}|k \text{ in error})) \\
&+ \Pr(E_1)D_{e,M}P_{e,M}^{(2)}(E_1)(1-\Pr(E_{e\to c,1}|M \text{ in error})) \\
&+ \Pr(E_1^c)\Pr(E_{c\to e,1})\left(\sum_{k=1}^{M-1} D_{e,k}P_{e,k}^{(2)}(E_1^c) + D_{e,M}P_{e,M}^{(2)}(E_1^c)\right) \\
&\overset{(a)}{\leq} D_q + \sum_{k=1}^{M-1} D_{e,k}P_{e,k}^{(1)}\Pr(E_{e\to c,1}|k \text{ in error}) \\
&+ D_{e,M}P_{e,M}^{(1)}\Pr(E_{e\to c,1}|M \text{ in error}) \\
&+ \left(\Pr(E_1)\sum_{k=1}^{M-1} D_{e,k}P_{e,k}^{(2)}(E_1) + \Pr(E_1^c)\sum_{k=1}^{M-1} D_{e,k}P_{e,k}^{(2)}(E_1^c)\right) \\
&+ \left(\Pr(E_1)D_{e,M}P_{e,M}^{(2)}(E_1) + \Pr(E_1^c)D_{e,M}P_{e,M}^{(2)}(E_1^c)\right)
\end{aligned}$$

$$
\begin{aligned}
&= D_q + \sum_{k=1}^{M-1} D_{e,k} P_{e,k}^{(1)} \Pr(E_{e\to c,1} | k \ \ in \ \ error) \\
&+ D_{e,M} P_{e,M}^{(1)} \Pr(E_{e\to c,1} | M \ \ in \ \ error) + \sum_{k=1}^{M-1} D_{e,k} P_{e,k}^{(2)} + D_{e,M} P_{e,M}^{(2)} \\
&\leq D_q + \sum_{k=1}^{M-1} D_{e,k} P_{e,k} + D_{e,M} P_{e,M} \qquad (6.51)
\end{aligned}
$$

where P_e is the probability of at least one source being in error upon completion of the protocol, $\Pr(E_1)$ is the probability of at least one source being in error after the first round of the protocol (event E_1) whereas its complement is denoted by $\Pr(E_1^c)$. In step (a) the probabilities of error to be detected given k and M sources are in error and the probability of mis-detection ($\Pr(E_{c\to e,1})$) are bounded by 1. The probability of not making an error at the end of the second round, i.e. $(1 - P_e)$, is also upper bounded by 1 in the same step. $P_{e,l}^{(1)}$ is the notation for Pr(l in error after round 1) whereas $P_{e,l}^{(2)}$ denotes Pr(l in error after round 2) for $l = 1, 2, ..., M$.

The average energy used by protocol can be derived and bounded as

$$
\begin{aligned}
\mathcal{E} &= \mathcal{E}_{\mathrm{D},1} + \sum_{k=1}^{M-1} \frac{k\mathcal{E}_{\mathrm{C},1}}{M} P_{e,k}^{(1)} + \mathcal{E}_{\mathrm{C},1} P_{e,M}^{(1)} \\
&+ \mathcal{E}_{\mathrm{D},2} \Bigg[\sum_{k=1}^{M-1} P_{e,k}^{(1)} \left(1 - \Pr(E_{e\to c,1} | k \ \ in \ \ error)\right) \\
&+ P_{e,M}^{(1)} \left(1 - \Pr(E_{e\to c,1} | M \ \ in \ \ error)\right) \Bigg] \\
&+ \mathcal{E}_{\mathrm{D},2} \left[\left(1 - \left(\sum_{k=1}^{M-1} P_{e,k}^{(1)} + P_{e,M}^{(1)} \right) \right) \Pr(E_{c\to e,1}) \right] \\
&\leq \mathcal{E}_{\mathrm{D},1} + \mathcal{E}_{\mathrm{C},1} P_e(\mathbf{m}) + \mathcal{E}_{\mathrm{D},2} [P_e(\mathbf{m}) + \Pr(E_{c\to e,1})] \qquad (6.52)
\end{aligned}
$$

Chapter 7

Résumé

Claude Shannon en 1948 grâce à son oeuvre [2] a montré qu'un codage séparé source-canal pour un système point-a-point ne provoque aucune perte d'optimalité (en termes de transmission fiable) dans la mesure que la longueur des mots de code tend vers l'infini. Ce résultat a été prouvé dans très peu d'autre topologies de transmission. Néanmoins, en raison de l'optimalité dans le cas d'une source unique, c'est la raison principale que l'on traite le codage source et canal séparément dans les reseaux sans-fils modernes. Du point de vue de la mise en réseau, il est également pratique de séparer les deux opérations afin de simplifier les protocoles, car les données numériques peuvent être multiplexés. Cependant, ces implémentations pratiques engendrent des retards élevés, qui se traduit par la latence, et une grande complexité en raison des encodages extrêmement longs. En combinant le codage canal et source, connue sous le nom de codage-canal source commune, la latence peut être limitée. On pourrait s'attendre à ce que cette technique fournira des améliorations significatives en termes de latence dans le cas d'une source avec une redondance importante combiné avec un canal avec des niveaux de bruit élevés. Cela est dû au fait que dans ce cas, le codage source-canal traditionnel, ou séparé, devrait d'abord utiliser le codage source afin d'éliminer la redondance et ensuite utiliser codage de canal pour insérer une redondance supplémentaire. Ainsi, il ne est pas surprenant que ce ne est pas l'approche la plus efficace, même lorsque la longueur des blocs est croit sans limite.

Un exemple moderne d'un système utilisant des approches de canal joint-sources (numérique) serait la norme HDMI actuelle utilisant une transmission OFDM sans fil à courte distance pour la vidéo haute définition avec une latence inférieure a 1ms. Cette technique exploite les niveaux variables du

signal source transformé (audio / vidéo) avec une protection d'erreur non-uniforme dans la couche physique qui varie en fonction des différents niveaux d'importance des signaux de source. Ici, l'information analogique n'est pas codé en utilisant un code source autre que la quantification scalaire. La latence est donc limitée et le schéma resemble au codage linéaire décrit par Goblick dans [4]. La remarque la plus importante à souligner est que cette approche est utilisée pour *minimiser la latence*.

Une autre raison motivant l'utilisation de nouvelles joint-source et canal paradigmes de codage serait les échelles de temps correspondants aux largeurs de bande de la source et du canal. Dans les réseaux de capteurs, par exemple, les sources peuvent être caractérisées par quelques échantillons indépendants d'un phénomène analogique qui doivent être transmis de façon très sporadique à travers un canal à large bande. Ce serait le cas lorsque nous intégrons des capteurs analogiques à faible coût / puissance au sein de l'infrastructure LTE. Ici, l'ergodicité de la source ne est pas un degré de liberté qui peut être exploitée par le système de codage. Curieusement, la performance ultime (en termes de reconstruction fidélité au récepteur) réalisables par un système de codage pour ce problème simple à formuler reste inconnue, bien que limites supérieures et inférieures sur la performance sont faciles à trouver.

Ce qui est sûr c'est que la transmission numérique des petites quantités de données généralement analogiques induira des surcoûts protocolaires, en particulier pour les réseaux massifs de nœuds simples, si on se limite aux techniques mis-en-place aujourd'hui. Le codage conjoint source-canal, qui combine les efforts du code canal et le code source, peut-être utile de ce point-de-vue. Dans cette étude, nous considérons la transmission de plusieurs échantillons spatialement répartis d'un champ aléatoire lentement variable dans le temps. Notre objectif principal est de fournir des mesures de la performance asymptotique et des stratégies de transmission réalisables et simples pour les grands réseaux de capteurs à un bond de transmission vers le centre de fusion (un canal à accés-multiples). On modélise les systèmes où chaque capteur mesure des signaux avec un nombre fini et petit de dimensions de la source, par rapport au nombre de dimensions de canal. Ceci est motivé par des applications telles que la télédétection en utilisant l'infrastructure sans-fil à large bande (par exemple les réseaux cellulaires) où les capteurs prélèvent des échantillons sporadiques d'un événement aléatoire, les envoient au réseau via des stations de base et reviennent ensuite à un état de repos pour économiser l'énergie. En conséquence, nous ne considérons pas le codage des séquences d'échantillons, mais plutôt exploitons l'expansion spatiale et la corrélation entre les noueds du réseau avec un bruit d'observation indépendante. Tenant compte que les applications ciblent les réseaux sans fil, il est raisonnable de supposer qu'une stratégie de transmission basé sur un canal de retour. Par conséquant les résultats asymptotiques ainsi que la stratégie de transmission étudié pourraient exploiter un canal

de retour. Ce dernier permet de stratégies simples et économes en énergie, même si les évaluations ne sont pas nécessairement optimale.

Imaginez le cas le plus simple d'un noeud avec un capteur qui suit une séquence aléatoire lentement variable dans le temps et qui envoi ses observations à un récepteur à travers un canal sans fil. La source est indiquée par un variable aléatoire U de moyenne nulle et de variance $\sigma_u^2 = 1$, représentant une seule réalisation de la séquence aléatoire à un moment donné t. Le capteur doit être considéré comme un petit appareil avec des contraintes énergétiques strictes. Le canal de communication entre l'émetteur et le récepteur est un canal à bruit blanc gaussien additif. Une question importante est de savoir comment coder de manière efficace le variable aléatoire U pour la transmission. L'efficité est mesuré dans ce cas en termes de la relation entre l'erreur de reconstruction et l'énergie utilisée pour réaliser cette transmission. A titre d'exemple, le capteur peut sporadiquement envoyer des informations analogiques (température, champ magnétique, le courant, la vitesse, etc.) à un noeud de collecteur. Le trafic serait à très faible taux (quasi nul) et pouvant nécessiter faible latence. Celle-ci pourrait se produire pour deux raisons, soit la réactivité d'un élément d'actionnement dans le réseau ou pour minimiser la consommation d'énergie dans le noeud de détection même en utilisant la transmission et la réception discontinue. Ici, le temps de latence de la transmission est directement liée au temps d'activation d'un circuit de communication du noeud de détection. Cet exemple fait ressortir l'essence de certains communications entre machines, ce que l'on appele le MTC ("machine-type communications") ou M2M ("machine-to-machine communications"), un terme qui fait référence aux machines (y compris les capteurs) interconnectées via des réseaux cellulaires et qui échangent des informations de façon autonome.

Pour ce scénario, la caractéristique de variation lente dans le temps de la source a deux principaux impacts sur la façon dont le problème de codage doit être adressée: premièrement, le temps entre deux observations est longue, et le capteur ne doit pas attendre une séquence d'observations pour encoder. Par conséquent, le capteur code seulement une observation avant de l'envoyer à travers le canal. Ensuite, pour chaque source réalisation le canal peut potentiellement être utilisé par de nombreuses dimensions dans l'espace des signaux, par exemple par codage sur une bande-passante large dans le domaine fréquentiel. Ce serait le cas pour les capteurs reliés directement aux réseaux cellulaires de quatrième génération. Par conséquent, on peut raisonnablement supposer qu'il n'y ait pas de contrainte sur la dimensionalité utilisée pour le codage de canal. Cette dernière condition revient à dire que les codes à rendement très faible devraient être utilisés. Dans [3], les auteurs affirment trois principales exigences qui doivent être satisfaites pour que la technologie 5G puissent accomoder les communications entre machines, le support d'un très grand nombre de périphériques connectés, le maintien de taux réduit et à faible latence. Cette thèse présente des modèles

de systèmes et stratégies de transmission qui tentent de répondre à ces trois principales exigences de la 5G.

Nous concentrons notre attention sur le cas où les échantillons unitaires de la source sont transmis de façon sporadique en raison de ralentir le temps de variation comme expliqué ci-dessus dans la motivation. Dans le problème d'une source unique, un codeur associe une réalisation de la source U dans $\mathbf{X} \triangleq (X_1, \ldots, X_n)$ où N désigne la dimension de l'entrée du canal. Nous allons faire usage d'une voie de retour causale afin que le codeur puisse aussi dépendre de sorties de canal dernières, c'est-à-dire que $X_i = f(U, y_1, \cdots, Y_{i-1})$. $\mathbf{X}$ est ensuite envoyé à travers le canal corrompu par une séquence de bruit blanche et gaussien, $\mathbf{Z}$, et est reçu comme $\mathbf{Y}$. Le récepteur est une fonction qui tente de construire une estimé $\widehat{U}$ de U étant donné $\mathbf{Y}$. Le critère de la fidélité que nous souhaitons minimiser est l'erreur quadratique moyen ("mean-squred error" ou MSE) défini comme $D \triangleq \mathbb{E}[(U - \widehat{U})^2]$, sous une contrainte d'énergie $\mathbb{E}[||\mathbf{X}||^2] \leq \mathcal{E}$. Une borne inférieure sur la distorsion sur tous les encodeurs et décodeurs possibles est facilement dérivés dans [4] utilisant la théorie de l'information classique, et donnée par

$$D \geq e^{-2\mathcal{E}/N_0} \tag{7.1}$$

où $N_0/2$ est bruit du canal par dimension. Notez que par rapport à la forme d'origine,(7.1) est adapté à un canal gaussien complexe en temps discret avec variance de bruit $N_0/2$ afin de rendre les comparaisons plus faciles avec notre informations théoriques bornes inférieures dans les autres chapitres.

Pour le cas d'un canal point-à-point sans retour, les études les plus récentes et importantes sont présentés par Merhav dans [13,14] pour les canaux AWGN et des canaux discret sans mémoire, respectivement. Dans [13, 15] la borne inférieure la plus serrée sur la MSE avec une détection cohérente et une bande passante du canal illimitée se comporte comme $e^{-\mathcal{E}/2N_0}$ pour U uniformément distribuée. $\mathcal{E}$ est l'énergie utilisée pour la transmission de U. En fait, l'auteur réalise cette limite inférieure sur la MSE en bornant la distribution complementaire de l'erreur,$|U - \hat{U}|$, plutôt que de se concentrer sur le MSE comme critère de performance elle-même. Afin de prouver des resultats sur la distribution de $|U - \hat{U}|$, il généralise la borne classique de Ziv-Zakai [16] en passant de deux à un nombre arbitraire,M, d'hypothèses. et le produit de dérivation que le Chazan-Zakai liés [17]. Dans le chapitre II, nous utilisons les résultats de [13] pour discuter de l'efficacité de notre schema de transmission pour le cas sans voie de retour.

7.0.5 Les systèmes exploitant une voie de retour

Dans les systèmes à deux voies, par exemple les réseaux cellulaires, nous pourrions imaginer clairement l'utilisation de la transission ultra-fiable de la liaison descendante (c'est à dire un retour parfait). Le principal inconvénient est l'exigence de l'énergie pour le récepteur qui aurait un impact le

budget énergétique globale du noeud de détection. Même s'il est difficile de modéliser, la latence du protocole devient un problème pour la consommation globale d'énergie. Certains des premiers travaux de la transmission analogique des sources à faible bande passante suppose la présence du signal de retour $f(\mathbf{Y}(n))$, c'est-à-dire le signal observé sans distortion. Grâce à une communication dans les deux sens, les approches de contrôle stochastique [19,20] peut atteindre, au moins asymptotiquement, la borne inférieure sur la distorsion dans (7.1). Ceci est au détriment du retard, puisque, comme dans de nombreux systèmes adaptatifs, le système avec un retour doit converger pour minimiser la distorsion. Il est raisonnable de supposer que les deux peuvent être étendus à la détection non-cohérente et canaux sélectifs en fréquence large bande, même pour la diversité. Cependant, les stratégies d'estimation sous-jacentes vont rapidement devenir très compliqué.

Les régimes réalisables proposés et analysés sur la base de leurs performances asymptotiques dans cette thèse sont inspirés par le schéma de transmission pour les canaux avec retour parfait proposé par Yamamoto et Itoh [1] qui est en fait le schéma Schalkwijk-Barron modifiée [24]. Le document d'origine [1] est applicable aux canaux à temps discret et AWGN. Un cycle de transmission dans les deux études réalisées par Yamamoto-Itoh et Schalkwijk-Barron est composé de deux phases que l'on appelle le mode de message, où le message de la source est transmis et réinjectée, et le mode de commande où la transmission du message de commande et la rétroaction se produisent.

7.0.6 Les cas de sources multiples

En ce qui concerne le problème de sources multiples. nous sommes particulièrement intéressés dans le cas où les variables aléatoires corrélées sont transmis sur des canaux à accès multiple, où l'information des sources sont envoyés via un canal AWGN. La question principale est de savoir comment faire le codage par rapport à la performance à atteindre lors de la reconstruction en fonction de l'énergie nécessaire. L'élément clé dans le scénario multi-capteur étant d'exploiter la corrélation, qui est supposé être connu, à la fois sur l'émetteur et le récepteur. En outre, nous cherchons à déterminer les régimes de fonctionnement d'un tel système à accès multiple en termes de corrélation joue le rôle dans la détermination de l'efficacité énergétique.

Le problème de sources multiples peut être considérée comme le problème CEO tel qu'il figure dans la littérature avec quelques différences. Le problème initial est introduit et formulé dans [26, 27] pour un discret sans mémoire source X. Le CEO dans un réseau de capteurs se intéresse à l'information d'une source $\{X(t)\}_{t=1}^{\infty}$ qui ne peut être obtenu directement ainsi le CEO utilise L agents qui observent une version bruyante de la source indépendante. Les agents envoient leurs observations, $Y_i(t) = X(t) + N_i(t)$, au directeur général qui est soumis à un taux de somme finie contrainte R.

Ici, le bruit d'observation gaussien est notée $N_i(t)$ qui est iid $\forall i = 1, \cdots, L$ et $t = 1, \cdots, n, \cdots$. Le CEO tente de reconstituer $\{X(t)\}_{t=1}^{\infty}$ qui se traduit par $D(R)$, la fonction de distorsion des taux de la source $X(t)$. Les auteurs dans [27] déterminé la fréquence d'erreur minime asymptotiquement dans L et R. [28] étudie un cas particulier du problème et qui considèrent la source $\{X(t)\}_{t=1}^{\infty}$ comme une variable aléatoire gaussienne iid et de montrer l'asymptotique la performance de la distorsion à la fois L et R ont tendance à l'infini. Il existe de nombreuses études dans la littérature qui traitent de ce problème dans différents contextes. [29] aborde le problème dans un système de communication source-canal multi-terminal avec sources corrélées transmis sur un MAC sans être soumis à un bruit de canal et fournit la région taux de distortion du codage de source multi-terminal. [30] peut être donné comme un autre exemple qui explore le problème de CEO où les auteurs introduisent le taux-région pour le cas gaussien quadratique tandis que dans un document assez récent [31] arrive avec une limite supérieure sur le taux -distortion région du vecteur gaussien problème de CEO pour le cas d'observation bruyant.

Une des principales différences entre le problème de sources multiples dans la façon dont est traitée au chapitre 4 de cette thèse et plusieurs études dans la littérature brièvement mentionné ci-dessus, ce est que tous les résultats obtenus au chapitre 4 sont considérés dans le contexte de taux zéro, savoir, un taux de fuite. Une autre différence majeure peut être déclaré que l'accent mis sur la transmission d'échantillons unitaires du message source au lieu de faire le codage séquentiel comme déjà mentionné ci-dessus dans la définition du problème et sera mis en évidence dans d'autres chapitres. Enfin, nous combinons le problème de CEO d'origine avec un canal d'accès multiple et discutons de la performance d'un système avec des sources analogiques corrélées sur une GMAC avec un lien de rétroaction du récepteur à chaque codeur comme on le verra en détail au chapitre 4.

Dans l'un des autres chapitres, dans le chapitre 4, nous allons montrer que le MSE qui en résulte pour le cas particulier d'un canal de vecteur avec une entrée gaussienne ([44, eq: 27]) répond à notre résultats de la limite inférieure dérivée de l'erreur de reconstruction d'un vecteur aléatoire simple mesurée par un réseau de capteurs et de multiples vecteurs de sources qui sont transmis à un récepteur commun sur une GMAC avec une rétroaction lien de causalité parfaite au codeur connecté à chaque capteur. Dans [44], Guo et al. définir la relation suivante entre l'information mutuelle du canal et le SNR erreur quadratique moyenne minimum (MMSE) dans des canaux gaussien pour les deux signaux d'entrée et scalaires du vecteur indépendamment de ses statistiques.

$$\frac{\mathrm{d}}{\mathrm{dsnr}} I(\mathrm{snr}) = \frac{\mathrm{MMSE}(\mathrm{snr})}{2}. \tag{7.2}$$

Considérons le cas simple d'un canal scalaire avec la paire de (X, Y) désig-

nant les signaux d'entrée et de sortie à travers la définition suivante de $Y = \sqrt{\text{SNR}}X + N$ où snr est non-négatif et le signal de bruit N est normalement distribué avec zéro écart moyen et de l'unité. Ainsi l'information mutuelle dans (7.2) est fondamentalement $I(X;Y) = I(X; \sqrt{\text{snr}}X+N)$ alors que le MMSE est défini par $\text{MMSE}(\text{snr}) = \text{MMSE}(X|\sqrt{\text{snr}}X + N)$.

7.0.7 Les principaux résultats

Tout d'abord, nous introduisons une faible latence, protocole bidirectionnel pour la transmission d'une seule variable aléatoire sur un canal à large bande et analysé son comportement asymptotique avec détection non cohérente sur les deux canaux en ligne de visée et plus généraux purs évanouissement. La stratégie de protocole et de la transmission pourrait être utilisé pour les capteurs limités en énergie futurs faisant usage de réseaux cellulaires à large bande. Nous montrons que l'écart entre le Goblick classique lié [4] et la limite obtenue par notre système de rétroaction envisagée ne peuvent pas être fermé en répétant le protocole plus de deux tours à moins de 3 dB. L'amélioration par rapport une transmission one-shot est de l'ordre de 3 à 4 dB et asymptotiquement 4,7 dB. Nous incluons également une discussion sur le cas des évaluations imparfaite et son effet sur le compromis entre l'énergie nécessaire pour le protocole et l'erreur de reconstruction dans l'estimation du message source. On montre que dans ce cas, si la consommation d'énergie requise par la liaison de rétroaction est représenté, ce qui réduit la fidélité de reconstruction. En outre, l'évaluation numérique des dernières limites inférieures de Merhav [13] pour la transmission one-shot sont inclus et la variante plus serré en utilisant ses techniques est déterminée. Tant l'évaluation des limites et de la performance du protocole de rétroaction ont été étendues à un modèle d'évanouissement multi-canal. L'amélioration du protocole de retour sur une transmission de tir est encore plus important que dans le cas de ligne de vue. Nous suggérons en outre que les techniques de délimitation plus strictes qui se appuient sur les canaux inconnus doivent être trouvées pour le canal à évanouissement. En outre, les systèmes utilisant la transmission à énergie variable devraient être considérées pour combler l'écart avec les limites inférieures.

Nous procédons à la dérivation des limites inférieures sur l'erreur de reconstruction pour la transmission de deux sources analogiques corrélées en présence de rétroaction causalité. Les bornes sont spécialisés pour le cas de canaux à large bande. Tous nos dérivations sont appliqués à résumer-canaux avec des sources à la fois uniforme et normalement distribués. Nous introduisons ensuite un protocole faible latence bidirectionnelle pour la transmission de deux variables aléatoires corrélées sur un canal à large bande et d'analyser son comportement asymptotique avec détection non-cohérente uniforme et distribution gaussienne. Nous montrons que la transmission de deux sources fortement corrélés peut atteindre l'efficacité énergétique d'une

source unique avec la même énergie totale, au moins dans certains régimes qui régissent le niveau de corrélation. Le cas de corrélation élevé donne le comportement exponentiel de l'affaire et bénéficie d'accumulation d'énergie, ou la collaboration des deux sources d'une source unique. Résultats faible corrélation insignifiante réduit l'efficacité énergétique.

La dernière partie de la thèse couvre une adaptation de deux voies à faible latence protocole de rétroaction pour une distorsion minimale à un grand scénario de réseau avec de multiples sources. Plus précisément, nous introduisons de nouvelles limites inférieures sur l'erreur de reconstruction des stratégies de transmission multi-capteurs arbitraires qui peuvent servir dans une étape ultérieure pour déterminer l'optimalité des stratégies particulières d'accès multiple et d'encodage. À cette fin, nous proposons une stratégie de collaboration tels exploiter corrélation entre capteurs. Haut-bornes asymptotiques sur l'erreur de reconstruction sont prévus pour le protocole proposé. Les deux-limites supérieure et inférieure montrent que la collaboration peut être atteint grâce à l'accumulation de l'énergie et de mettre en lumière un compromis dans la source et le canal SNR qui lui permet de se produire. La performance pratique du protocole de retransmission proposé a été étudiée par l'évaluation numérique de la Haute-limites dans le régime de l'énergie non-asymptotique, qui correspond à l'aide de poids faible quantification dans les capteurs. Les performances du protocole est améliorée par l'introduction d'une modification mineure de la stratégie de contre-réaction qui permet la la performance sans erreur à atteindre rapidement. Les comparaisons avec une transmission one-shot ne pas exploiter les évaluations montrent que gagne avec un tour de rétroaction sont de l'ordre de 2 à 3 dB par rapport à un système de rétroaction-moins et sont souvent moins de 5 dB de la borne inférieure. Il est en outre montré que l'augmentation de la taille du réseau apporte des avantages en termes de performances, mais que le gain en termes d'efficacité énergétique diminue rapidement à des énergies finies en raison d'une perte combinant non cohérente.

Bibliography

[1] H. Yamamoto and K. Itoh, "Asymptotic performance of a modified Schalkwijk-Barron scheme for channels with noiseless feedback," *IEEE Transactions on Information Theory*, vol. 25, pp. 729–733, November 1979.

[2] C. E. Shannon, "A mathematical theory of communication," *The Bell System Technical Journal*, vol. 27, pp. 379–423,623–656, July, October 1948.

[3] F. Boccardi, R. W. Heath, A. E. Lozano, T. L. Marzetta, and P. Popovski, "Five disruptive technology directions for 5G," *CoRR*, vol. abs/1312.0229, 2013. [Online]. Available: http://arxiv.org/abs/1312.0229

[4] T. Goblick, "Theoretical limitations on the transmission of data from analog sources," *IEEE Transactions on Information Theory*, vol. 11, pp. 558–567, October 1965.

[5] P. Elias, "Networks of Gussian channels with applications to feedback systems," *IEEE Transactions on Information Theory*, vol. 13, pp. 493–501, July 1967.

[6] M. Gastpar, "To code or not to code," Ph.D. dissertation, EPFL, Dec. 2002.

[7] F. Abdallah and R. Knopp, "Source-channel coding for very-low bandwidth sources," in *Information Theory Workshop, 2008. ITW '08. IEEE*, may 2008, pp. 184 –188.

[8] F. Abdallah, "Source-channel coding techniques applied to wireless networks," Ph.D. dissertation, University of Nice-Sophia Antipolis, Dec. 2008.

[9] J. Wozencraft and I. M. Jacobs, *Principles of Communication Engineering*. Wiley, New York, 1965.

[10] V. Vaishampayan and I. Costa, "Curves on a sphere, shift-map dynamics, and error control for continuous alphabet sources," *IEEE Transactions on Information Theory*, vol. 49, pp. 1658–1672, July 2003.

[11] B. Hochwald and K. Zeger, "Tradeoff between source and channel coding," *IEEE Transactions on Information Theory*, vol. 43, pp. 1412–1424, Sept. 1997.

[12] B. Hochwald, "Tradeoff between source and channel coding on a Gaussian channel," *IEEE Transactions on Information Theory*, vol. 44, pp. 3044–3055, Nov. 1998.

[13] N. Merhav, "On optimum parameter modulation-estimation from a large deviations perspective," *IEEE Transactions on Information Theory*, vol. 58, pp. 7215–7225, December 2012.

[14] ——, "Exponential error bounds on parameter modulation-estimation for discrete memoryless channels," *IEEE Transactions on Information Theory*, vol. 60, pp. 832–841, February 2014.

[15] ——, "Data processing inequalities based on a certain structured class of information measures with application to estimation theory," *IEEE Transactions on Information Theory*, vol. 58, pp. 5287–5301, July 2012.

[16] J. Ziv and M. Zakai, "Some lower bounds on signal parameter estimation," *IEEE Transactions on Information Theory*, vol. 15, pp. 386–391, November 1969.

[17] D. Chazan, M. Zakai, and J. Ziv, "Improved lower bounds on signal parameter estimation," *IEEE Transactions on Information Theory*, vol. 15, pp. 386–391, November 1969.

[18] K. Bell, Y. Steinberg, Y. Ephraim, and H. Van Trees, "Extended ziv-zakai lower bound for vector parameter estimation," *IEEE Transactions on Information Theory*, vol. 43, pp. 624–637, March 1997.

[19] J. Schalkwijk and L. Bluestein, "Transmission of analog waveforms through channels with feedback," *IEEE Transactions on Information Theory*, vol. 13, pp. 617–619, October 1967.

[20] J. Omura, "Optimum linear transmission of analog data for channels with feedback," *IEEE Transactions on Information Theory*, vol. 14, pp. 38–43, January 1968.

[21] J. Schalkwijk, "A coding scheme for additive noise channels with feedback–II: Band-limited signals," *IEEE Transactions on Information Theory*, vol. 12, pp. 183–189, April 1966.

[22] R. G. Gallager and B. Nakiboğlu, "Variations on a theme by Schalkwijk and Kaliath," *IEEE Transactions on Information Theory*, vol. 56, no. 1, pp. 6–17, Jan. 2010.

[23] J. Schalkwijk and T. Kaliath, "A coding scheme for additive noise channels with feedback–I: no bandwith constraint," *IEEE Transactions on Information Theory*, vol. 12, pp. 172–182, April 1966.

[24] J. Schalkwijk and M. Barron, "Sequential signaling under a peak power constraint," *IEEE Transactions on Information Theory*, vol. 17, pp. 278–282, May 1971.

[25] A. Viterbi, "The effect of sequential decision feedback on communication over the Gaussian channel," *Inform. Contr.*, vol. 8, no. 1, pp. 80–92, Feb 1965.

[26] T. Berger and Z. Zhang, "Source-channel coding for very-low bandwidth sources," in *IEEE International Symposium on Information Theory, ISIT 1994*, june 1994.

[27] T. Berger, Z. Zhang, and H. Viswanathan, "The CEO problem," *IEEE Transactions on Information Theory*, vol. 42, pp. 887–902, may 1996.

[28] H. Viswanathan and T. Berger, "The quadratic Gaussian CEO problem," *IEEE Transactions on Information Theory*, vol. 43, pp. 1549–1559, september 1997.

[29] J. Xiao and Z. Luo, "Multiterminal source-channel communication over an orthogonal Multiple-Access Channel," *IEEE Transactions on Information Theory*, vol. 53, pp. 3255–3264, September 2007.

[30] V. Prabhakaran, D. Tse, and K. Ramchandran, "Rate region of the quadratic Gaussian CEO problem," in *IEEE International Symposium on Information Theory, ISIT 2004*, june 1994.

[31] E. Ekrem and S. Ulukus, "An outer bound for the vector Gaussian CEO problem," in *IEEE International Symposium on Information Theory, ISIT 2012*, june 1994.

[32] A. Lapidoth and S. Tinguely, "Sending a bivariate Gaussian source over a Gaussian MAC with feedback," *IEEE Transactions on Information Theory*, vol. 56, pp. 1852–1864, April 2010.

[33] ——, "Sending a bivariate Gaussian source over a Gaussian MAC," *IEEE Transactions on Information Theory*, vol. 56, pp. 2714–2752, June 2010.

[34] Y. Oohama, "Gaussian multiterminal source coding," *IEEE Transactions on Information Theory*, vol. 43, pp. 1912–1923, November 1997.

[35] A. Wagner, S. Tavildar, and P. Viswanath, "Rate region of the quadratic Gaussian two-encoder source-coding problem," *IEEE Transactions on Information Theory*, vol. 54, pp. 1938–1960, May 2008.

[36] L. Ozarow, "The capacity of the white Gaussian Multiple-Access Channel with feedback," *IEEE Transactions on Information Theory*, vol. 30, pp. 623–629, July 1984.

[37] A. Lapidoth and M. Wigger, "On the Gaussian MAC with imperfect feedback," in *Proc. 24th IEEE Conv. Elec. Electron. Eng. in Israel (IEEEI'06)*, November 2006, pp. 203–207.

[38] A. Jain, D. Gündüz, S. R. Kulkarni, H. V. Poor, and S. Verdú, "Energy-distortion tradeoff with multiple sources and feedback," in *Information Theory and Applications Workshop, ITA 2010, San Diego, California, USA, January 31 - February 5, 2010*, 2010, pp. 142–146.

[39] ——, "Energy-distortion trade-offs in Gaussian joint-source channel coding problems," *IEEE Transactions on Information Theory*, vol. 58, pp. 3153–3168, Mai 2012.

[40] A. Jain, D. Gündüz, S. R. Kulkarni, H. V. Poor, and S. Verdú, "Energy efficient lossy transmission over sensor networks with feedback." in *ICASSP*. IEEE, 2010, pp. 5558–5561. [Online]. Available: http://dblp.uni-trier.de/db/conf/icassp/icassp2010.html#JainGKPV10

[41] M. Gastpar, "Uncoded transmission is exactly optimal for a simple Gaussian 'sensor' network," *IEEE Transactions on Information Theory*, vol. 54, pp. 5247–5251, November 2008.

[42] R. Soundararajan and S. Vishwanath, "Communicating linear functions of correlated Gaussian sources over a MAC," *IEEE Transactions on Information Theory*, vol. 58, pp. 1853–1860, March 2012.

[43] A. Wagner, "An outer bound for distributed compression of linear functions," in *Information Sciences and Systems, CISS 2008*, March 2008, pp. 435–440.

[44] S. Guo, D. Shamai (Shitz) and S. Verdu, "Mutual information and minimum mean-square error in Gaussian channels," *IEEE Transactions on Information Theory*, vol. 51, pp. 1261–1282, April 2005.

[45] J. Barros and S. D. Servetto, "Network information flow with correlated sources," *IEEE Transactions on Information Theory*, vol. 52, pp. 155–170, 2006.

[46] 3GPP TS 36.211 V11.3.0 (2013-06), "3rd Generation Partnership Project; Technical Specification Radio Access Network Aspects;

Evolved Universal Terrestrial Radio Access Network (E-UTRA); Physical Channels and Modulation(Release 11)," no. 36.211, June 2013.

[47] M. Simon and M.-S. Alouini, "Exponential-Type Bounds on the Generalized Marcum Q-Function with Application to Error Probability Analysis over Fading Channels," *IEEE Trans. on Communications*, vol. 48, no. 3, pp. 359 –366, march 2000.

[48] J. Proakis, *Digital Communications*. McGraw-Hill, Third Ed., 1995.

[49] C. E. Shannon, "Probability of error for optimal codes in a Gaussian channel," *The Bell System Technical Journal*, vol. 38, pp. 611–656, May 1959.

[50] M. Steiner, "The strong simplex conjecture is false," *IEEE Transactions on Information Theory*, vol. 40, no. 3, pp. 721–731, 1994.

[51] L. MacColl, "Signalling in the presence of thermal noise, I, II, and III," *Bell Laboratories internal memoranda issued May 27, June 30, and September 13*, 1948.

[52] Y. Sun, "Stochastic iterative algorithms for signal set design for Gaussian channels and optimality of the l2 signal set," *IEEE Transactions on Information Theory*, vol. 43, no. 5, pp. 1574–1587, 1997.

[53] R. Scholtz and C. Weber, "Signal design for phase-incoherent communications," *IEEE Transactions on Information Theory*, vol. 12, no. 4, pp. 456–463, 1966.

[54] LOLAD4.4, European project deliverable, 2013, http://www.ict-lola.eu/deliverables.

[55] A. Unsal and R. Knopp, "Low-latency transmission of low-rate analog sources," in *EUSIPCO 2012, European Signal Processing Conference, August, 27-31, 2012, Bucharest, Romania*, 08 2012. [Online]. Available: http://www.eurecom.fr/publication/3798

[56] ——, "Distortion bounds and a protocol for one-shot transmission of correlated random variables on a non-coherent Multiple-Access Channel," in *SCC 2013, 9th International ITG Conference on Systems, Communications and Coding, January 21-24, 2013, Munich, Germany*, Munich, GERMANY, 01 2013. [Online]. Available: http://www.eurecom.fr/publication/3898

[57] ——, "Transmission of correlated Gaussian samples in a Multiple-Access Channel," in *CISS 2014, 48th Annual Conference on Information Sciences and Systems, March 19-21, 2014, Princeton, USA*, Princeton, UNITED STATES, 03 2014. [Online]. Available: http://www.eurecom.fr/publication/4225

[58] M. Gastpar and M. Vetterli, "On the capacity of large Gaussian relay networks," *IEEE Transactions on Information Theory*, vol. 51, pp. 765–779, March 2005.

[59] Y. Oohama, "The rate-distortion function for the quadratic Gaussian CEO problem," *IEEE Transactions on Information Theory*, vol. 44, pp. 1057–1070, May 1998.

[60] P. Kam and R. Li, "Simple tight exponential bounds on the first-order Marcum Q-Function via the geometric approach," in *Proc. International Symposium on Information Theory*, July 2006, pp. 1085–1089.

[61] A. Unsal and R. Knopp, "Transmission of sporadic analog samples on wireless channels," *Submitted to IEEE Transactions on Wireless Communications, February 2014*, 02 2014. [Online]. Available: http://www.eurecom.fr/publication/4081